Microbial life at the glass-palagonite interface

Dissertation

zur Erlangung des

Doktorgrades der Naturwissenschaften

(Dr. rer. nat.)

am Fachbereich Geowissenschaften

der Universität Bremen

vorgelegt von

Andreas Türke

Bremen, August 2016

Referent:

Prof. Dr. Wolfgang Bach

Korreferent:

Dr. Magnus Ivarsson

Table of Contents

Abstract

The majority of the upper 500 m of oceanic crust is made up from extrusive volcanic rocks, predominantly basalts and hyaloclastites (volcanic rocks very rich in fresh glass). When the upper oceanic crust alters under the influence of seawater, its geochemistry, hydrology, and physical conditions change considerably, which shapes the bioenergetical landscape, i.e. the thermodynamics of chemical reactions, which microorganisms can exploit for their energy gain. Basalt that is exposed to oxygenated aqueous solutions, forms rims of palagonite along fractures at the expense of glass. Electron microprobe and LA-ICP-MS (laser ablation inductively coupled plasma mass spectrometry) analyses of fresh glass, adjacent palagonite crusts, and zeolites were employed to determine the geochemical changes involved in the alteration reactions. Samples were retrieved from drill cores taken in the North Pond Area, located on the western flank of the Mid-Atlantic Ridge at 22°45'N and 46°05'W, as well as from the Louisville Seamount Trail in the Pacific, off New Zealand. The crust in the North Pond area is about 8 Ma old and has only been altered oxidatively, whereas the > 60 Ma old rocks from Louisville Seamounts are more severely altered, including anoxic phases. We also analyzed whole rock powders to determine the overall crust-seawater exchange in ridge flanks.

Radioactive elements are enriched in palagonite relative to fresh glass, reaching concentrations where radiolytic production of molecular hydrogen (H_2) may play a significant role. In older flanks, crustal sealing and sediment accumulation have slowed down seawater circulation and radiolytically produced hydrogen might reach concentrations where molecular hydrogen (H_2) may be a significant energy source. Based on these results, the hypothesis that microbial ecosystems in ridge flank habitats undergo a transition in the principal energy carrier, fueling carbon fixation from Fe oxidation in very young crust to H_2 consumption in older crust, was formed. Unless the H_2 is swept away by rapid fluid flow (i.e., in young flanks), it may easily accumulate to levels high enough to support chemolithoautotrophic life. In older flanks the influence of H_2 for catalytic energy supply is expected to increase greatly. Similar habitats on other planetary surfaces are theoretically possible; as accumulation of radiolytically produced hydrogen merely requires the presence of H_2O molecules and a porous medium, from which the hydrogen is not lost. Within these fluids, Si concentrations increases due to palagonitization and eventually void space is (partially) filled by zeolites. Alteration of primary phases also changes the mineral interface to the fluid. One of the major factors controlling radiolytic H_2 production is the mineralogy in the immediate proximity of void space in the basalts, as the radioactive doses decrease, while traveling through a mineral matrix. Micro-tomography results show

that radiolysis is most effective when the void space is small (more radioactive material from minerals in close proximity) and near U, Th, and K bearing minerals. Biosignatures compared strongly vary from the two distinctly different study sites.

Furthermore, biosignatures associated with the 8 Ma North Pond Region, which is built up by young well-oxygenated crust, are characterized by little textural diversity. However, the organic matter associated with those textures, shows evidence for the occurrence of complex molecules like proteins. In contrast, the biosignatures from the Louisville Seamounts are much more texturally diverse, whereas the organic molecules are more degraded and suggest Archaeal origin. This implied that microbial communities change significantly during crustal evolution and suggest that microbes associated with older and severely altered crust, are not responsible for the trace fossils commonly found within subseafloor basalt glass.

Kurzfassung

Der Großteil der oberen 500 m der Ozeankruste ist durch effusive vulkanische Gesteine aufgebaut – größtenteils Basalte und Hyaloclastite (vulkanische Gesteine mit sehr hohem Glasanteil). Sobald ozeanische Kruste mit Meerwasser in Kontakt kommt und alteriert, ändert sich ihre Geochemie, Hydrologie und physikalischen Bedingungen erheblich. Dies formt die bioenergetische Landschaft der Ozenankruste, d.h. es formt die Thermodynamik der chemischen Reaktionen, welche Mikroorganismen zur Energiegewinnung nutzen können. Basalte, die wässrigen Lösungen ausgesetzt sind, bilden Palagonitkrusten entlang von Rissen und Brüchen aus, wobei frisches Glas ersetzt wird. Elektronenstrahlmikrosonden und Laser-Ablations induktiv-gekoppelte-Plasma Massenspektrometrie Analysen von frischem Glas, benachbarten Palagoniten und Zeoliten wurden durchgeführt, um geochemische Änderungen durch Alterationsreaktionen zu erfassen. Die Proben stammen aus Bohrkernen von der North-Pond Region an der westlichen Flanke des Mittel-Atlantischen Rückens bei 22°45'N und 46°05'W, sowie vom Louisville Seamount Trail im Pazifik, nahe Neuseelands. Die Kruste in der North-Pond Region ist ca 8 Millionen Jahre alt und wurde nur oxidativ alteriert, während die Gesteine der Louisville Seamounts deutlich stärker und auch anoxisch alteriert wurden. Des Weiteren wurden Gesamtgesteinsdaten durch Analyse von Pulverproben erhoben, um den Stoffumsatz in ozeanischen Rückenflankensystemen zu quantifizieren.

Radioaktive Elemente sind besonders im Palagonit angereichert im Vergleich zum primären frischen Glas. Die Konzentrationen erreichen Werte, bei denen Radiolyse signifikante Mengen an molekularem Wasserstoff (H_2) produziert. In alten Rückenflankensystemen bewirkt die Sedimentation, dass die Meerwasserzirkulation abklingt und radiolytisch produzierter Wasserstoff sich ansammeln kann. Hier kann molekularer Wasserstoff dann als Energiequelle für mikrobielle Organismen dienen. Darauf basierend entstand die Hypothese, dass mikrobielle Ökosysteme in Rückenflanken sich einem Wandel in der dominanten Energiequelle unterziehen. In junger Kruste wird Kohlenstoff vor allem durch Eisenoxidation fixiert, während in älterer Kruste H_2 als dominiert. Sofern der Wasserstoff nicht durch rapiden Fluidfluss weggespühlt wird, wie etwa in jungen Rückenflanken, kann er sich ansammeln und so chemoautotrophes Leben antreiben. In älteren Flanken ist das Potenzial für Leben basierend auf molekularem Wasserstoff dementsprechen deutlich größer. Ähnliche Habitate auf anderen planetaren Oberflächen sind theoretisch möglich und denkbar, da die Ansammlung von Wasserstoff lediglich die Anwesenheit von H_2O Molekülen und ein festes poröses Medium benötigt, so dass der Wasserstoff nicht verloren geht. Innerhalb dieser Fluide sammelt sich durch die voranschreitende Palagonitisierung

außerdem die Si Konzentration und Porenraum wird durch ausfallenden Zeolite teilweise ersetzt. Somit ändert sich mit der Zeit auch die Mineraloberfläche, mit welcher das Fluid interagiert. Einer der entscheidenden Faktoren bei der radiolytischen Produktion von Wasserstoff ist eben diese Mineralisierung in direkter Umgebung des fluidgefüllten Porenraums im Basalt, da die radioaktive Dosis sich bei der Ausbreitung durch ein Mineral abschwächt. Die µ-Computer Tomography Ergebnisse zeigen deutlich, dass Radiolyse dann am effektivsten ist, wenn der Porenraum klein und nah an Mineralen mit hohen Konzentrationen von radioaktiven Elementen ist.

Des Weiteren zeigen Biosignaturen große Unterschiede in den beiden miteinander verglichen Lokationen. In der North Pond Region sind diese nur durch geringe texturelle Diversität geprägt,. Die organischen Moleküle hingegen zeigen Hinweise auf komplexe Strukturen, wie etwa Proteine. Wohingegen in den Gesteinen des Louisville Seamount Trails texturell deutliche diversere Alterationstexturen zeigen, aber die organischen Moleküle dafür deutlich simpler und stärker abgebaut sind, sowie auf archäischen Ursprung hindeuten. Dies spricht dafür, dass sich mikrobielle Lebensgemeinschaften stark verändern während der krustalen Evolution. So scheinen die Mikroben, die man in älteren Rückenflankensystemen findet, nicht die selben Organismen zu sein, die in jüngeren Systemen für die Alterationstexturen verantwortlich sind.

1 Introduction

1.1 The subseafloor as a habitat

Oceanic crust covers more than 60% of Earth's surface and harbors myriads of different life forms, many of which are fueled directly or indirectly by geological processes. The diversity of terrestrial life we are familiar with is ultimately supported by primary production of photosynthetic organisms, building the foundation of complex food webs. However, life below the seafloor cannot rely on sunlight as an energy source. Instead, subseafloor microbial communities and their energy sources vary greatly depending on the geological setting. Microorganisms thriving in sediments depend on organic matter that is deposited from the overlying ocean as so-called 'marine snow' or brought in by diffusion from seawater or underlying crustal fluids.

The metabolic pathway that is used to oxidize organic matter in sediments is ultimately dependent on thermodynamics. Oxygen as an electron acceptor yields the highest amount of energy for microorganisms and is thus the preferred pathway. Consequently, oxygen is the oxidant that is depleted first in marine sediments, leaving them anoxic after a few centimeters to meters (depending on the amount of organic matter that is deposited). Other pathways that will be utilized in deeper parts of the sediment include iron-, manganese-, and sulfate reduction (Fig. 1). Unique ecosystems form around specific geological feature, e.g. cold seeps or mud volcanoes on continental shelves or –slopes, where methane rich fluids can migrate towards the sediment surface and be released into the seawater, supporting microbial communities (Orphan et al., 2002; Lösekann et al, 2007).

The volcanic ocean crust on the other hand, represents a physically and chemically different ecosystem, as fluid pathways and composition are influenced more by the rock type, compared to sedimentary ecosystems. Fresh magmatic ocean crust is constantly produced at mid-ocean ridges (MOR) and the approximately upper 500 m are made up from very permeable basalts (the most abundant volcanic rock in ocean crust). The MOR system is a global phenomenon, which covers a vast area of about 70000 km in length. From here freshly formed volcanic rocks move off-axis towards subduction zones where the crustal material is eventually recycled in the Earth's mantle. Close to the MOR, seawater penetrates the oceanic crust, is heated to temperatures of more than 400 °C near the magma chamber, and takes up significant amounts of metals and dissolved gases. As the chemically strongly modified hot

fluid rises through the crust, it is rapidly discharged in hydrothermal vents (Fig. 1) as it reaches the seafloor and mixes with seawater. Microorganisms can exploit the resulting chemical disequilibria by catalyzing redox reactions for metabolic energy gain (e.g. Amend et al., 2011; Wankel et al., 2011; Edwards et al., 2011). Further off-axis, in the so-called 'ridge flanks', fluid flow through the crust still prevails at lower temperatures (< 20 °C) and seawater-rock interactions continues to support microbial life (e.g. Jungbluth et al., 2013; Orcutt et al., 2013). Nearing the continental shelves, the volcanic ocean crust is usually covered by up to several kilometers thick impermeable sediments, which inhibit the exchange of seawater from the ocean and the subseafloor fluids. While samples from deeply buried ocean crust are scarce and thus evidence for microbial life very limited, active microbial communities have been detected even in very deep sediments of several kilometers (Whitman et al., 1998). These subseafloor microbes significantly influence their environment and shape the geochemical evolution of the Earth by mediating biogeochemical cycles. Hence, we need to address their impact on all oceanic settings, when discussing environmental issues such as the fate of pollutants, climate change, or redox chemistry kinetics in geological processes.

Microbiological incubation studies on volcanic rocks have revealed that carbon fixation, in subseafloor basalt hosted microbial communities, in fact reaches significant rates at different MORs and hotspots (Orcutt et al., 2015). Extended to global scale these rates extrapolate to 10^9 – 10^{12} g C yr^{-1}, which is in good agreement with theoretical approaches using thermodynamic and bioenergetics calculations (Bach and Edwards, 2003). The majority of all oceanic crust could in principle serve as a suitable habitat for microbial life as prevailing temperatures are below the upper temperature limit for life (slightly > 120 °C; Takai et al., 2008) and energy sources are provided through both chemical and physical processes when volcanic rocks (which make up the majority of the hydrologically active oceanic crust) are exposed to seawater. Hence, the oceanic crust represents Earth's potentially largest habitat. Yet we know very little about the controlling factors of its habitability and the actual subseafloor biosphere's extent both in cellular mass and spatial distribution. Sedimentary subseafloor habitats have been studied in more detail and they have been estimated to account for a total of 5.6 – 30.3 x 10^{16} g of cellular carbon (Parkes et al., 1994; Whitman et al., 1998; Lipp et al., 2008), which accounts for 10 – 30 % of the total biomass on Earth.

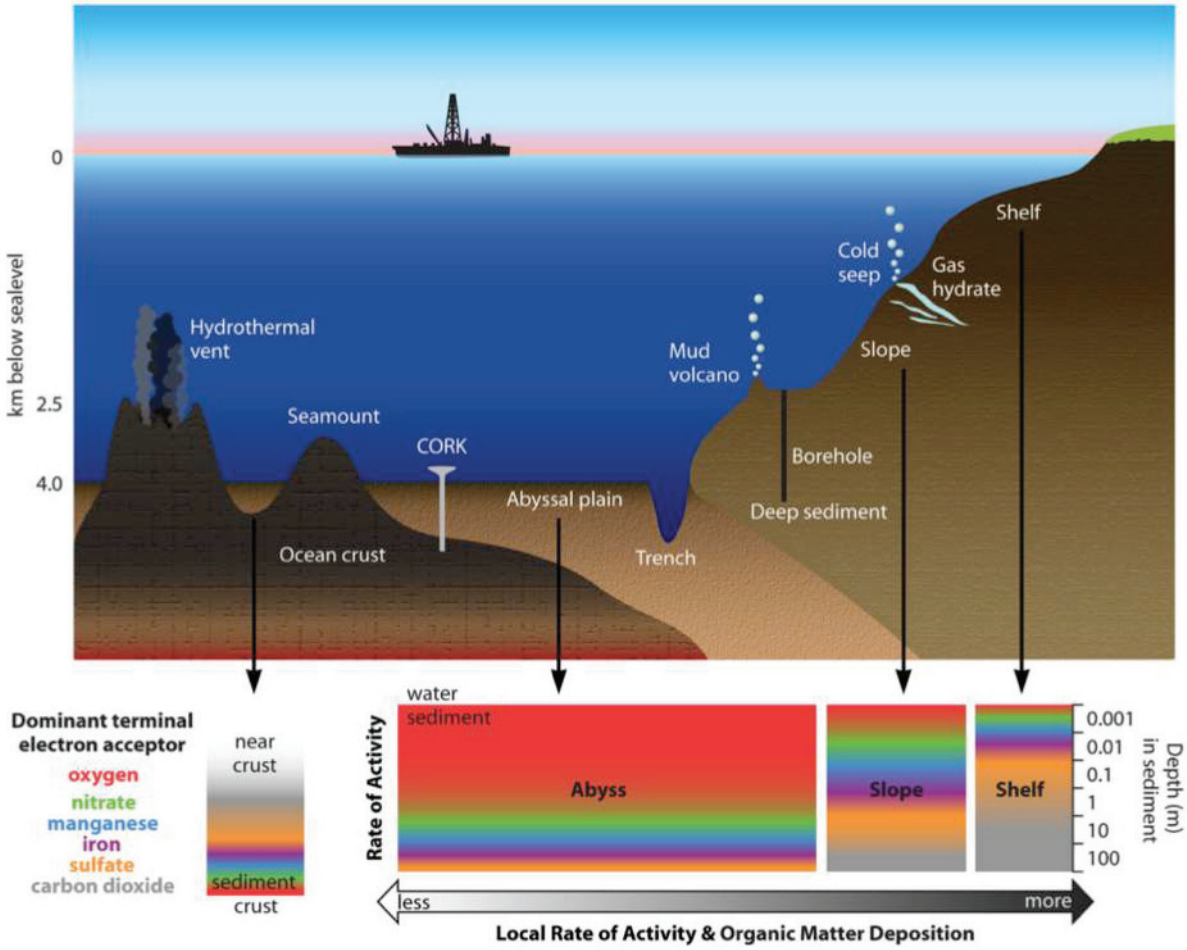

Fig. 1: Sketch of possible habitats within the subseafloor by Orcutt et al. (2011). Microbial life is supported by redox reactions. Oxygen is the electron acceptor that will be used first by microbes, since oxidation by oxygen yields more energy compared to nitrate, manganese, iron, sulfate, and carbon dioxide (decreasing yield per oxidized mol of organic matter).

However, it remains a vital task to grasp the subseafloor communities' impact on global element cycles, in particular the carbon cycle, in order to accurately account for this potentially large and active reservoir of carbon in modern climate models.

In the following sections I will review the physical properties of oceanic crust, its interaction with seawater, and the resulting chemical disequilibria, which can be exploited by microorganisms for energy gain and make the subseafloor habitable.

1.1.1 The architecture of oceanic crust

The igneous ocean crust consists of several distinct zones (Fig 2). The uppermost approximately 800 meters consist of basaltic lava flows and when these are being erupted at the seafloor they rapidly cool and the outer rim is chilled forming basalt glass. It provides the opportunity to indirectly sample the liquid phase of the initial lava, which is slightly fractionated compared to the whole-rock composition, as it does not contain any crystals. The basaltic lava flows are followed by a transition zone of a few tens of meters, which separates the extrusive volcanic rocks from the underlying sheeted dike complex. These dikes can range from several hundreds of meters to more than a kilometer and they are usually 0.5 m to 2 m in width. The lowest part of the oceanic crust is formed by intrusive gabbros, which also make up the largest section of oceanic crust with 3.5 – 5.5 km in thickness and are underlain by lithospheric mantle peridotites.

However, only the upper approximately 500 m of oceanic crust are significantly fractured and are being penetrated by seawater, which circulates through volcanic rocks. These make up the most habitable section of the ocean crust, as permeability decreases drastically with depth (Fisher et al., 2008). The subseafloor aquifer is thought to occur mainly in these upper few hundred meters of ocean crust. This so-called 'subseafloor ocean' is Earth' largest aquifer with 2% of the oceans volume and an equivalent to the water in the global oceans is passed through the crust on average about every 10^5 to 10^6 years (Wheat et al., 2003; Johnson and Pruis, 2003). Very close to the MOR fluid temperatures can exceed 300 °C and the vast amount of fluid rock reactions can be witnessed in hydrothermal systems (see section 1.1.2). In ridge flanks, away from the heat source – the magma chamber at the MOR – fluid temperatures are more moderate (< 20 °C) and water-rock reactions become more sluggish as reaction kinetics slow down.

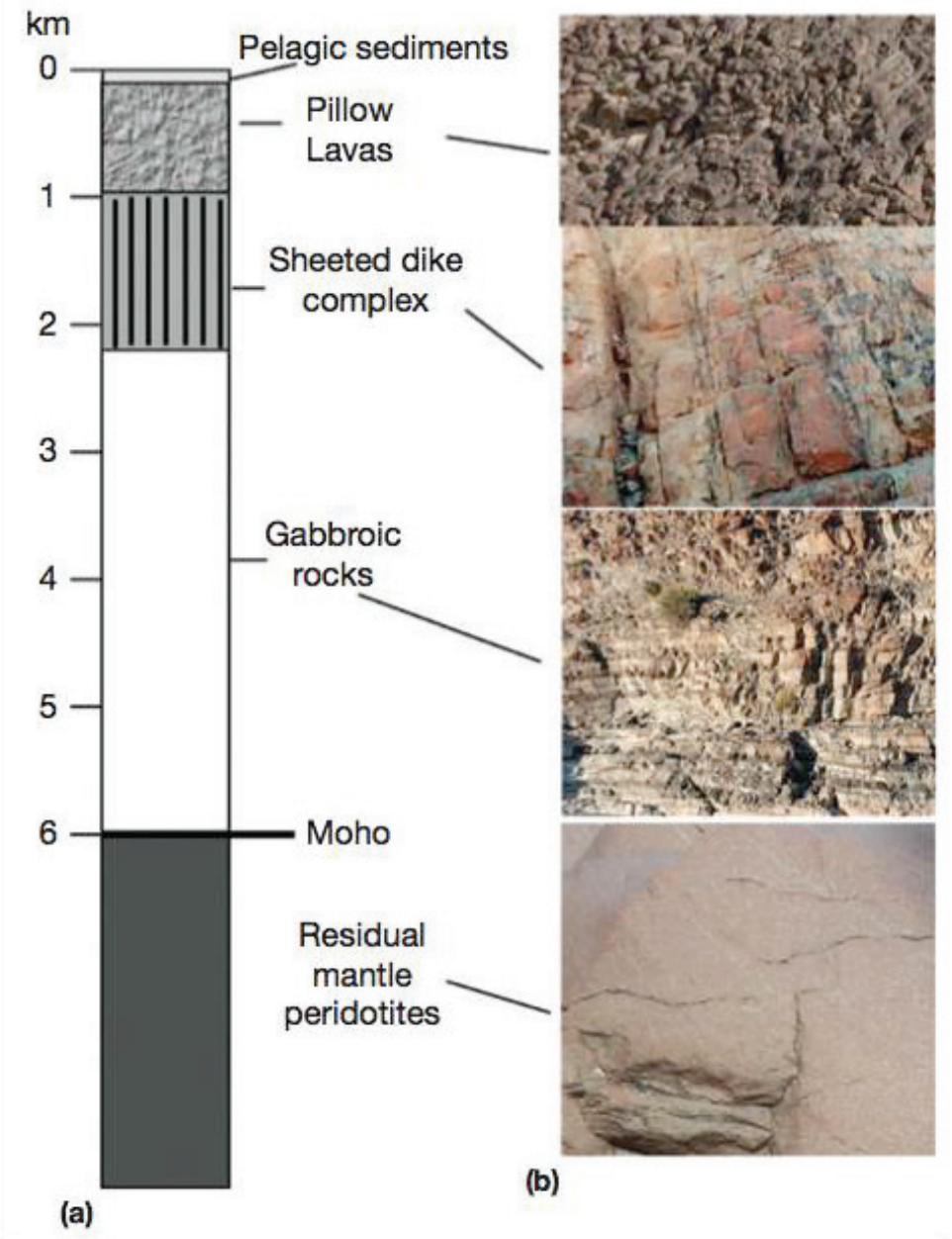

Fig. 2: Schematic overview of the oceanic lithosphere (a) and photographs of the respective rock types exposed in ophiolites (b). Figure by White and Klein (2014).

As oceanic crust moves even further off-axis and approaches the continental margins (where it will be subducted) it leaves the oligotrophic regions and sediments accumulate, eventually covering the crust. These sediments prevent exchange between the ocean and the underlying subseafloor ocean. Initially sedimentation results in channeled fluid flow between, which are not yet completely covered. In the latest stages of crustal evolution, circulation within the crust will be entirely closed, exchange with the ocean will be permitted. Now, subseafloor crustal fluids can probably become anoxic, resulting in very different chemical conditions for microbial life, compared to young oceanic crust. With these changes in mind it

becomes evident that the heterogeneity of oceanic crust has profound impact on shaping the (energetical) landscape for the subseafloor biosphere.

1.1.2 Water-rock interactions

The interaction between rocks and seawater plays a vital role in cycling elements through the ocean crust. The unique chemical environment that is created by hydrothermal fluid circulation does not only fuel a unique biosphere, but also forms precious metal deposits. Near fast spreading MORs seawater penetrates the permeable crust and interacts with the ocean crust by forming a fluid that becomes slightly acidic, anoxic, rich in alkalis, and poor in Magnesium (Fig. 3).

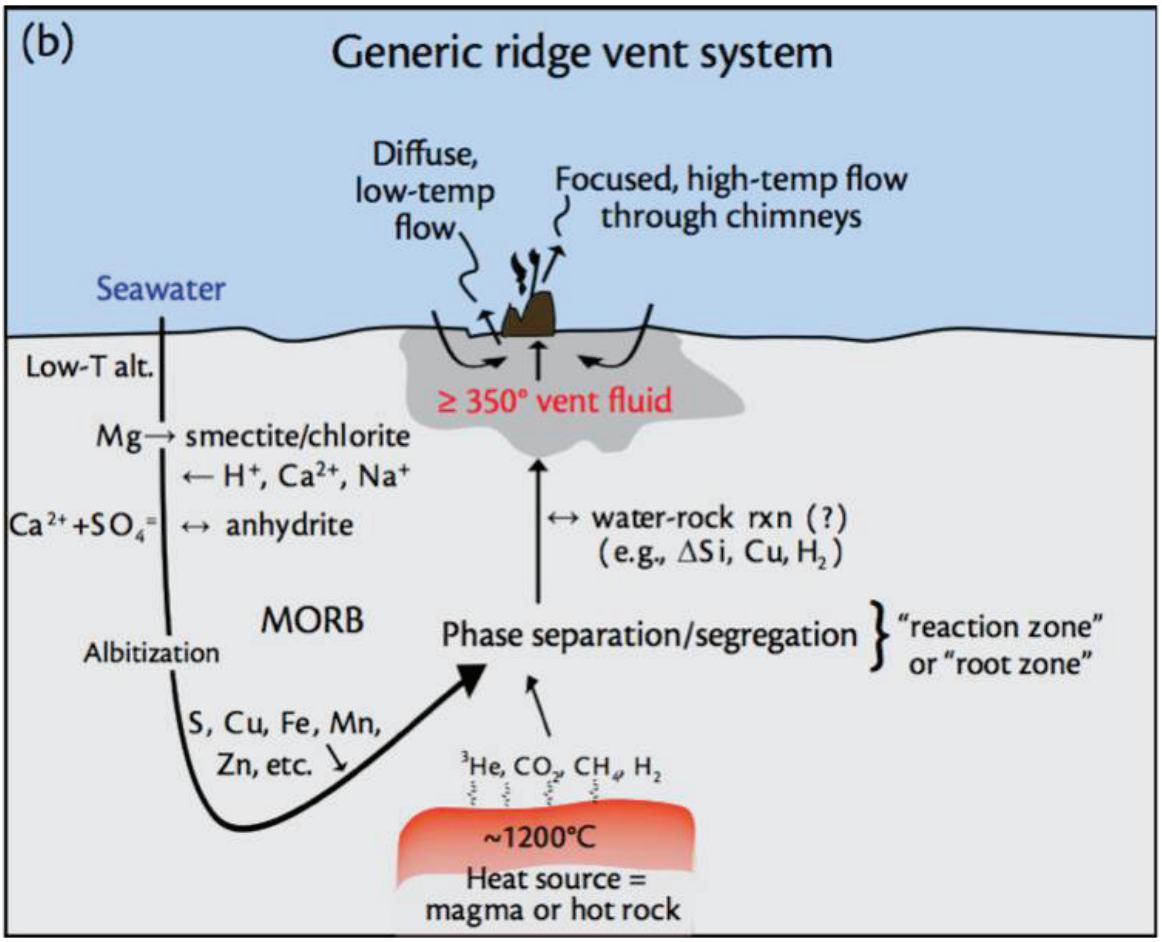

Fig. 3. Schematic overview of a hydrothermal vent system by Tivey (2007). Seawater enters the permeable ocean crust and is chemically changed by water-rock interaction. The resulting fluid eventually discharges rapidly on the seafloor to form a hydrothermal vent.

This fluid can then leach significant amounts of sulfur and metals at high temperatures of > 300 °C. Depending on the temperature a phase separation can occur to form a low-salinity and vapor-rich fluid as

well as a brine phase. In any case the hot fluid will become buoyant and rapidly rise to the seafloor, where it is expelled in hydrothermal vents. However, this process mainly occurs very close to the MOR, as it requires a heat source (usually magma under the MOR).

At lower temperatures, as they prevail in ridge flanks, alteration of basalts exposed to seawater forms ferric smectites and Fe-(oxy)hydroxides by replacing plagioclase, olivine, and basalt glass. The glassy rims in basalt pillows represent the least stable and therefore most reactive part in oceanic (sub)seafloor basalts. The abiotic process in which basalt glass is dissolved and hydrated by seawater is called palagonitization and the resulting mixture of several authigenic minerals (mostly smectites and zeolites (Stroncik and Schmincke, 2002)) is called palagonite. However, the rates and mechanisms controlling this process are poorly understood. A recent study in different environments has found strongly varying trends in major element changes (Pauly et al., 2011), with only MgO being highly mobile in all environments. The main factor appears to be original sample porosity, since palagonitization terminates as soon as cavities fill and water circulation ceases. The ageing of ocean crust occurs along with changes to its hydrological state – from open circulation of oxygenated seawater in young crust to closed-system or even ceased circulation in older crust (e.g., Fisher and Wheat, 2010). Conceptually the upper igneous crust is treated as an aquifer "sealed" by low permeability sediments, such that exchange with seawater occurs only at seamounts (Harris et al., 2004; Anderson et al., 2012). The seafloor is decorated with 10^6 – 10^7 seamounts of elevations >100 m (Wessel et al., 2010), acting as "breathing holes" that sustain seawater circulation within the crust. Estimations suggest that roughly 2×10^{16} kg of seawater circulate through oceanic crust per year, which is equivalent to the yearly discharge of global river systems into oceans (Wheat et al., 2003). Within the upper igneous crust, pillows, breccia, and fault zones are usually most altered, implying that these lithologies represent areas of highest fluid throughput (Alt, 2004).

1.1.3 Energy sources in the subseafloor ocean

Oceanic subsurface habitats span a variety of physical and chemical conditions, characterized by different rock types, fluid throughput, and temperatures. These factors ultimately decide whether a specific chemical reaction is a viable source for microbial energy gain. In principle any reaction, with a negative Gibbs energy is going to go forward in nature. However, reactions typically require activation energy to undergo a chemical or physical change (e.g. phase change), which allows many metastable phases to persist in nature (e.g. metastable diamonds at surface pressure, which are supposed to become graphite). Thermodynamic computations have been used to identify viable catabolic reactions

as well as estimate the size of the biomass supported by redox equilibria between hot hydrothermal vent fluids and seawater (McCollom & Shock, 1997; Amend et al., 2011). The models suggest that basalt-hosted systems offer maximal potential for sulfide oxidation and to a lesser extent iron and methane oxidation (Amend et al., 2011). These computations use measured vent fluid compositions and assess reactions of dissolved aqueous species. Reduced elements (Fe, Mn, S) in rocks and minerals are an additional source of energy, and are colonized as substrates by specifically adapted microorganisms (e.g., Einen et al., 2008; Santelli et al., 2008). These solids, in theory, can release similar amounts of energy as hydrothermal venting (McCollom, 2000; Bach and Edwards, 2003). Microorganisms select specific solid phases in seafloor settings, indicating a prominent mineralogical control on the community composition of the attached microorganism (e.g., Toner et al., 2012). Energetics may be one of the master variables in causing this selectivity. The community compositions change rapidly as the seafloor ages and the mineralogical composition of rocks evolves (Santelli et al., 2009).

However, microbial metabolism is not only influenced by the catalysis of chemical reactions that are exploited as energy source (the so called catabolism), but also by the thermodynamics for their anabolism (i.e. the synthesize of biomolecules). Anabolism is one of the key factors, that determines how much maintenance energy a microorganism requires, which is the amount of energy necessary to keep all vital cell activities going (e.g. cell repair). In an environment where cell anabolism is energetically favored, microorganisms can thus thrive even under less catabolically favorable conditions. Hydrothermal systems are environments, where many biomolecules are energetically very stable (Fig. 4) and also formed abiotically (McDermott et al., 2015).

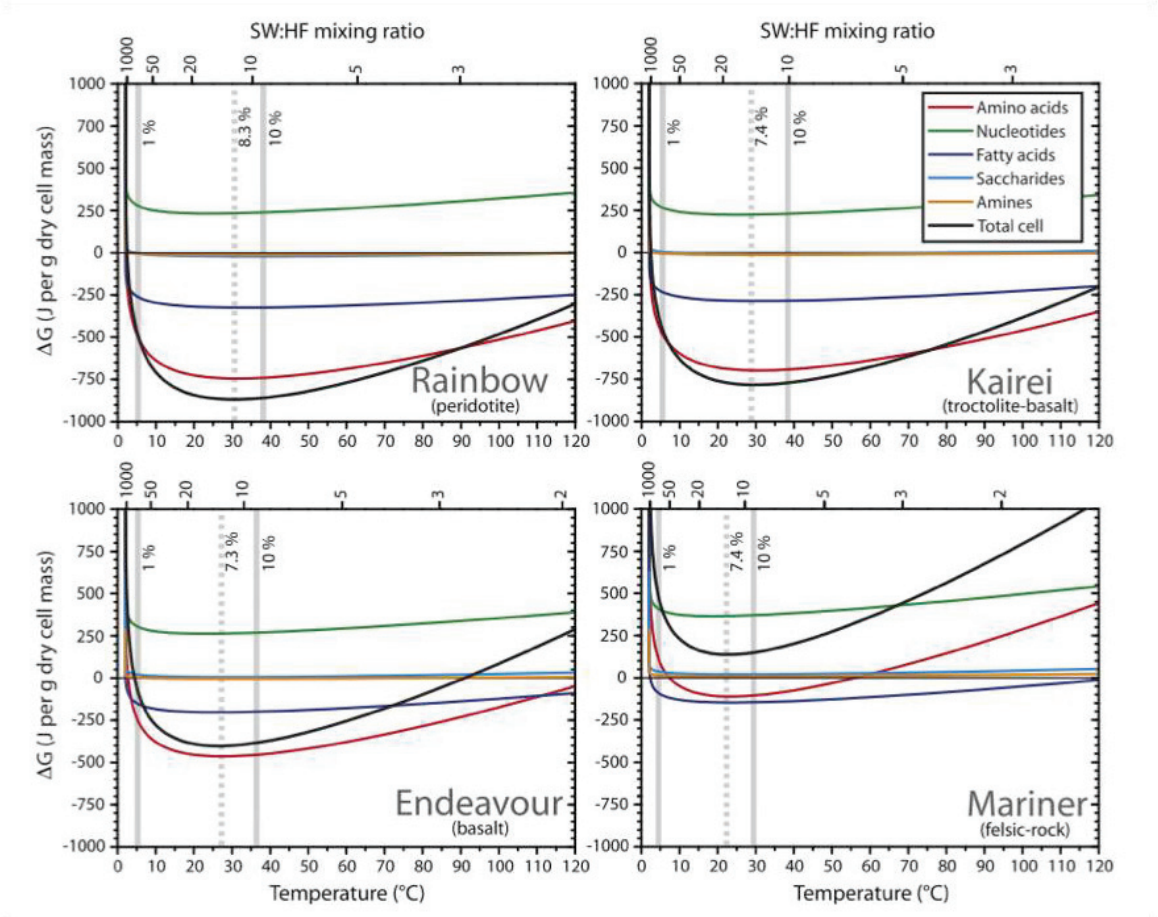

Fig. 4: Gibbs free energies of anabolic synthesize of individual biomolecules (amino acids, nucleotides, fatty acids, saccharides, and amines) and the sum of the total cell biomass for different ratios of seawater and hydrothermal fluids mixing (SW:HF mixing ratio). This computation was done for hydrothermal systems hosted in different rock types. Figure by Amend et al. (2011).

The flanks of MOR systems represent a different environment in terms of metabolism. The crustal fluids are not characterized by the vigorous changes that fluids in hydrothermal systems undergo and thus do not offer such favorable anabolic conditions. Nevertheless, ridge flanks represent Earth's largest reservoir of basalt glass, which theoretically is an ideal habitat for chemoauthotrophic catabolic energy gain. When seawater is flowing through in-situ oceanic crust, an environment with differing redox chemistry is created where basaltic rocks, containing reduced forms of Fe, S, Mn and other metals, which are in disequilibrium with oxidants such as O_2 in the seawater, form an environment suitable for microbial colonization. The most likely reactions to be catalyzed by chemoautotrophs in this environment are: Fe(II) oxidation (1), Mn(II) oxidation (2) and sulfide oxidation (3) (Edwards et al., 2005).

(1) $Fe^{2+} + ¼\ O_{2(aq)} + H^{+} \rightarrow Fe^{3+} + ½\ H_2O$

(2) $Mn^{2+} + ½\ O_2 + H_2O \rightarrow MnO_{2(solid)} + 2H^{+}$

(3) $HS^{-} + 2O_2 \rightarrow SO^{2-}_{4} + H^{+}$

1.2 Biosignatures in volcanic rocks

Several lines of evidence for active microbial life in volcanic rocks have been observed over the past decades. The most obvious are bioalteration textures, which refer to empty or mineral-filled pits (granular alteration textures) and channels (tubular alteration textures) (Fig. 5) within volcanic glass. Their size of a few µm in width and their shape are comparable to modern microbes (Furnes et al., 2007). These textures are always associated with fluid pathways like fractures or vesicles. In some cases they are overgrown by palagonite, which forms as rims around individual glass shards or along fractures. This textural observation indicates that the abiotic palagonitization is a slower process, which is in good agreement with a biotic origin of the bioalteration textures, as catalysis by microbes would enhance the reaction kinetics. The mechanism with which these bioalteration textures form, is unclear, however it has been suggested that microbes cause local variations in pH, allowing them to chemically 'drill' into fresh glass (Thorseth et al., 1992).

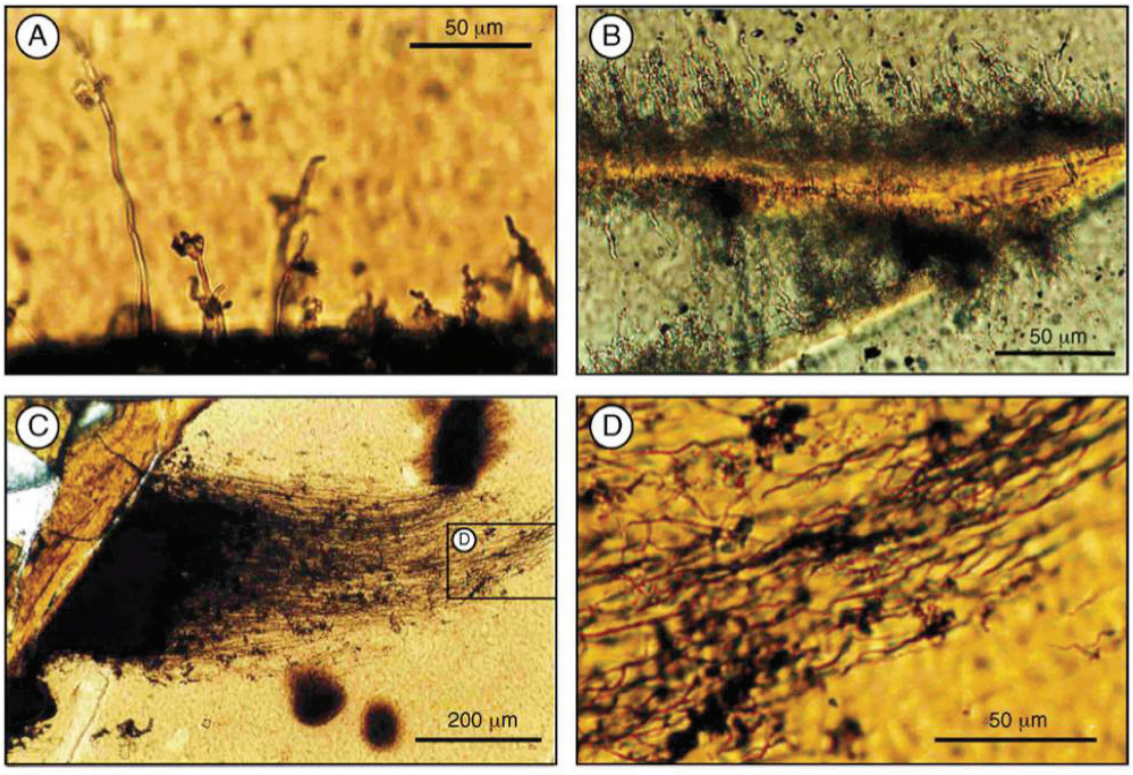

Fig. 5: Tubular alteration textures in fresh basalt glass as seen under a plane polarized light transmission microscope. A: Close up view on several individual tubes that show branching at the terminus. B: Close up of several tubes originating at a palagonite rim. C: Thick network of tubes, again originating from palagonite. D: Close up of C, individual tubes are visible; yet crosscutting cannot be observed. Figure by Furnes et al. (2007).

Other evidence for an active subseafloor biosphere comes from fossilized fungal colonies, which have been reported from several seamounts in different oceans (Schumann, et al., 2004; Ivarsson et al., 2012; Bengtson et al., 2014; Ivarsson et al., 2015). These include cryptoendolithic communities preserved in vesicles and mineralized by Mn oxides, as well as large (10s of µm) body like structure and hyphae preserved in calcite (Fig. 6). The presence of fungi in subseafloor volcanic rocks in remarkable, since all known fungi are heterotrophs, which meaning they rely on a source of primary production for their energy gain. While this source is unknown, it appears feasible to assume that the primary production is carried out by chemolithoautotrophic microbes, as highlighted in section 1.1.3.

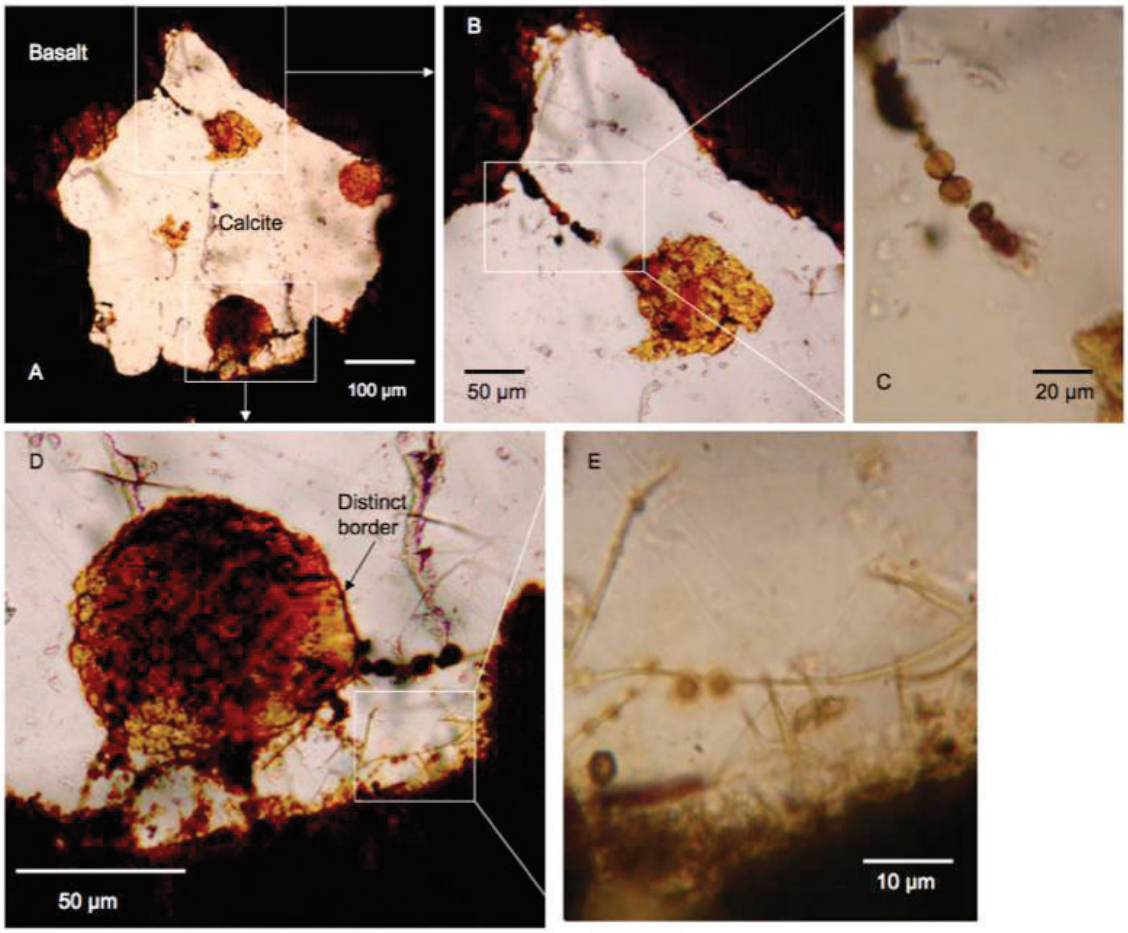

Fig. 6: Microphotographs of a vesicle (A) with close-ups of fossilized body-like structures (B, C, D) and fungal hyphae structures (E). These can be found in basalt among several oceans illustrating the diverse and active subseafloor communities in volcanic rocks. Figure by Ivarsson et al. (2012).

1.2.1 Biomolecules in microbial organisms and their preservation

In some cases trace fossils are accompanied with the presence of organic molecules, however the relationship between the two is difficult to assess. When we sample rocks from an environment with the intent of finding out if they harbor or harbored life, we need to understand what kind of biomolecules make up a living organism and what their fate is, once they decay.

Life is build up from four groups of basic organic molecules: sugars, amino acids, fatty acids, and nucleotides, which then make up the four key macromolecules of a microbial cell: proteins, nucleic acids, lipids, and polysaccharides. They are built from the essential elements C, N, O, S, P, and H and several non-essential elements that contribute to individual molecules (e.g. metals acting as a co-factor in proteins). Some molecules are very specific for certain organisms or metabolism and act as biomarkers that reveal insights into modern or ancient microbial ecosystems.

While carbohydrates are not very useful tracers for microbial life in rocks due to their rapid degradation, proteins, lipids and nucleic acids reveal significant insights into community structures found in the subseafloor.

Microbiological studies focusing on nucleic acids include gene-based methods such as the extraction of DNA or RNA followed by amplification (e.g. quantitative polymerase chain reaction (Q-PCR)) or hybridization with probes targeting for specific molecules (e.g. fluorescent in-situ hybridization (FISH)). In particularly the 16S ribosomal RNA (16S rRNA) gene sequencing technique, have been applied to a series of microbiological studies among all oceanic habitats. The 16S rRNA is a component of a prokaryotic ribosome and it is widely applied for phylogenetic studies, due to the slow evolution rates of this region of the gene. The main idea of using biomolecules as biomarkers is that DNA is transcribed into mRNA, which translates into proteins. As all these molecules have different lifetimes in nature, they can be used to decipher different processes. Based on 16S rRNA studies, significant differences in bacterial community structures have been detected for the different (sub)seafloor habitats (deep sediments, surface sediments, basalts, hydrothermal deposits, and hydrothermal fluids), especially compared to seawater and terrestrial habitats (Fig. 7).

While gene-based methods reveal substantial insights into the composition of subseafloor microbial communities, there are limitations. They selectively suppress the detection of certain archaea (Lipp et al., 2008; Teske and Sørensen, 2008) and the massive amount of data that is produced is often difficult to decipher. Furthermore they require isolation and cultivation of an individual microbial species, which can be difficult for microorganisms that live symbiotically or grow very slowly. These obstacles highlight the necessity for multi-method studies as attempted in the scope of this thesis.

Studies focusing on enzyme activity on basalt exposed at the seafloor from the Loihi seamount revealed activity similar in order of magnitude as from communities in continental shelf sediments and significantly higher than in the overlying water column (Meyers et al., 2014). Such studies provide insights into the geochemical role of a microbial biosphere in the marine environment. However, preservation of enzymes in the rock record is not very likely, due to its rapid degradation.

All microbial cells' exterior is covered by a cell membrane, separating the inside and the outside of a cell and being made up by lipids. These lipids have been incredibly useful in identifying life forms in deep sea sediments, since they are highly specific for the different domains of life. Even though they can suffer from thermal breakdown when buried in the sedimentary record, they tend to be a very long-lived biomolecule.

Once a microbial cell dies, its molecular components will either degrade abiotically or be metabolized by other microbes, if present. Whether the molecule (or parts of it) can be preserved in the rock record depends on several factors, for example its thermodynamic stability in the environment or the time it is exposed to a reactive fluid or other microbial organisms. Many life building blocks are remarkably stable within hydrothermal fluids, mixing with seawater (Amend et al., 2011). Amino acids and fatty acids tend to be the thermodynamically most stable biomolecules (see Fig. 3).

Summarizing, once we detect biomolecules or their remnants in the rock record, we need to assess their biogenicity and syngenicity. This means carefully addressing the potential origin of the different groups of molecule and whether any abiotic origin can be excluded (biogenicity criteria) and whether the biomolecule can be directly associated with the rock (syngenicity criteria). Once again, given the significant differences in preservation of the different biomolecules in (sub)seafloor environments, an approach with complementary methods is often useful.

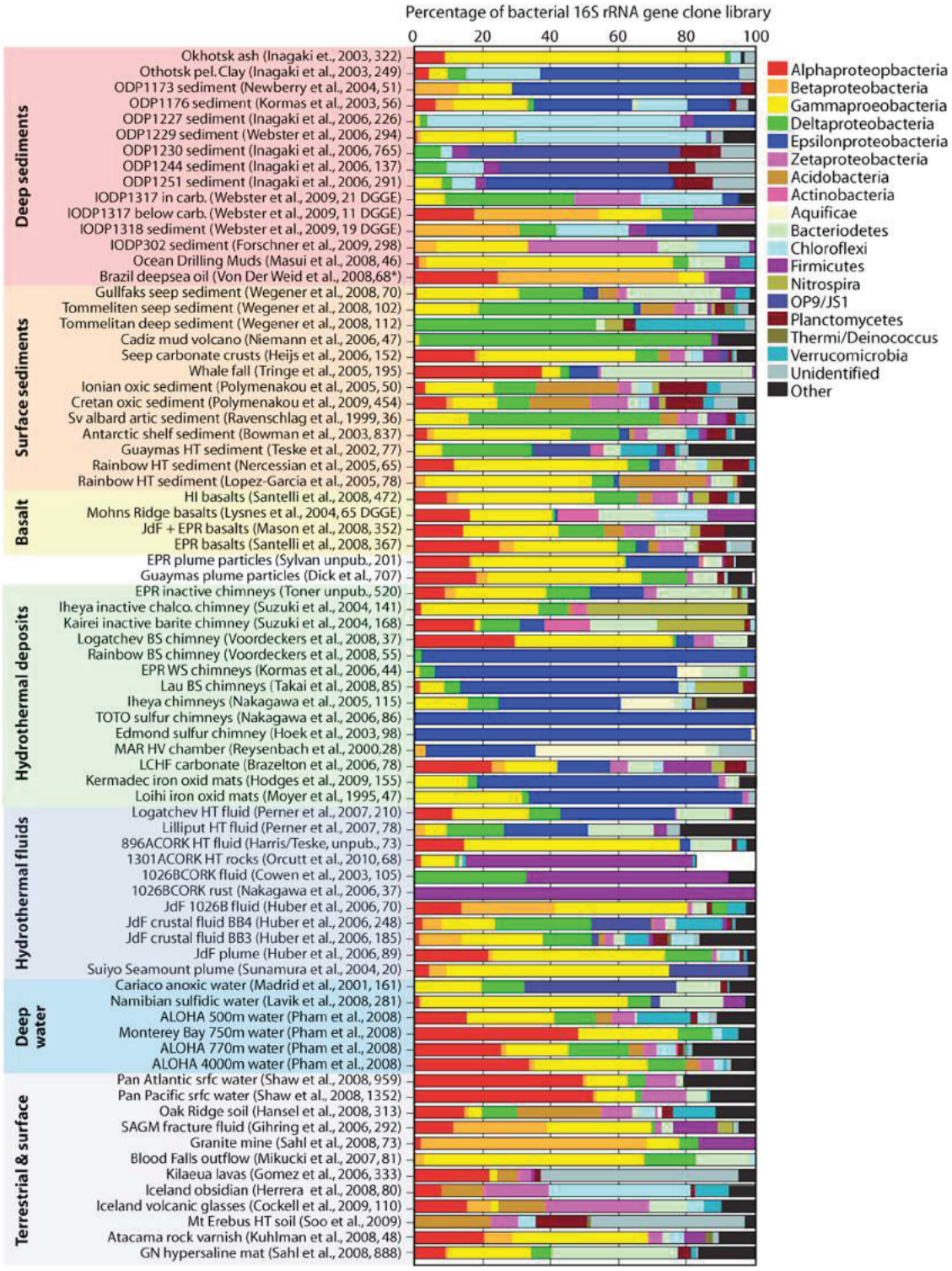

Fig. 7: Composition of bacterial communities by Orcutt et al. (2011) derived from clone libraries of the 16S rRNA gene from different oceanic environments. Individual samples are grouped based on the habitat they were recovered from.

1.2.2 Significance of biosignatures for astrobiology

Investigating biosignatures on Earth plays a crucial role in the search for extraterrestrial life, as we need to learn to clearly distinguish between abiotic and biotic origin of potential biosignature candidates to decipher their biogenicity in extraterrestrial material. We can group potential habitats according to the physical and chemical conditions of the respective environment and evaluate whether these are habitable or not for life as we know it on Earth. However, identifying biosignatures associated with a rock is the most plausible evidence for the habitability of an environment. Many planetary surfaces meet all requirements to be habitable but are likely uninhabited due to the lack of an origin of life (Cockell, 2011). Moreover we likely overestimate the uninhabitable space in the universe, since our knowledge about the limits of life is probably not complete.

When we consider the earliest life on Earth - the Last Universal Common Ancestor (LUCA) – i.e. an organism before the diversion into bacteria and archaea in the tree of life, it must have had an autotroph catabolism, as heterotrophy was impossible due to the lack of other life forms (Lane et al., 2010). As was pointed out in section 1.1.3, particularly hydrothermal systems, but also basalts in ridge flanks provide an environment, where thermodynamic conditions favor chemoautotrophic life. However, the latter environment may not be the one where life originated, given the less favorable anabolic conditions for the synthesis of organic molecules and thus higher maintenance energy demands. However, here we find abundant and easily recognizable biosignatures within the secondary mineral phases and as bioalteration textures in basalt glass. This makes volcanic rocks that were altered by an aqueous fluid one of the prime targets for the search extraterrestrial life and highlights the necessity to clearly identify the chemical and physical conditions under which biosignatures in volcanic rocks are formed on Earth.

1.3 Motivation

The interface between basaltic glass and palagonite is of considerable interest to geomicrobiological studies of the subseafloor, as it represents a unique environment that is slowly changing its chemical, physical, and mineralogical conditions with the ageing of the ocean crust. These environmental changes drive a change in bioenergetical conditions and raise the question of whether the upper oceanic crust is habitable only for a short duration of its existence or throughout the entire phase from formation at the MOR to the subduction at the continental margin.

However, unraveling these parameters for different stages of crustal evolution is a challenging task. Very fresh basalts are erupted constantly at MORs, but these are typically too hot to serve as a habitat in the initial stages. As soon as they are exposed to seawater for longer periods of time, oxidative alteration occurs and tubular and granular alteration textures witness the microbial colonization of the upper oceanic crust. Eventually more altered basalts will travel off-axis due to plate spreading and buried by sedimentation, which increases as the oceanic crust moves closer to the continental margins. Sampling rocks buried under hundreds of meters of sediment is a difficult task and thus samples are rare and often limited to seamounts, where crustal material is exposed at the seafloor even far off-axis. These seamounts also act as 'breathing holes' for the ocean crust, fueling the subseafloor basaltic aquifer with seawater.

This thesis aims at deciphering the small-scale mineralogical changes that occur with the initial oxidative alteration of basalts (predominantly palagonitization) and discusses the bioenergetical changes that are accompanied. Furthermore organic molecules were detected, associated with textural alteration features, some of which are indicative of microbial activity. Therefore, basalts from the North Pond region, Mid-Atlantic Ridge and from the Louisville Seamount Trail were analyzed with geochemical techniques. The North Pond region is characterized by 8 Ma old basalts that have only been altered oxidatively and gives a snapshot into the onset and initial stages of crustal alteration. The Louisville Seamount Trail on the other hand is characterized by > 60 Ma old basalts, which have a more diverse history of alteration, including exposure to anoxic fluids. Comparing the two, this thesis provides new insights into the habitability of subseafloor aquifers on Earth and provides valuable information that can be adapted for habitability studies on other planetary bodies.

Additionally, micro-tomography techniques were utilized to study alteration phases in 3-D at small scale of only a few µm. Void space in basalts plays a crucial role in determining how trapped crustal fluids evolve chemically and thus how the bioenergetical regime changes in these cavities. Micro-tomography is the perfect tool to observe the relationship of secondary phases that are precipitated or formed from primary phases and the void space, which is retreating in favor of precipitating minerals.

1.4 Outline and Scientific contributions

The scientific work conducted in the framework of my PhD studies resulted in three first-author manuscripts that are presented in chapter 2, 3, and 4.

Manuscript I:

Title: Palagonitization of Basalt Glass in the Flanks of Mid-Ocean Ridges: Implications for the Bioenergetics of Oceanic Intracrustal Ecosystems

Authors: A. Türke, K. Nakamura, W. Bach

Published in *Astrobiology* 10/15, DOI: 10.1089/ast.2014.1255

Manuscript I investigates the uptake of radioactive elements in the process of oxidative alteration of basalt glass (palagonitization) in the North Pond region on the western flank of the Mid-Atlantic Ridge. U, Th, and K are taken up from seawater during palagonitization and lead to radiolytic production of molecular hydrogen. As basalts alter the interface of fresh glass and water is eventually eliminated, which results in a very different micro-environment for chemolithoautotrophic microbes in the subseafloor aquifer. The leaching of Si from glass creates a fluid from which zeolites are precipitated. These seal fractures and form closed areas of fluids, where the radiolytically produced hydrogen can accumulate and potentially support microbial life, even in very old samples that do not offer any other primary chemotrophic energy source.

Authors' contributions:

Andreas Türke wrote the manuscript (except for 2.3.4 and 2.4.4) created the figures (except for Figure 6), analyzed the thin sections and calculated the radiolytic hydrogen yields. Contribution approximately 75 % of the total work.

Wolfgang Bach wrote the section 2.3.4 “Thermodynamic computation of hydrogen production during palagonitization” and 2.4.4 “Comparison between the amounts of hydrogen expected from radiolysis versus water-rock reactions”, produced Figure 6 and 7, and contributed with scientific input into the discussion. Contribution approximately 20 % of the total work.

Kentaro Nakamura produced and analyzed the whole rock powders by X-ray fluorescence for Fe and K contents. Contribution approximately 5 % of the total work.

Manuscript II:

Title: Comparing biosignatures in aged basalt glass from North Pond, Mid-Atlantic Ridge and the Louisville Seamount Trail, off New Zealand

Authors: A. Türke, W. Bach, B. Menez

Submitted to *PlosOne* on 25/08/2016

Manuscript II compared tubular alteration textures and organic molecules associated with them in fresh glass and palagonite from the North Pond area, Mid-Atlantic Ridge and the Louisville Seamount Trail, off New Zealand. Biosignatures were clearly different from one another, which coincides with the significant differences in alteration history of the two sites. Tubular alteration textures seem to be formed rather early within the approximately first 10 Ma of crustal evolution. The organic molecules found in the older samples from the Louisville Seamount Trail were associated with secondary phases and are likely not remnant of the organisms that form tubular textures in fresh glass.

Authors’ contributions:

Andreas Türke wrote the manuscript, created the figures, prepared all samples and carried out the analytical measurements. Contribution approximately 85 % of the total work.

Benedicte Menez helped significantly with the detection of organic molecules at the IPGP in Paris, France and contributed to the interpretation of the results and the discussion. Contribution approximately 10 % of the total work.

Wolfgang Bach was involved in the planning of the project and gave scientific input into the discussion of the results. Contribution approximately 5 % of the total work.

Manuscript III:

Title: The coupled evolution of void space geometry and alteration reactions in the ageing oceanic crust

Authors: A. Türke, W-A. Kahl, W. Bach

To be submitted to *Geochemistry, Geophysics, Geosystems* (G^3)

Manuscript III reports geochemical data on altered basalt from the North Pond region, Mid-Atlantic Ridge, as well as micro-tomography measurements of the void space geometry and its evolution during alteration reactions. Alteration of primary phases also changes the mineral interface to the fluid, which is what drives the bioenergetic landscape. Molecular hydrogen produced by radioactive decay from elements in the basalt has been proposed as an important energy source in old ocean crust. One of the major factors controlling radiolytic H_2 production is the mineralogy in the immediate proximity of void space in the basalts, as radioactive doses decrease, while traveling through a mineral matrix. We show that radiolysis is most effective when the void space is small (more radioactive material from minerals in close proximity) and near U, Th, and K bearing minerals.

Authors' contributions:

Andreas Türke wrote the manuscript, created the figures (except for Figure X), prepared all samples and carried out the analytical measurements (except for the µ-CT measurements). Contribution approximately 85 % of the total work.

W-A. Kahl carried out the µ-CT analyses and the post-processing of the data. He also implemented the four phase segmentation of the tomography data. He wrote section 4.4.3 and created Figure 7. Contribution approximately 10 % of the total work.

Wolfgang Bach helped with designing the project and gave scientific input into the discussion of the results. Contribution approximately 5 % of the total work.

1.5 References

Alt, J. C., 2004. Alteration of the upper oceanic crust: Mineralogy, chemistry, and processes. In: Davies, E.E., and Elderfield H. (Eds.) Hydrogeology of the Oceanic Lithosphere, pp. 495–533. Cambridge University Press.

Amend, J. P., McCollom, T. M., Hentscher, M., and Bach, W., 2011, Catabolic and anabolic energy for chemolithoautotrophs in deep-sea hydrothermal systems hosted in different rock types. Geochim. Cosmochim. Acta 75, 5736–5748.

Anderson, B. W., Coogan, L. A., and Gillis, K. M., 2012. The role of outcrop-to-outcrop fluid flow in off-axis oceanic hydrothermal systems under abyssal sedimentation conditions, Journal of Geophysical Research: Solid Earth, 117, B05103.

Bach, W., and Edwards, K. J. 2003, Iron and sulfide oxidation within the basaltic ocean crust : Implications for chemolithoautotrophic microbial biomass production. 67, 3871–3887.

Bengtson S, Ivarsson M, Astolfo A, Belivanova V, Broman C, Marone F, et al., 2014, Deep-biosphere consor- tium of fungi and prokaryotes in Eocene sub-seafloor basalts. Geobiology 2014; 12: 489–496.

Cockell, C. S., 2011, Vacant habitats in the Universe. Trends Ecol. Evol. 26, 73–80.

Einen, J., Thorseth, I.H., and Ovreås, L., 2008, Enumeration of Archaea and Bacteria in seafloor basalt using real-time quantitative PCR and fluorescence microscopy. FEMS Microbiology Letters, 282(2), 182 – 187.

Fisher, A. T., Davis, E. E., and Becker, K., 2008, Borehole-to-borehole hydrologic response across 2.4 km in the upper oceanic crust: Implications for crustal-scale properties, J. Geophys. Res., 113, B07106

Furnes, H., Banerjee, N. R., Staudigel, H., Muehlenbachs, K., McLoughlin, N., de Wit, M., and Van Kranendonk, M., 2007, Comparing petrographic signatures of bioalteration in recent to Mesoarchean pillow lavas: Tracing subsurface life in oceanic igneous rocks. Precambrian Research 158, 156–176.

Harris, N. H., Fisher, A. T. & Chapman, D. S., 2004, Fluid flow through seamounts and implications for global mass fluxes. Geology, v. 32; no 8, p. 725 – 728.

Ivarsson, M., 2012, Subseafloor basalts as fungal habitats. *Biogeosciences Discuss.* 9, 2277–2306.

Ivarsson, M., Peckmann, J., Tehler, A., Broman, C., Bach, W., Behrens, K., Reitner, J., Böttcher, M. E., and Ivarsson, L. N., 2015, Zygomycetes in Vesicular Basanites from Vesteris Seamount, Greenland Basin – A New Type of Cryptoendolithic Fungi. PLoS One 10.

Johnson, H. P., and Pruis, M. J., 2003. Fluxes of fluid and heat from the oceanic crustal reservoir. Earth Planet. Sci. Lett. 216, 565–574.

Jungbluth, S. P., Grote, J., Lin, H.-T., Cowen, J. P., and Rappé, M. S., 2013, Microbial diversity within basement fluids of the sediment-buried Juan de Fuca Ridge flank. ISME J. 7, 161–72.

Lane, N., Allen, J. F., and Martin, W., 2010, How did LUCA make a living? Chemiosmosis in the origin of life. Bioessays 32, 271–80.

Lipp, J. S., Morono, Y., Inagaki, F., and Hinrichs, K. U., 2008, Significant contribution of Archaea to extant biomass in marine subsurface sediments. Nature, 454(7207), 991-994.

Lösekann, T., Knittel, K., Nadalig, T., Fuchs, B., Niemann, H., Boetius, A., and Amann, R., 2007, Diversity and abundance of aerobic and anaerobic methane oxidizers at the Haakon Mosby Mud Volcano, Barents Sea. Applied and environmental microbiology, 73(10), 3348-3362.

McCollom, T. M., 2000, Geochemical constraints on primary productivity in submarine hydrothermal vent plumes. Deep Sea Research Part I: Oceanographic Research Papers, 47(1), 85 – 101.

McCollom, T. M. and Shock, E. L., 1997, Geochemical constraints on chemolithoautotrophic metabolism by microorganisms in seafloor hydrothermal systems. Geochimica et Cosmochimica Acta, 61, 4375 – 4391.

McDermott, J. M., Seewald, J. S., German, C. R., and Sylva, S. P., 2015, Pathways for abiotic organic synthesis at submarine hydrothermal fields. Proceedings of the National Academy of Sciences, 112(25), 7668-7672.

Meyers, M. E. J., Sylvan, J. B., and Edwards, K. J., 2014, Extracellular enzyme activity and microbial diversity measured on seafloor exposed basalts from loihi seamount indicate the importance of basalts to global biogeochemical cycling. Applied and environmental microbiology, 80(16), 4854-4864.

Orcutt, B. N., Sylvan, J. B., Knab, N. J., and Edwards, K. J., 2011, Microbial ecology of the dark ocean above, at, and below the seafloor. *Microbiol. Mol. Biol. Rev.* 75, 361–422.

Orcutt, B. N., Wheat, C.G., Rouxel, O., Hulme, S., Edwards, K. J., and Bach, W., 2013, Oxygen consumption rates in subseafloor basaltic crust derived from a reaction transport model. Nat. Commun. 4, 2539.

Orcutt, B. N., Sylvan, J. B., Rogers, D. R., Delaney, J., Lee, R. W., and Girguis, P. R., 2015, Carbon fixation by basalt-hosted microbial communities. Front. Microbiol. 6, 1–14.

Orphan, V. J., House, C. H., Hinrichs, K. U., McKeegan, K. D., and DeLong, E. F., 2002, Multiple archaeal groups mediate methane oxidation in anoxic cold seep sediments. Proceedings of the National Academy of Sciences, 99(11), 7663-7668.

Parkes, R. J., Cragg, B. A., Bale, S. J., Getlifff, J. M., Goodman, K., Rochelle, P. A., Fry, J. C., Weightman A. J., and Harvey, S. M., 1994, Deep bacterial biosphere in Pacific Ocean sediments. Nature, 371(6496), 410-413.

Pauly, B. D., Schiffman, P., Zierenberg, R., and Clague, D., 2011, Environmental and chemical controls on palagonitization. Geochemistry Geophysics Geosystems (12).

Santelli, C. M., Edgcomb, V. P., Bach, W., and Edwards, K. J., 2009, The diversity and abundance of bacteria inhabiting seafloor lavas positively correlate with rock alteration. Environmental Microbiology Vol 11, Issue 1, 86 – 98.

Santelli, C.M., Orcutt, B.N., Banning, E., Bach, W., Moyer, C.L., Sogin, M.L., Staudigel, H., and Edwards, K.L., 2008, Abundance and diversity of microbial life in ocean crust. Nature 453, 653 – 656.

Schumann G, Manz W, Reitner J, and Lustrino M., 2004, Ancient fungal life in North Pacific eocene oceanic crust. Geomicrobiol. J. 2004; 21: 241–246.

Stroncik, N.A. & Schmincke, H.U., 2002, Palagonite — a review. International Journal of Earth Sciences 91, 680–697.

Takai, K., Nakamura, K., Toki, T., Tsunogai, U., Miyazaki, M., Miyazaki, J., Hirayama, H., Nakagawa, S., Nunoura, T., and Horikoshi, K., 2008, Cell proliferation at 122°C and isotopically heavy CH4 production by a hyperthermophilic methanogen under high-pressure cultivation: National Academy of Sciences Proceedings, v. 105, p. 10949–10954.

Teske A. and Sørensen K. B., 2008, Uncultured archaea in deep marine subsurface sediments: have we caught them all? The ISME J. 2, 3–18.

Thorseth, I. H., Furnes, H., and Heldal, M., 1992, The importance of microbiological activity in the alteration of natural basaltic glass. Geochimica et Cosmochimica Acta 56.2: 845-850.

Tivey, M. K., 2007, Generation of seafloor hydrothermal vent fluids and associated mineral deposits. Oceanography Vol. 20, No. 1.

Toner, B. M., Lesniewski, R. A., Marlow, J. J., Santelli, C. M., Bach, W., Orcutt, B. N., and Edwards, K. J., 2012, Mineralogy drives bacterial biogeography of hydrothermally inactive seafloor sulfide deposits, Geomicrobiology Journal.

Wankel, S. D., Germanovich, L. N., Lilley, M. D., Genc, G., DiPerna, C. J., Bradley, A. S., Olson, E. J., and Girguis, P. R., 2011, Influence of subsurface biosphere on geochemical fluxes from diffuse hydrothermal fluids. Nat. Geosci. 4, 461–468.

Wessel, P., Sandwell, D. T. & Kim, S.-S. ,2010, The global seamount census. Oceanography 23, 24 – 33.

Wheat, C. G.,McManus, J.,Mottl, M. J., and Giambalvo, E., 2003. Oceanic phosphorous imbalance: the magnitude of the ridge-flank hydrothermal sink. Geophys.Res. Lett. 30,OCE5.1– OCE5.4.

White, W. M., and Klein, E. M., 2014, Composition of the Oceanic Crust. Treatise on Geochemistry (Second Edition) 457-492.

Whitman, W. B., Coleman, D. C., and Wiebe, W. J., 1998, Prokaryotes: the unseen majority. Proceedings of the National Academy of Sciences, 95(12), 6578-6583.

2 Palagonitization of basalt glass in the flanks of mid-ocean ridges: implications for the bioenergetics of oceanic intracrustal ecosystems

Andreas Türke[1,*], Kentaro Nakamura[2], Wolfgang Bach[1,3,*]

[1] Department of Geosciences and MARUM, University of Bremen, Klagenfurter Str. GEO, 28357, Bremen, Germany

[2] Department of Systems Innovation, School of Engineering, The University of Tokyo, 7-3-1 Hongo, Bunkyo-ku, Tokyo 113-8656, Japan

[3] Centre of Excellence in Geobiology and the Department of Earth Sciences, Realfagbygget, University of Bergen, Allegaten 41, N-5007 Bergen, Norge

[*] Correspondence authors: atuerke@uni-bremen.de, wbach@uni-bremen.de

2.1 Abstract

When basalt is exposed to oxygenated aqueous solutions, rims of palagonite form along fractures at the expense of glass. We employed electron microprobe and LA-ICP-MS (laser ablation inductively coupled plasma mass spectrometry) analyses of fresh glass and adjacent palagonite crusts to determine the geochemical changes involved in palagonite formation. Samples were retrieved from drill cores taken in the North Pond Area, located on the western flank of the Mid-Atlantic Ridge at 22°45'N and 46°05'W. We also analyzed whole rock powders to determine the overall crust-seawater exchange in a young ridge flank. Radioactive elements are enriched in palagonite relative to fresh glass, reaching concentrations where radiolytic production of molecular hydrogen (H_2) may be a significant energy source. Based on these results, we hypothesize that microbial ecosystems in ridge flank habitats undergo a transition in the principal energy carrier,

fueling carbon fixation from Fe oxidation in very young crust to H_2 consumption in older crust. Unless the H_2 is swept away by rapid fluid flow (i.e., in young flanks), it may easily accumulate to levels high enough to support chemolithoautotrophic life. In older flanks, crustal sealing and sediment accumulation have slowed down seawater circulation, and the significance of radiolytically produced H_2 for catalytic energy supply is expected to increase greatly. Similar habitats on other planetary surfaces are theoretically possible, as accumulation of radiolytically produced hydrogen merely requires the presence of H_2O molecules and a porous medium, from which the hydrogen is not lost.

Key words: Palagonite, microbial glass alteration, ridge flanks, abiotic hydrogen production, chemolithoautotrophy

2.2 Introduction

Interaction of fresh volcanic rock and seawater theoretically provides energy to sustain microbial life (Amend et al., 2011). At mid-ocean ridges, volcanic rocks are constantly formed and exposed to seawater, thus representing an environment energetically favorable to sustaining a subseafloor biosphere. The interaction of water and rock causes redox disequilibria, and the associated Gibbs energy can be utilized as metabolic energy gain by chemolithoautotrophic microorganisms. Most of the seawater circulation takes place in ridge flanks, where temperatures are low and the rates of water-rock reaction are sluggish, allowing chemolithoautotrophs to harness the redox energy. An initial appraisal of the potential size of biomass living in these ridge flanks suggests that the cell numbers may resemble those in the sedimentary deep biosphere (Bach and Edwards, 2003). Chemolithoautotrophy is of particular interest to astrobiologists, because it is thought to be the metabolic pathway of the first, and most primitive, organisms on Earth (Lane et al., 2010). Moreover, submarine habitats, such as ridge flanks, provide a large source of water (the overlying ocean) at temperatures < 120°C, a source of constantly forming fresh rocks (mid-ocean ridges) as well as protection from solar radiation, such that chemolithoautotrophic microorganisms can thrive.

Alteration textures have been reported from a variety of modern glassy subseafloor basalt (the volcanic rock type formed at most mid-ocean ridges) (e.g., Banerjee et al., 2010; Cockell et al.,

2010; Fisk et al., 2003; Heberling et al., 2010; Fliegel et al., 2012) and have been interpreted as microbial borings into fresh basalt glass. Similar textures in ancient rocks suggest that endolithic microbes may have lived in subseafloor as early as 3.22 – 3.48 Ga (Furnes et al., 2004). However, the biogenicity of ancient samples has been questioned recently (Grosch and McLoughlin, 2014). Experiments with microbes have yet to produce comparable biosignatures in volcanic glass, so their biotic origin remains unproven to date. Nevertheless, the presence of microbial life in basaltic crust is undoubted (Santelli et al., 2008; Einen et al., 2008), even though their role in rock alteration has not been revealed yet.

Oceanic subsurface habitats span a variety of physical and chemical conditions, based on rock type, fluid throughput, and temperature. Thermodynamic computations have been used to identify viable catabolic reactions and estimate the size of the biomass supported by redox equilibria between hot hydrothermal vent fluids and seawater (McCollom & Shock, 1997; Amend et al., 2011). Basalt-hosted systems offer maximal potential for sulfide oxidation and to a lesser extent iron and methane oxidation (Amend et al., 2011). These models are based on measured vent fluid compositions and assess reactions of dissolved aqueous species. Reduced elements (Fe, Mn, S) in rocks and minerals are an additional source of energy, and these substrates are colonized by specifically adapted microorganisms (e.g., Einen et al., 2008; Santelli et al., 2008). These solids, in theory, can release similar amounts of energy as hydrothermal venting (McCollom, 2000; Bach and Edwards, 2003). Microorganisms select specific solid phases in seafloor settings, indicating a prominent mineralogical control on the community composition of the attached microorganism (e.g., Toner et al., 2012). Energetics may be one of the master variables in causing this selectivity. The community compositions change rapidly as the seafloor ages and the mineralogical composition of rocks evolves (Santelli et al., 2009).

The aging of ocean crust occurs along with changes to its hydrological state – from open circulation of oxygenated seawater in young crust to closed-system or even ceased circulation in older crust (e.g., Fisher and Wheat, 2010). How this crustal ageing affects the energetic landscape for subcrustal chemolithoautotrophic microorganisms has only been addressed for the Juan de Fuca Ridge.

In this communication, we focus on the potential for metabolic energy gain in aging off-axis settings, where hydrothermal circulation at low temperatures (< 25°C) is limited to outcrop-to-outcrop flow, and eventually exchange between ocean and subseafloor fluids is negated (Figure 1).

The conceptual model treats the upper igneous crust as an aquifer "sealed" by low permeability sediments, such that exchange with seawater only occurs at seamounts (Harris et al., 2004; Anderson et al., 2012). The seafloor is decorated with 10^6 – 10^7 seamounts of elevations >100 m (Wessel et al., 2010), acting as "breathing holes" that sustain seawater circulation within the crust. Estimations suggest that roughly 2×10^{16} kg of seawater circulate through oceanic crust per year, which is equivalent to the yearly discharge of global river systems into oceans (e.g., Wheat et al., 2003). Within the upper igneous crust, pillows, breccia, and fault zones are usually most altered, implying that these lithologies represent areas of highest fluid throughput (Alt, 2004). Pillows and breccia in ridge flanks are the largest reservoir of basalt glass on Earth. The glass is thermodynamically unstable and is altered to palagonite when exposed to seawater (e.g., Stroncik and Schmincke, 2001).

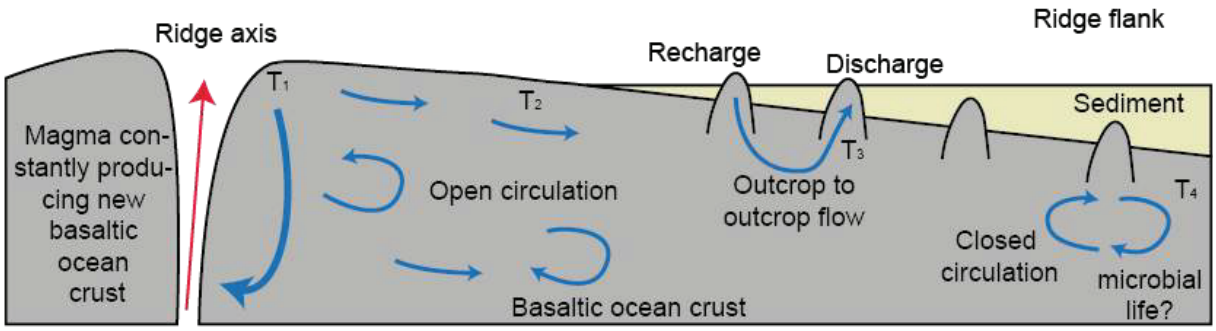

FIG. 1. Sketch illustrating changes in fluid circulation through oceanic crust with increasing age (T_1/T_4). Young ocean crust (T_1 and T_2) is characterized by open circulation and short fluid residence times. As sediments start to accumulate, outcrop-to-outcrop fluid flow dominates (T_3). Eventually, impermeable sediments seal the igneous oceanic crust, and exchange between ocean and the basaltic aquifer is inhibited (T_4).

This communication discusses possible bioenergetical implications of the aging of ocean crust for ridge flank habitats. Based on chemical compositions of glass, palagonite rims, and whole rock samples, we assess changes in composition and redox state of iron, and discuss how palagonitization may influence the bioenergetics landscape in ridge flanks and its implication for habitability of extraterrestrial subsurfaces.

2.3 Material and Methods

2.3.1 Sample material and geological setting

North Pond (Figure 2) is a sediment pond structure of 8 x 15 km located on the western flank of the Mid-Atlantic Ridge at 22°45'N, 46°05'W in about 4450 m water depth surrounded by steep rift mountains rising with elevations of 1 to 2 km. Heat flow measurements suggest significant fluid flow, below the up to 270 m thick sediments, with seawater circulating from the SW part to the NNE part (Langseth et al., 1992). North Pond is an area of low temperature of ~ 2 - 15 °C, high fluid flux (Becker et al., 2001), and hence overall high water-to-rock ratios. Sediment thickness decreases from the center towards the edges of the pond, where oxygen profiles indicate that basement fluids are oxygenated (Ziebis et al., 2012). Orcutt et al. (2013) proposed that a south-to-north decline in the oxygen concentrations of the basal pore waters is due to microbial respiration of oxygen by microorganisms inhabiting the basaltic aquifer underlying North Pond.

We analyzed the geochemical composition of a set of four thin sections (with fresh glass and adjacent palagonite) and 59 whole rock powder samples, from the North Pond Area. They were drilled during Integrated Ocean Drilling Program (IODP) Expedition 336, dedicated to investigating ridge flank microbiology (Edwards et al., 2012). Samples are from two cores (U1382A and U1383C). Hole U1382A recovered 32 m of core between 110 and 210 meters below sea-floor (mbsf). Numerous volcanic flow units with distinct geochemical and petrographic characteristics and a sedimentary breccia containing clasts of basalt, gabbroic rocks, and mantle peridotite were recovered. Drilling in Hole U1383C retrieved 50.3 m of core from between 69.5 and 331.5 mbsf. Three volcanic units were identified, of which the top and bottom one consist of aphyric basalts with abundant glassy rinds. Rocks from both holes are fresh to moderately altered. Secondary phases are palagonite as well as clay minerals (saponite, nontronite, and celadonite), Fe oxyhydroxide, carbonate, and zeolites (Edwards et al., 2012).

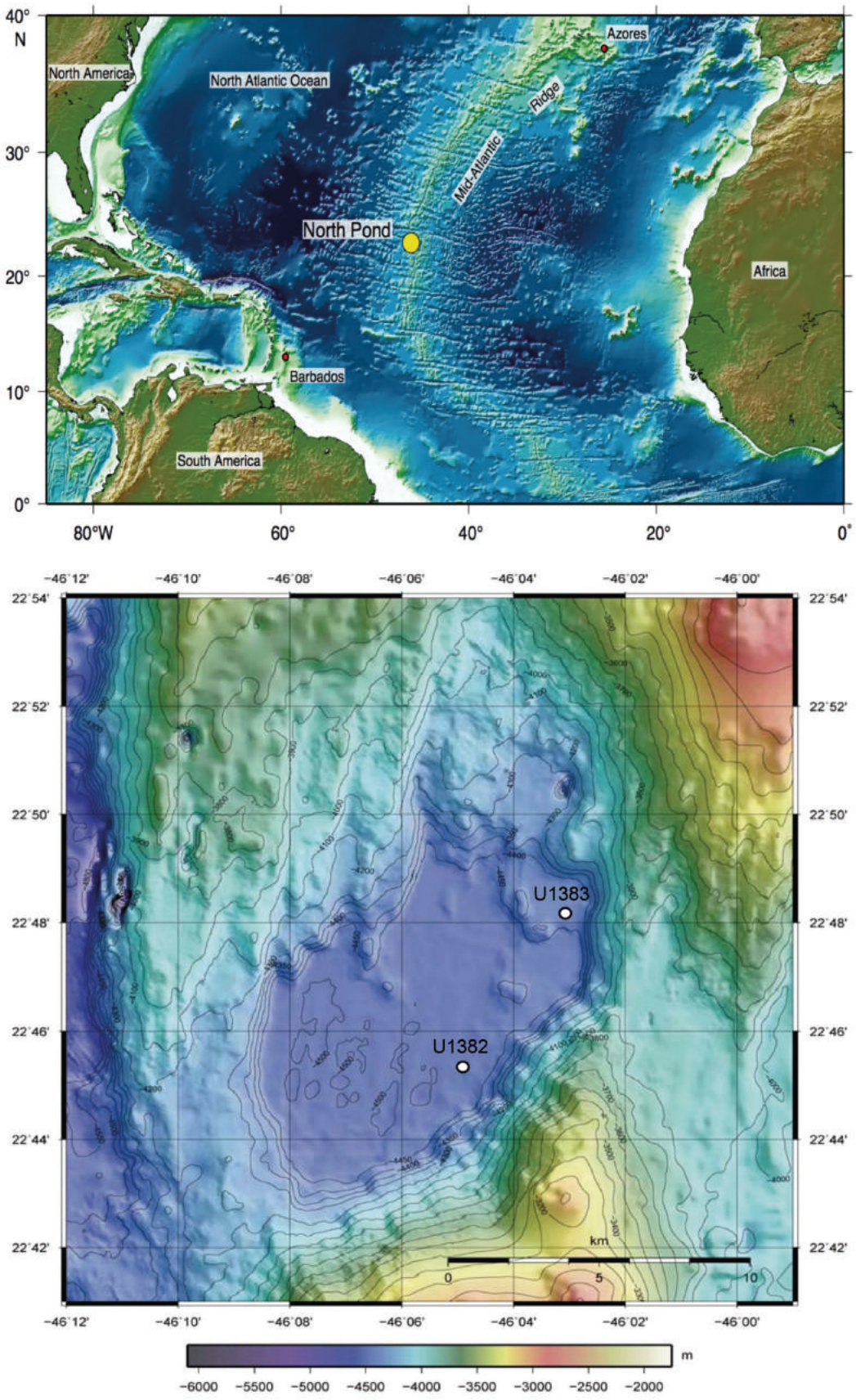

FIG. 2. Map showing the location of North Pond at 22°45'N, 46°05'W in about 4450 m water depth at the western flank of the Mid-Atlantic Ridge. Modified after Edwards et al. (2012).

2.3.2 Analytical Methods

2.3.2.1 Whole rock analyses

Whole rock geochemical composition for 59 samples from different depths in Holes U1382A and U1383C. Major element concentrations were determined by x-ray Fluorescence (XRF) at the University of Tokyo. Trace element concentrations of the whole rock powders were determined by a ThermoScientific Element 2, ICP-MS at the University of Bremen, Germany, following HF-HCl-HNO_3 acid digestion. Relative external precision of these analyses can be assumed as 1 – 5 % for major elements, and 5 – 10 % for trace elements.

In addition to total Fe contents (determined by XRF), FeO concentrations were measured by manganometric titration (Querol, 1952) at the GeoForschungsZentrum Potsdam. From the difference between the actual FeO (by titration) and FeO,total (by XRF), the abundance of Fe_2O_3 can be calculated as follows:

$$Fe_2O_3 = (FeO,total - FeO) \times 1.11134.$$

The extent of Fe oxidation ($Fe(III)/Fe_{(tot)}$) can then be expressed as $Fe_2O_3/FeO,total$.

Grain densities of powdered whole rock samples were determined by using ~ 1 g of sample and a 25 ml pycnometer with heptane as liquid phase.

2.3.2.2 Thin section microanalytical techniques

Thin sections of four samples were analyzed to determine the enrichments of radioactive elements (K, Th, and U) in palagonites relative to the composition of the fresh glass precursor. Spot measurements for major element contents were carried out along traverses spanning from altered palagonite rims into fresh glass, using a Jeol JXA 8900R electron probe microanalyzer (EPMA) at the University of Kiel. The instrument was operated with an acceleration voltage of 15 kV, a probe current of ~ 20 nA, and a defocussed electron beam with an elliptical spot of 5 µm in diameter.

Trace element contents were determined with a ThermoScientific Element 2 ICP-MS coupled to a NewWave UP193ss laser ablation system at the Geosciences Department, University of Bremen.

Both standards and thin section samples were ablated with an irradiance of ~ 1 GW/cm². Beam diameter was set to 75 µm for spot measurements. Pulse rate was 5 Hz for alteration minerals and 10 Hz for basalt glass. Helium (0.7 L/min) was used as the carrier gas and argon (0.9 L/min) was added as the make-up gas. External calibration standard was NIST612 using a composition according to Jochum et al. (2011). Areas of fresh glass and palagonite previously measured by EPMA were selected for LA-ICPMS analyses. Silicon was used as the internal standard, and Si concentration previously established by EPMA were used in computing concentrations with the Cetac GeoPro™ software. Analytical precision and accuracy were checked regularly by analyzing the SRM BCR2-G (basaltic glass; Jochum et al. 2005) and NIST612 reference materials.

2.3.3 Hydrogen yield calculations

Radiolysis of water refers to the process of dissociation of water molecules by alpha, beta, and gamma radiation, released by decaying radioactive elements. In natural water-rock systems, U, Th, and K are the dominant sources of radioactivity. Radiation ionizes water molecules and short-lived reactive species, such as aqueous electrons, protons, as well as hydrogen and hydroxyl radicals that are formed as primary products of radiolysis (Draganic & Draganic, 1971; LaVerne & Tandon, 2002; Gales et al., 2004). The subsequent reactions then form molecular hydrogen.

Hydrogen yields by radiolysis of water were calculated based on protocols utilized by Lin et al. (2005) and Blair et al. (2007). Hydrogen production $P_{H2,rock}$ of a rock, due to alpha, beta and gamma radiation can be calculated with equation 1:

$$P_{H2,rock} = (G_{H2,\alpha}(D_{\alpha,^{238}U} + D_{\alpha,^{235}U} + D_{\alpha,^{232}Th})) + (G_{H2,\beta}(D_{\beta,^{238}U} + D_{\beta,^{235}U} + D_{\beta,^{232}Th} + D_{\beta,^{40}K})) + (G_{H2,\gamma}(D_{\gamma,^{238}U} + D_{\gamma,^{235}U} + D_{\gamma,^{232}Th} + D_{\gamma,^{40}K}))$$

(1)

with $G_{H2,i}$ as radiation chemical yield for each radiation type, and D_i the radiation doses. Values for $G_{H2,\alpha} = 1.57 \times 10^4$ H_2 molecules/MeV, $G_{H2,\beta} = 5.3 \times 10^3$ H_2 molecules/MeV and $G_{H2,\gamma} = 4.5 \times 10^3$ H_2 molecules/MeV, were taken from the work of Spinks and Wood (1990), respectively.

Radiation doses D_i can be calculated based on activity A_i, decay energy sums ΣE_i of the respective decay series, grain density ρ_r and S_i the relative stopping power ratios of alpha and beta particles or gamma radiation, respectively:

$$D_\alpha = (\rho_r/(1/(1-\Phi) + 1/(S_\alpha\Phi)) (A_{238U}\,\Sigma E_{\alpha,238U} + A_{235U}\,\Sigma E_{\alpha,235U} + A_{232Th}\,\Sigma E_{\alpha,232Th}) \quad (2)$$

$$D_\beta = (\rho_r/(1/(1-\Phi) + 1/(S_\beta\Phi)) (A_{238U}\,\Sigma E_{\beta,238U} + A_{235U}\,\Sigma E_{\beta,235U} + A_{232Th}\,\Sigma E_{\beta,232Th} + A_{40K}\,\Sigma E_{\beta,40K}) \quad (3)$$

$$D_\gamma = (\rho_r/(1/(1-\Phi) + 1/(S_\gamma\Phi)) (A_{238U}\,\Sigma E_{\gamma,238U} + A_{235U}\,\Sigma E_{\gamma,235U} + A_{232Th}\,\Sigma E_{\gamma,232Th} + A_{40K}\,\Sigma E_{\gamma,40K}) \quad (4)$$

Decay energy sums ΣE_i were calculated from the World Wide Web Table of Radioactive Isotopes (Ekström & Firestone, 1999). Relative stopping power ratios were assumed as $S_\alpha = 1.5$, $S_\beta = 1.25$ and $S_\gamma = 1.14$ (Aitken, 1995). A summarizing table of factors relevant for hydrogen yield calculations is attached as supplementary material.

2.3.4 Thermodynamic computation of hydrogen production during palagonitization

Besides radiolytic production, hydrogen may also be produced by water-rock reactions, when ferrous iron in the basalt is oxidized by water:

$$2FeO + H_2O \Rightarrow Fe_2O_3 + H_2(aq).$$

in glass in seawater in palagonite

This process may produce abundant hydrogen in ultramafic rocks (Mayhem et al., 2013) and, to much lesser extents, in basalts (e.g., Stevens and McKinley, 1998). We therefore compare (in section 4.4) the amounts of hydrogen produced from oxidation of basalt glass by water (all other oxidants were suppressed to maximize the model's hydrogen yields) with those expected to form by radiolysis. We employed a standard thermodynamic-kinetic reaction path model to compute the amount of hydrogen produced by reactions between basalt glass and seawater, assuming a water-to-rock ratio of 10. The calculations were conducted for a temperature of 10 °C, expected for the upper basement at North Pond. Geochemist's Workbench (Bethke, 1996) and a 250 bar thermodynamic database compiled from SUPCRT92 (Boettger et al., 2013) were employed. Included in the database was mid-ocean ridge basalt glass as a phase, for which thermodynamic properties were calculated with a polyhedral approach (cf. Oelkers and Gislasson, 2001). Also included were the secondary Fe(III) phases, such as Fe-Al celadonite and goethite (Wolery, 2004). We assume that basalt glass dissolution is the rate-limiting step in the production of hydrogen and estimated a 10 °C dissolution rate of 10^{-16} mol m^{-2} sec^{-1} from 25 °C rates of 10^{-15} mol cm^{-2} sec^{-1} in

Oelkers (2001) and rates of 10^{-7} mol cm^{-2} sec^{-1} at 90 °C (Daux et al., 1997). A specific surface area of 1m^2 g^{-1} was assumed for the basalt glass.

2.4 Results

2.4.1 Microanalytical data

We found that palagonite rims show very significant enrichments in both K_2O (enriched by a factor of up to 49) and U (up to 15), but also slight enrichment in Th (up to 3), compared to the precursor glass composition. These enrichments were found in all palagonite rims analyzed. The profiles did not show differences in enrichment along the traverses (see Figure 3, Figure 4 and supplementary data).

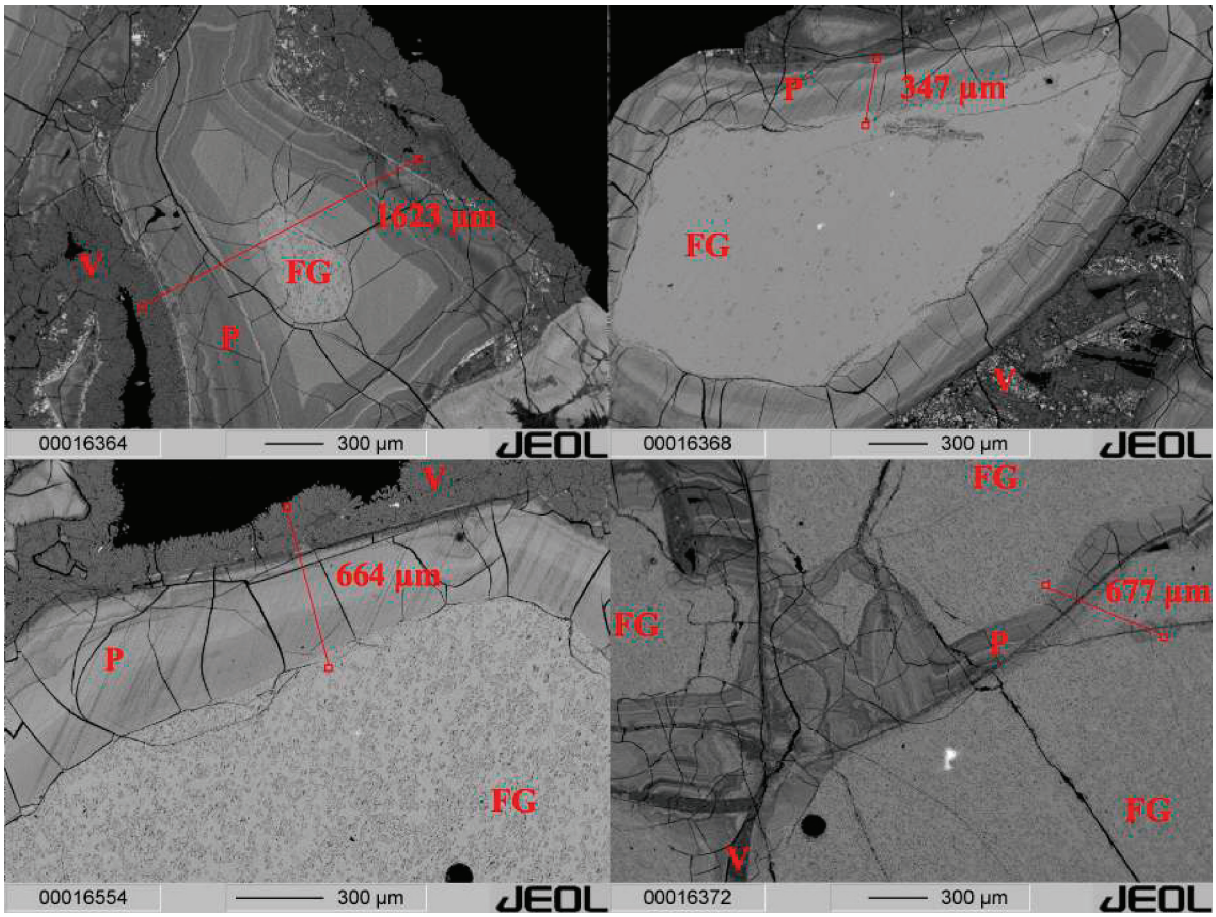

FIG. 3. Four backscattered electron images of spots analyzed by electron microprobe. Point measurements were carried out with approximately 10 µm spacing along indicated lines, covering both palagonite (P) and fresh glass (FG). Secondary vein-filling minerals (V) are also visible.

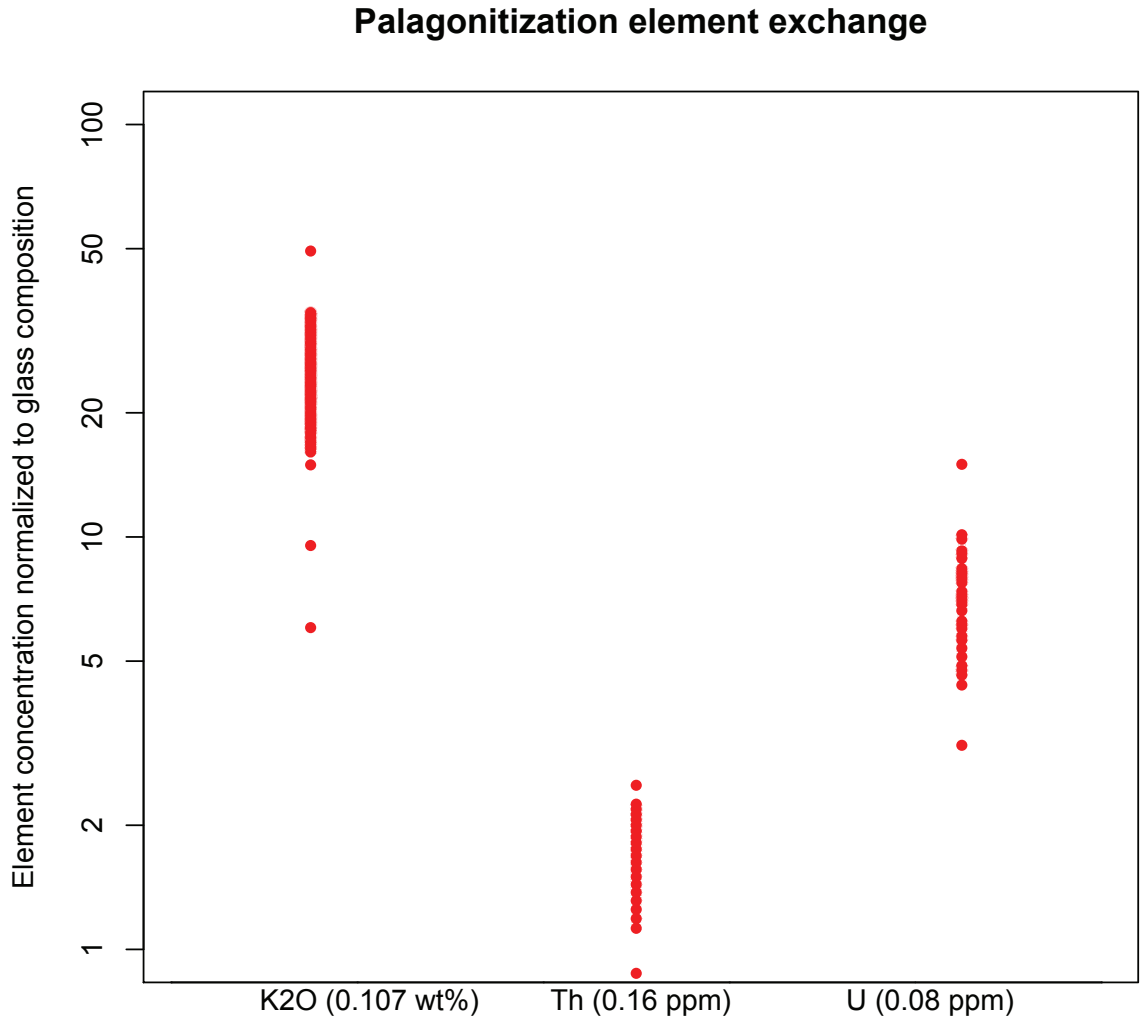

FIG. 4. Element exchange involved in palagonitization. All elements are normalized to fresh glass composition, which is given in the abscissa. Palagonite rims show significant enrichment in radioactive elements.

2.4.2 Whole rock compositions

The results of the whole rock analyses show a strong enrichment of U in rocks with increased Fe(III)/$Fe_{(tot)}$ ratios (Figure 5). U contents in least altered rocks (Fe(III)/$Fe_{(tot)}$ < 0.4) are generally around 0.1 ppm, whereas samples with Fe(III)/$Fe_{(tot)}$ > 0.6 have between 0.2 – 1 ppm of U. We could not observe any systematic down-section trends in core from either hole. Rather, alteration is highly

non-uniform, with fresh interiors of lava flows intercalating with extensively altered rocks. These most intensely altered zones are the most oxidized and enriched in U.

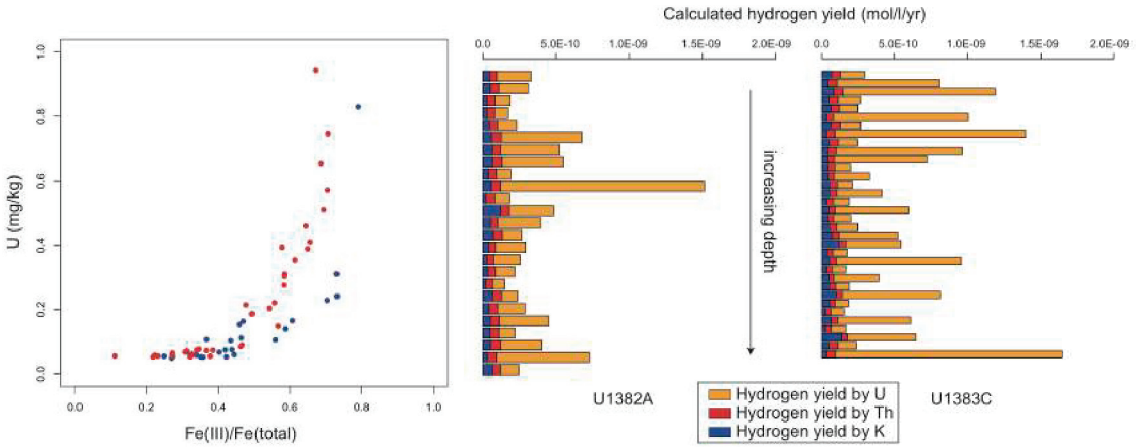

FIG. 5. Left: Uptake of U with increasing Fe-oxidation state in whole rock composition. Samples from U1382A in red and U1383C in blue. Right: Calculated hydrogen yields in mol/L/yr. Bars are structures to indicate individual contribution of U, Th, and K.

2.4.3 Hydrogen production by radiolysis

From the measured concentrations of U, Th, and K, radiolytic hydrogen yields in palagonite were calculated, ranging between 4.65 x 10^{-15} and 1.73 x 10^{-13} mol yr^{-1} cm^{-3} and averaging at 2.26 x 10^{-14} mol yr^{-1} cm^{-3} (Figure 5). Uranium is the main provider of radiolytically produced H_2, contributing between 46 and 94% of the expected hydrogen production (Figure 5). The hydrogen production rates in palagonite were converted to hydrogen accumulation rates in the rocks' intergranular water by using the measured porosities, which range between 2.2 and 16.6% (IODP LIMS database). The accumulation rates that were estimated that way range between 0.15 and 1.65 nM yr^{-1} (average 0.45 nM yr^{-1}).

2.4.4 Comparison between the amounts of hydrogen expected from radiolysis versus water-rock reactions

We now assess the role of radiolysis as a source of hydrogen in relation to the other main source of hydrogen (water-rock reaction). In a kinetic reaction path model, basalt glass was turned

into palagonite at a rate of 10^{-16} mol cm^{-2} s^{-1}. Only water was allowed as an oxidant to maximize non-radiolytic hydrogen yields. We assumed that there is no loss of rock mass from the system and that the basalt glass dissolving will be turned into palagonite with the average U, Th, and K contents established for palagonite in this study. The palagonite formed will hence produce radiolytic hydrogen at a rate of 2×10^{-14} mol cm^{-3} yr^{-1} (cf. 4.3.). The model results are depicted in Figure 6. For the first million years of closed-system water-rock evolution (at a water-to-rock ratio of 10), radiolytic hydrogen yields are expected to outcompete those from the reduction of water (Figure 6). The closed-system assumption is a necessity of the comparative model calculation. In reality, the computed levels of hydrogen will be diluted by the recharge of seawater taking place in the system (section 5.1), but the relative contributions from both sources will not be affected by this dilution. The model results indicate that radiolytic hydrogen is expected to be more important than hydrogen coming off water-basalt reactions for the North Pond system. It is important to note that the calculated hydrogen yields from water-rock reactions are absolute maximum estimates, as in reality oxidants other than water (foremost: O_2,aq) will oxidize Fe(II) released by dissolution of basalt glass.

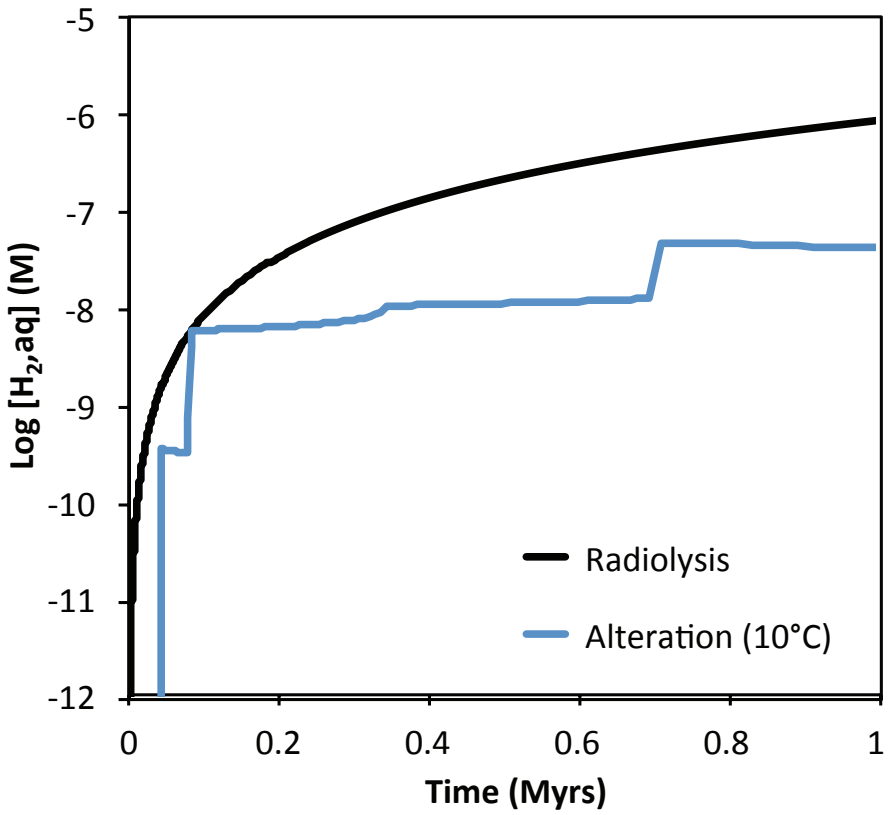

FIG. 6. Kinetic reaction path model for hydrogen production via radiolysis and reduction of water at 10 °C. At low temperatures, radiolytic hydrogen production is expected to be more important than hydrogen coming off water-basalt reaction.

2.5 Discussion

2.5.1 Accumulation of H_2 in the ridge flank at North Pond

The North Pond Area is a rather young ridge flank (8 Ma) with open fluid circulation beneath a sediment pond. We have established that the glassy flow margins are most intensely altered (palagonitized and more oxidized) and enriched in U and K. This relationship likely results from extensive oxidative alteration in discrete zones, probably along the contacts of different lava flow units, where seawater flow was channelized. Wire-line borehole logging data indicate that circulation of seawater is focused in discrete subseafloor aquifers, which likely correspond to glassy contacts of major flow units and breccia (Becker et al., 2001). Moreover, formation microscanner data (Edwards et al., 2012) indicate that these partly palagonitized glassy zones are the most fractured. The void space in these fractured and highly altered zones is filled with seawater, which would facilitate ongoing oxidative alteration and extant microbial activity. Ingress of oxygenated seawater into these permeable zones causes replacement of basalt glass with <20% ferric iron (i.e., $Fe(III)/Fe_{tot}$ <0.2) by ferric iron-rich palagonites ($Fe(III)/Fe_{tot}$ up to >0.8; Donnelly et al., 1977).

What we can learn about the hydrology and water-rock reaction at North Pond may be applicable to many young ridge flanks in areas that are sparsely sedimented. A compilation of geochemical data from drill core indicates that ferrous iron is actively oxidized in crust up to about 10 Myrs old (Bach and Edwards, 2003). Based on this observation, and supported by thermodynamic calculation, these authors deduced that Fe-oxidizing metabolisms may support a large fraction of the primary biomass production in young ridge flanks. In very young ridge flank crust, close to the spreading center, conditions are probably ideal for Fe-oxidizing bacteria, because a lot of fractured glass is exposed to oxygenated seawater. However, as the crust ages, permeability goes down, and palagonite rinds overgrow previously exposed glass surfaces. These processes will slow down oxidation and make it more difficult for colonizing microorganisms to gain access to the fresh glass. The palagonite rinds, however, contain high concentrations of the radioactive elements,

in particular U and K. These elements are located in water-logged sections of the rock, as palagonite only forms around fractures and voids. Palagonite contains large contents of molecular water (14 – 38 wt% H_2O; Pauly et al., 2011), and radiolysis of water can therefore occur within the palagonite rind and away from the interface with liquid water (Gournis et al., 2000; Allard & Calas, 2009). Will this radiolytic hydrogen production within these palagonite rinds be sufficient to support microbial life in altered crust?

We have shown (in section 4.3.) that the annual accumulation of radiolytically produced hydrogen may be on the order of nanomoles per liter of water in the permeable basement. Known hydrogenotrophic microorganisms require threshold hydrogen concentrations in sediment pore waters that depend on the terminal electron acceptor: Fe-oxyhydroxide (0.1 – 0.8 nM), sulfate (1 – 15 nM), and methane (5 – 95 nM) (Löffler et al., 1999). Habitat temperature and physiological state of the microbial community (e.g., growth versus maintenance) also influence the minimum $H_2(aq)$ concentrations required for hydrogenotrophy (Hoehler, 2004). At the low temperatures prevailing in the upper basement at North Pond (<20°C, Becker et 2001), $H_2(aq)$ concentrations on the order of tens of nanomoles per kilogram are expected to provide sufficient energy for maintenance of iron and sulfate reducers. Hence, if the intergranular fluids at North Pond were stagnant, several years of accumulation time could be enough to reach these threshold values for hydrogenotrophs. Vigorous circulation of seawater, however, would prevent the accumulation of radiolytic hydrogen to contents critical for hydrogenotrophic life. For young oceanic crust, such as the eastern Juan de Fuca Ridge flank, fluid residence times of only several thousands of years were estimated (Elderfield et al., 1999). Likewise, heat flow data suggest fast lateral flow of seawater within the basement at North Pond, on the order of 2-3 m yr^{-1} if a well-mixed basement aquifer is assumed (Langseth et al., 1992). Even faster flow velocities would be implied, if lateral flow were channelized in discrete aquifers (Fisher and Becker, 2000), such as those identified by wire-line borehole logging in the North Pond basement (Becker et al., 2001). Can radiolytic hydrogen in such an environment accumulate to levels sufficient to support hydrogenotrophic life?

To address this question, we calculated the water flux (F) required to transport a certain amount of heat (Q) for different extents of heating (ΔT) of the circulating seawater with a heat capacity (C_p) of 4 J g^{-1} K^{-1}, according to $F = Q / (C_p \Delta T)$. The amount of heat (Q) transported by circulating seawater can be calculated from the difference between the total heat flow predicted from cooling of the lithospheric plate (180 mW m^{-2} for 8 Ma old lithosphere at North Pond; Langseth et al., 1992)

and the measured conductive heat flow. Measure conductive heat flow at North Pond varies between 10 mW m^{-2} in the southeastern part and >100 mW m^{-2} in the northwest (Langseth et al., 1992). For the entire North Pond area, conductive heat flow averages <80 mW m^{-2}. Hence, heat flow is reduced by >100 mW m^{-2} relative to the predicted heat flow. Assuming that removal of this amount of heat is due to seawater circulation, we calculate a heat deficit of roughly 10 megawatts (MW) for the 8 x 15 km North Pond area. With Q fixed, the water flux is simply a measure of the amount of heating of the seawater circulating underneath the North Pond sediments. The relation between ΔT and F corresponding to Q=10 TW is depicted in Figure 7. Langseth et al. (1992) estimated that about 7.5 billion Liters of seawater flow annually through the basement at North Pond. This flux would correspond to a temperature anomaly (ΔT) of 10 °C (Figure 7).

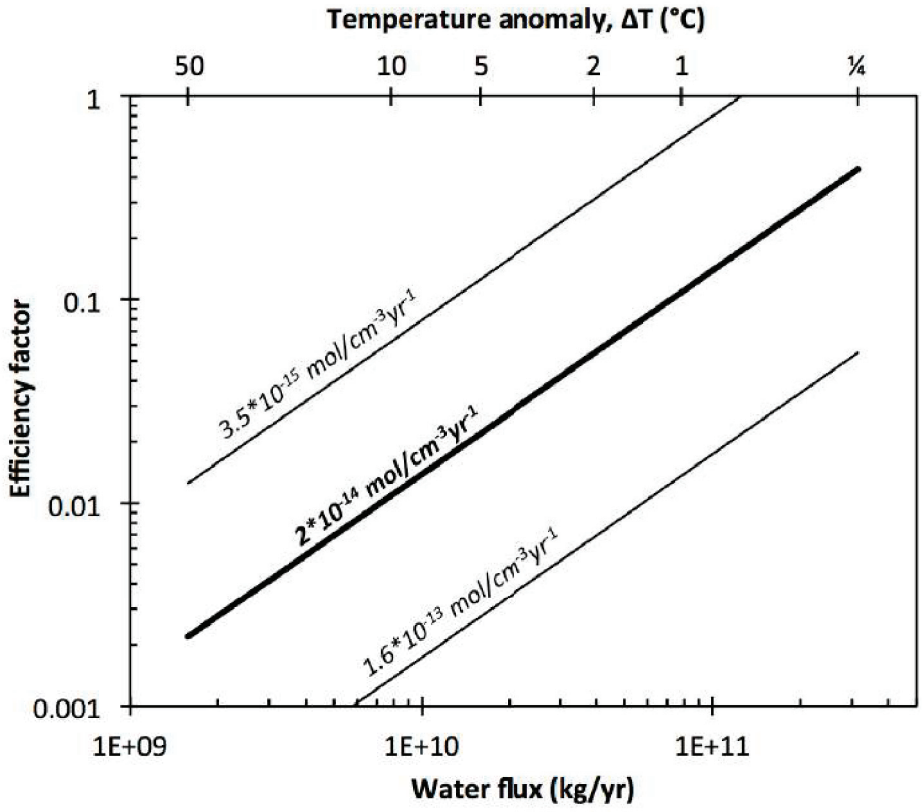

FIG. 7. Yield efficiency of radiolytic hydrogen production versus water flux (and temperature anomaly) corresponding to 10 MW of advective heat transport. The bold line represents the efficiency required to yield 1 nmol H_2/kg of water given the average radiolytic hydrogen production of altered rock. The thin lines represent the equivalent numbers for the maximum and minimum H_2 yields determined for basalt from North Pond basement.

We next compare this water flux estimate with the expected hydrogen accumulation in the North Pond system. An average H_2 production of 2×10^{-14} mol cm^{-3} yr^{-1} in the upper 300 m of basement at North Pond would yield 720 moles of H_2 yr^{-1}. Based on the range of U, K, Th contents, minimum and maximum hydrogen production of 126 and 5760 moles per year can be calculated. When these numbers are divided by the proposed water flux of 7.5×10^9 kg yr^{-1}, H_2(aq) concentrations between 17 and 770 nM (average of 96 nM) can be estimated. Theses numbers compare favorably with the minimum required H_2(aq) concentrations for hydrogenotrophy. However, in the calculation of the hydrogen yields a highly favorable geometry is assumed, which allows efficient production of hydrogen by radiolysis (cf. Blair et al., 2007). The actual produced amount of hydrogen is much smaller in a fractured rock, where the site of radioactive decay relative to the availability of water molecules may not be conducive to radiolysis in many instances. Hence, the efficiency factor (i.e., the ratio of calculated over actual hydrogen production for radiolysis in basalt) is <1 because not all alpha particles will interact with water to cause radiolysis. Both the recharge rate of seawater and the efficiency factor will therefore determine whether or not hydrogen levels sufficient for sustaining hydrogenotrophic life may arise in a ridge flank setting. The relation between the efficiency factor and flow rate required to yield a threshold H_2(aq) concentration of 1 nM are plotted in Figure 7. Given the flow rates estimated by Langseth et al. (1992) and using average contents of U, K, and Th, an efficiency factor of only 0.01 (i.e., 1% efficiency) is sufficient to have 1 nM H_2(aq) (i.e., the approximate threshold concentration for hydrogenotrophy) in aquifer seawater. The heat flow studies provide a minimum estimate of water flow, and more water flow would dilute the dihydrogen produced. The computed numbers may hence represent maximum estimates of the concentrations of radiolytic H_2 in the aquifers underneath North Pond. Nonetheless, our calculation results lend strong support to the concept that hydrogenotrophic life is energetically feasible in ridge flank settings, in particular in those with slow fluid flow and highly altered basement.

2.5.2 Transition in energetic landscapes from Fe-oxidation to hydrogenotrophy in ridge flanks and its implication for astrobiology

We hypothesize that there may be a shift in bioenergetic landscape in ageing ridge flank systems from ferrous iron- towards hydrogen-based dominance (Figure 8). In very young ridge flank

crust, there is plenty of fresh glass and ferrous silicates available to support Fe-oxidizing microorganisms. Palagonitization has not yet advanced far enough, so neither is there much U and K enrichment leading to increased radiolytic hydrogen production nor do the palagonite rinds inhibit microbial attack of the fresh glass. As the palagonite rind thickness builds up in the aging crust, the amount of radiolysis increases, while access to fresh glass is limited. Net oxidation of the basaltic basement ceases, as interfaces between fresh glass and seawater are no longer available; hence, Fe-oxidation may no longer be a significant energy source. Instead, dihydrogen accumulation is facilitated in aged crust, due to both the enrichment of U and K in alteration products such as palagonite and the reduced crustal permeability that leads to less vigorous circulation of seawater and, therefore, less dilution of the radiolytic hydrogen. Our estimations of radiolytic hydrogen yield in aging ridge flanks suggest that even hydrologically inactive parts of the subseafloor may not be energy-starved, possibly extending the range of habitable areas on Earth.

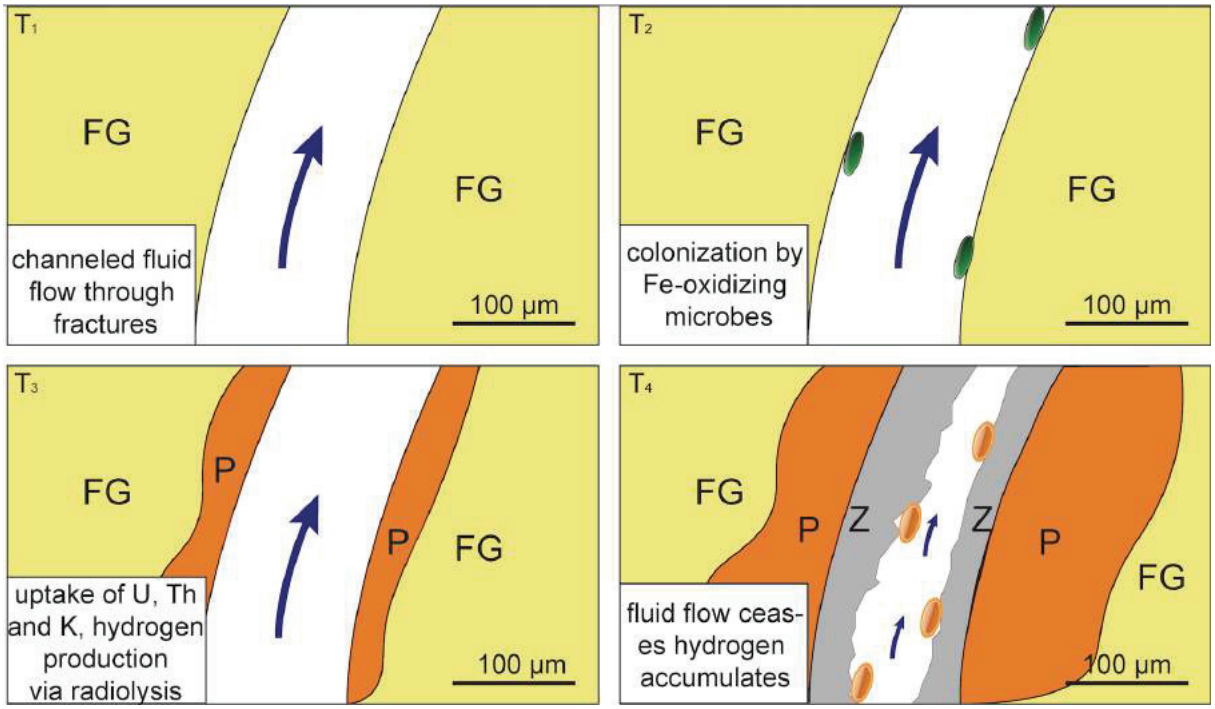

FIG. 8. Conceptual model as hypothesis for a change in bioenergetical conditions in aging ridge flank systems. T_1: Only fresh glass (FG) in hyaloclastite samples, with available Fe(II). T_2: Microbial colonization and initiation of tubular boring textures. T_3: Sluggish palagonitization (P) begins, resulting in uptake of U, Th, and K and increased Fe-oxidation state. Fe(II) is no longer readily available. Microbes might disappear. T_4: Minerals (Z) precipitate and fill veins, ceasing fluid flow and hydrogen produced by radiolysis could initiate re-colonization (by a different type of microbe?) and a change in microbial metabolism towards hydrogen consumption.

Basaltic environments exist beyond our planet, and alteration conditions on Mars may have been akin to seafloor environments on Earth (Grosch et al., 2014). Basalts appear to be the dominant rock type on the martian surface (Singer and McSween, 1993). While the presence of palagonite on Mars or other extraterrestrial planetary surfaces remains uncertain, palagonite is typically seen as a martian dust analogue (Merikallio et al., 2013; Warner and Farmer, 2010). It should be noted that radiolytic hydrogen production is not limited to palagonite. Radiolysis of water merely requires (1) presence of H_2O molecules (not necessarily in liquid form), (2) radioactive decay and (3) a trapping mechanism (e.g. closed fluid circulation due to impermeable sediment coverage) that prevents exchange with an atmosphere with lower concentration in molecular hydrogen, so that molecular hydrogen can accumulate and, in theory, support microbial life.

There is evidence for (1) groundwater upwelling in martian rocks exhumed from deep basins, large craters, and subsurface alteration of ancient basaltic lavas (Michalski et al., 2013, Ehlmann et al., 2013), as indicated by the presence of Mg and Fe bearing clays, which are hydrated alteration minerals typically formed in aqueous settings. Bulk Mars composition (K 76.5 – 920 ppm, Th 56 – 125 ppb, U 16 – 35 ppb) suggests that (2) radioactive decay might even be – on average – more prominent than on Earth (K 550 ppm, Th 29 ppb, U 7.4 ppb) (Wänke and Dreibus, 1994; Morgan and Anders, 1979; Lodders and Fegley, 1997). It remains an open question as to whether (3) a trapping mechanism similar to marine deep-sea sediments exists, or ever existed, on Mars that would allow for accumulation of significant H_2 concentrations that could potentially support hydrogenetrophy.

2.6 Summary and outlook

We have estimated hydrogen yield from radiolysis based on physical rock parameters and U, Th, and K concentrations in the upper igneous crust at the North Pond Area. Results of EPMA and LA-ICP-MS analyses suggest that palagonite rims are the main host of these radioactive elements. As palagonite rims form around fresh glass, access to ferrous iron in basalts is inhibited. Hence, the importance of iron oxidation for microbial metabolism likely decreases, and we hypothesize that radiolytically produced hydrogen might become the universal electron donor in aging ridge flank systems, possibly extending our view of habitable areas on Earth.

Our findings raise further questions that are beyond the scope of this paper. For instance, the termination of Fe-oxidation as a metabolic energy source in highly altered regions may be indicated either by the absence or by the presence of different kinds of biosignatures, when palagonite rims inhibit microbial access to ferrous iron in the fresh glass, preventing further microbial mediation of glass alteration. The hypothesis to be tested in future studies, therefore, is that Fe-oxidizers are responsible for the bioalteration textures abundantly observed in ridge flank crust.

Other questions that might be addressed in future studies concern the timing and thresholds in habitat evolution and their relation to crustal alteration and seawater circulation. Are older and more altered rocks colonized by different types of microbes (maybe from overlying sediments) than younger and fresher rocks? Are there population changes in bioenergetically different parts of igneous oceanic ridge flanks, similar to sedimentary settings (e.g., Jorgensen et al., 2012)? And finally, since radiolysis can also break down water molecules structurally bound in minerals, can we find habitats on other planetary bodies in which hydrogen might accumulate similarly?

Acknowledgements

This research used samples and data provided by the Integrated Ocean Drilling Program (IODP). Funding for this research was provided the German Research Foundation DFG (grant BA1605/11) and the and the MARUM Center for Marine Environmental Sciences. We are grateful to Jörg Erzinger at the GFZ-Potsdam for support with the Fe(II) determinations. We also acknowledge support from Olivier Rouxel during the cruise. Two anonymous reviewers are thanked for numerous helpful comments. We dedicate this contribution to our late colleague and friend, Katrina Edwards.

Disclosure statement

No competing financial interests exist.

Reference

Aitken, M.J. (1985). Thermoluminescence Dating, Academic Press, Orlando, FL.

Allard T. & Calas, G. (2009). Radiation effects on clay mineral properties. Applied Clay Science 43, 143–149.

Alt, J.C. (2004). Alteration of the upper oceanic crust: Mineralogy, chemistry, and processes. In: Davies, E.E., and Elderfield H. (Eds.) Hydrogeology of the Oceanic Lithosphere, pp. 495–533. Cambridge University Press

Amend, J.P., McCollom, T.M., Hentscher, M. & Bach, W. (2011). Catabolic and anabolic energy for chemolithoautotrophs in deep-sea hydrothermal systems hosted in different rock types. Geochimica et Cosmochimica Acta, 75(19), 5736–5748.

Anderson, B.W., Coogan, L.A. & Gillis, K.M. (2012). The role of outcrop-to-outcrop fluid flow in off-axis oceanic hydrothermal systems under abyssal sedimentation conditions, Journal of Geophysical Research: Solid Earth, 117, B05103.

Bach, W. & Edwards, K.J. (2003). Iron and sulphide oxidation within the basaltic ocean crust: implications for chemolithoautotrophic microbial biomass production. Geochimica et Cosmochimica Acta 67, 3871–3887.

Banerjee, N.R., Izawa, M.R.M., Sapers, H.M. & Whitehouse, M.J. (2010). Geochemical biosignatures preserved in microbially altered basaltic glass. Surface and Interface Analysis, 43, 452–457.

Becker, K., Bartetzko, A. & Davis, E.E. (2001). Leg 174B Synopsis: Revisiting Hole 395A for logging and long-term monitoring of off-axis hydrothermal processes in young oceanic crust. Proceedings of the Ocean Drilling Program, Scientific Results Volume 174B.

Bethke, C.M. (1996). Geochemical Reaction Modeling. Oxford University Press, New York.

Blair, C.C., D'Hondt, S., Spivack, A.J. & Kingsley, R.H. (2007). Radiolytic Hydrogen and Microbial Respiration in Subsurface Sediments. Astrobiology Volume 7, Number 6, 951-970.

Boettger, J., Lin, H.-T., Cowen, J.P., Hentscher, M. & Amend, J.P. (2013). Energy yields from chemolithotrophic metabolisms in igneous basement of the Juan de Fuca ridge flank system. Chemica Geology 337 – 338, 11 – 19.

Cockell, C.S., van Calsteren, P., Mosselmans, F.W., Franchi, I.A., Gilmour, I., Kelly, L., Olsson-Francis, K., Johnson, D. & the JC24 Shipboard scientific party (2010). Microbial endolithic colonization and the geochemical environment in young seafloor basalts. Chemical Geology 279, 17 – 30.

Daux, V.C., Guy, T., Advocat, J.-L., Crovisier, J. & Stille, M. (1997). Kinetic Aspects of basaltic glass dissolution at 90°C: Role of silicon and aluminum. Chemical Geology 142, 109 – 128.

Draganic, I.G. & Draganic Z.D. (1971). The Radiation Chemistry of Water, Academic Press, New York.

Donnelly, T.W., Thompson, G. & Salisbury, M.H. (1977). The chemistry of altered basalts at site 417, Deep Sea Drilling Project Leg 51, in: Donnelly, T.W., Francheteau, J., Bryan, W.B., Robinson, P.T. (Eds.), Initial Reports of the Deep Sea Drilling Project. U.S. Government Printing Office, Washington, D.C., pp. 1319 – 1330.

Edwards, K.J., Bach, W., Klaus, A., and the Expedition 336 Scientists (2012). Proceedings of IODP, 336: Tokyo (Integrated Ocean Drilling Program Management International, Inc.).

Ehlmann, B.L., Berger, G., Mangold, N., Michalski, J.R., Catling, D.C., Ruff, S.W., Chassefiere, E., Niles, P.B., Chevrier, V. & Poulet, F. (2013). Geochemical consequences of widespread clay mineral formation in Mars' ancient crust. Space Sci. Rev. 174, 329 – 364.

Einen, J., Thorseth, I.H. & Ovreås, L. (2008). Enumeration of Archaea and Bacteria in seafloor basalt using real-time quantitative PCR and fluorescence microscopy. FEMS Microbiology Letters, 282(2), 182 – 187.

Ekström, L.P. & Firestone, R.B. (1999). World Wide Web Table of Radioactive Isotopes, database version 02/28/99, from http://ie.lbl.gov/toi/index.htm (last accessed 03/15/13).

Elderfield, H., Wheat, C.G., Mottl, M.J., Monnin, C. & Spiro, B. (1999). Fluid and geochemical transport through oceanic crust: a transect across the eastern flank of the Juan de Fuca Ridge. Earth and Planetary Science Letters 172: 151 – 165.

Fisher, A. T. & Becker, K. (2000). Channelized fluid flow in oceanic crust reconciles heat-flow and permeability data. Nature, 403, 71 – 74.

Fisher, A. T. & Wheat, C.G. (2010). Seamounts as conduits for massive fluid, heat, and solute fluxes on ridge flanks. Oceanography, 23, 74 – 87.

Fisk, M.R., Storrie-Lombardi, M.C., Douglas, S., Popa, R., McDonald, G. & Di Meo-Savoie, C. (2003). Evidence of biological activity in Hawaiian subsurface basalts. Geochemistry Geophysics Geosystems, Vol 4, doi:10.1029/2002GC000387.

Fliegel, D., Knowles, E., Wirth, R., Templeton, A., Staudigel, H., Muehlenbachs, K. & Furnes, H. (2012). Characterization of alteration textures in Cretaceous oceanic crust (pillow lava) from N-Atlantic (DSDP Hole 418A) by spatially-resolved spectroscopy. Geochimica et Cosmochimica Acta 96, 80 – 93.

Furnes, H., Banerjee, N.R., Muehlenbachs, K., Staudigel, H., de Wit, M. (2004). Early life recorded in archean pillow lavas. Science 304, 578 – 581.

Gales, G., Libert, M-F., Sellier, R., Cournac, L., Chapon, V. & Heulin, T. (2004). Molecular hydrogen from water radiolysis as an energy source for bacterial growth in a basin containing irradiating waste. FEMS Microbiology Letters 240, 155 – 162.

Gournis, D., Mantaka-Marketou, A.E., Karakassides, M.A. & Petridis, D. (2000). Effect of γ-irradiation on clays and organoclays: a Mössbauer and XRD study. Physics and Chemistry of Minerals, 27: 514 – 521.

Grosch, E.G. & McLoughlin, N. (2014). Reassessing the biogenicity of Earth's oldest trace fossil with implications for biosignatures in the search for early life. Proceedings of the National Academy of Science. doi/10.1073/pnas.1402565111

Grosch, E.G., McLoughlin, N., Lanari, P., Erambert, M. & Vidal, O. (2014). Microscale mapping of alteration conditions and potential biosignatures in basaltic-ultramafic rocks on early Earth and beyond. Astrobiology 14, 216 – 228.

Harris, N.H., Fisher, A.T. & Chapman, D.S. (2004). Fluid flow through seamounts and implications for global mass fluxes. Geology, v. 32; no 8, p. 725 – 728.

Heberling, C., Lowell, R.P., Liu, L. & Fisk, M.R. (2010). Extent of the microbial biosphere in the oceanic crust. Geochemistry Geophysics Geosystems, Vol 11. Q08003, doi:10.1029/ 2009GC002968

Hoehler, T.M. (2004). Biological energy requirements as quantitative boundary conditions for life in the subsurface. Geobiology, v. 2, issue 4, p. 205 – 215.

Jochum, K.P., Willbold, M., Raczek, I., Stoll, B. & Herwig, K. (2005). Chemical Characterisation of the USGS Reference Glasses GSA-1G, GSC-1G, GSD-1G, GSE-1G, BCR-2G, BHVO-2G and BIR-1G Using EPMA, ID-TIMS, ID-ICP-MS and LA-ICP-MS. Geostandards and Geoanalytical Research, v. 29, issue 3, p. 285 – 302.

Jochum, K.P., Weis, U., Stoll, B., Kuzmin, D., Yang, Q., Raczek, I., Jacob, D.E., Stracke, A., Birbaum, K., Frick, D.A., Günther, D. & Enzweiler, J. (2011). Determination of Referemce Values for NIST SRM 610– 617 Glasses Following ISO Guidelines. Geostandards and Geoanalytical Research, v. 35, issue 4, p. 397 – 429.

Jørgensen, S. L., Hannisdal, B., Lanzen, A., Baumberger, T., Flesland, K., Fonseca, R., Ovreås, L., Steen, I.H., Thorseth, I.H., Pedersen, R.B. & Schleper, C. (2012). Correlating microbial community profiles with geochemical data in highly stratified sediments from the Arctic Mid-Ocean Ridge.

Proceedings of the National Academy of Sciences 109, 2846 – 2855.

Lane, N., Allen, J.F. & Martin, W. (2010). How did LUCA make a living? Chemiosmosis in the origin of life. BioEssays 32, 271 – 280.

Langseth, M.G., Becker, K., Von Herzen, R.P. & Schultheiss, P. (1992) Heat and fluid flux through sediment on the western flank of the Mid-Atlantic ridge: a hydrogeological study of North Pond. Geophysical Research Letters 19, 517 – 520.

LaVerne, J. & L. Tandon (2002). H_2 Production in the Radiolysis of Water on CeO_2 and ZrO_2. The Journal of Physical Chemistry B 2002, 106, 380 – 386.

Lin, L., Slater, G.F., Sherwood Lollar, B., Lacrampe-Couloume, G. & Onstott, T.C. (2005). The yield and isotopic composition of radiolytic H_2, a potential energy source for the deep subsurface biosphere. Geochimica et Cosmochimica Acta 69, 893 – 903.

Lodders, K. & Fegley Jr. B. (1997). An oxygen isotope model for the composition of Mars. Icarus 126, 373 – 394.

Löffler, F.E., Tiedje, J.M. & Sanford, R.A. (1999). Fraction of Electrons Consumed in Electron Acceptor Reduction and Hydrogen Thresholds as Indicators of Halorespiratory Physiology. Applied and Environmental Microbiology, Sept. 1999, p. 4049 – 4056.

Mayhew, L.E., Ellison, E.T., McCollom, T.M., Trainor, T.P. & Templeton, A.S. (2013). Hydrogen generation from low-temperature water–rock reactions. Nature Geosciences 6, 478 – 484.

McCollom, T.M. (2000). Geochemical constraints on primary productivity in submarine hydrothermal vent plumes. Deep Sea Research Part I: Oceanographic Research Papers, 47(1), 85 – 101.

McCollom, T.M. & Shock, E.L. (1997). Geochemical constraints on chemolithoautotrophic metabolism by microorganisms in seafloor hydrothermal systems. Geochimica et Cosmochimica Acta, 61, 4375 – 4391.

Merikallio, S., Nousiainen, T., Kahnert, M. & Harri, a-M. (2013). Light scattering by the Martian dust analog, palagonite, modeled with ellipsoids. Opt. Express 21, 179, 72 – 85.

Michalski, J.R., Cuadros, J., Niles, P.B., Parnell, J. & Rogers, A.D. (2013). Groundwater activity on Mars and implications for a deep biosphere. Nature Geoscience 6, 133 – 138.

Morgan, J.W. & Anders, E. (1979). Chemical composition of Mars. Geochimica et Cosmochimica Acta 43, 1601 – 1610.

Oelkers, E.H. (2001). General kinetic description of multioxide silicate mineral and glass dissolution. Geochimica Cosmochimica Acta 65, 3703 – 3719.

Oelkers, E.H. & Gislason, S.R. (2001). The mechanism, rates and consequences of basaltic glass dissolution: I. An experimental study of the dissolution rates of basaltic glass as a function of aqueous Al, Si and oxalic acid concentration at 25°C and pH = 3 and 11. Geochimica Cosmochimica Acta 65, 3671 – 3681.

Orcutt, B.N., Wheat, C.G., Hulme, S., Edwards, K.J., Bach, W. (2013). Oxygen consumption in the subseafloor basaltic crust derived from a reactive transport model. Nature communications 4, doi:10.1038/ncomms/2539.

Pauly, B. D., Schiffman, P., Zierenberg, R. A. & Clague, D. A. (2011). Environmental and chemical controls on palagonitization. Geochemistry Geophysics Geosystems, 12(12), Q12017 doi:10.1029/2011GC003639

Querol, M.C.A., (1952). Manganometric microtitration of iron. Mikrochimica acta, Springer-Verlag, p. 126 – 132.

Santelli, C.M., Edgcomb, V.P., Bach, W. & Edwards, K.J. (2009). The diversity and abundance of bacteria inhabiting seafloor lavas positively correlate with rock alteration. Environmental Microbiology Vol 11, Issue 1, 86 – 98.

Santelli, C.M., Orcutt, B.N., Banning, E., Bach, W., Moyer, C.L., Sogin, M.L., Staudigel, H. & Edwards, K.L. (2008). Abundance and diversity of microbial life in ocean crust. Nature 453, 653 – 656.

Singer, R.B. & McSween Jr., H.Y. (1993). The igneous crust of Mars: compositional evidence from remote sensing and SNC meteorites. Resources of Near-Earth Space, edited by J.S. Lewis, M.S. Mettews and M.M.L. Guerrieri, pp. 709 – 736, University of Arizona Press, Tuscon.

Spinks, J. W. T., & Woods, R. J. (1990). An introduction to radiation chemistry. John Wiley, New York.

Stevens, T.O. & McKinley, J.P., 1995. Lithoautotrophic microbial ecosystems in deep basalt aquifers. Science 270, 450 – 454.

Stroncik, N.A. & Schmincke, H.-U. (2001). Palagonite – a review. International Journal of Earth Sciences, 91(4), 680 – 697.

Toner, B.M., Lesniewski, R.A., Marlow, J.J., Santelli, C.M., Bach, W., Orcutt, B.N., Edwards, K.J. (2012). Mineralogy drives bacterial biogeography of hydrothermally inactive seafloor sulfide deposits, Geomicrobiology Journal, doi 10.1080/01490451.2012.688925.

Wänke, H. & Dreibus, G. (1994). Chemistry and accretion history of Mars. Philosophical Transactions of the Royal Society of London A349, 285 – 293.

Warner, N.H. & Farmer, J.D. (2010). Subglacial Hydrothermal Alteration Minerals in Jökulhlaup Deposits of Southern Iceland, with Implications for Detecting Past or Present Habitable Environments on Mars. Astrobiology. June 2010, 10(5): 523 – 547.

Wessel, P., Sandwell, D.T. & Kim, S.-S. (2010). The global seamount census. Oceanography 23, 24 – 33.

Wheat, C.G., McManus, J., Mottl, M.J. & Giambalvo, E. (2003). Oceanic phosphorus imbalance: the magnitude of the ridge-flank hydrothermal sink. Geophysical Research Letters 30(17).

Wolery, T.J. (2004). Qualification of Thermodynamic Data for Geochemical Modeling of Mineral-Water Interactions in Dilute Systems, in: Energy, U.S.D.o. (Ed.). Bechtel SAIC Company, LLC.

Ziebis, W., McManus, J., Ferdelman, T., Schmidt-Schierhorn, F., Bach, W., Muratli, J., Edwards, K. J. & Villinger, H. (2012). Interstitial fluid chemistry of sediments underlying the North Atlantic gyre and the influence of subsurface fluid flow. Earth and Planetary Science Letters, 323 – 324, 79 – 91.

2.7 Supplementary material

Table 1. Summary of factors used in the hydrogen yield calculations and their respective references.

Variable	Description	Unit	Reference/Source
$P_{H2,rock}$	Total hydrogen yield from radiolysis	H_2 molecules/s/cm$^3_{rock}$	Equation 1
$G_{H2,i}$	radiation chemical yield for each radiation type	H_2 molecules/MeV	Spinks & Woods, 1990
D_i	radiation doses absorbed by the rock	MeV/s/cm^3	Equation 2-4
Φ	porosity	volume water / volume rock	IODP LIMS database
A_i	Activities of ^{238}U, ^{235}U, ^{232}Th and ^{40}K, respectively	decays/s/g_{rock}	XRF and ICP-MS
ΣE_i	decay energy sums for each respective decay series	MeV/decay series	Ekström & Firestone, 1999
S_i	relative stopping power of alpha, beta particles and gamma radiation	-	Aitken, 1985

Table 2. Analytical results from EPMA. LA-ICP-MS and ICP-MS. Measurements on thin section are given as averages of each respective sample. WR=whole rock.

Sample	Phase	Depth (mbsf)	K_2O (wt%)	Th (ppm)	U (ppm)	$Fe(III)/Fe_{(tot)}$
U1383C 29R-1W 6-9	Glass	299.29	0.11	0.12	0.08	-
U1383C 29R-1W 6-9	Palagonite	299.29	3.06	0.27	0.57	-
U1383C 20R-1W 139-141	Glass	220.61	0.11	0.11	0.07	-
U1383C 20R-1W 139-141	Palagonite	220.61	2.66	0.26	0.62	-
U1383C 22R-1W 24-27	Glass	237.97	0.10	0.11	0.06	-
U1383C 22R-1W 24-27	Palagonite	237.97	2.62	0.27	0.55	-
U1383C 19R-1W 67-79	Glass	212.27	0.10	0.11	0.08	-
U1383C 19R-1W 67-79	Palagonite	212.27	2.91	0.18	0.54	-
U1382A 3R-3W 21-27	WR	116.46	0.19	0.12	0.14	0.59
U1382A 3R-3W 64-69	WR	116.88	0.19	0.12	0.11	0.56
U1382A 3R-3W 114-119	WR	117.38	0.10	0.11	0.05	0.42

U1382A 3R-4W 1-7	WR	118.56	0.11	0.12	0.05	0.35
U1382A 4R-1W 90-96	WR	123.86	0.18	0.13	0.08	0.44
U1382A 4R-2W 32-36	WR	124.70	0.24	0.14	0.31	0.73
U1382A 4R-2W 92-98	WR	125.32	0.26	0.13	0.23	0.70
U1382A 4R-3W 34-39	WR	126.20	0.27	0.15	0.24	0.73
U1382A 4R-3W 40-44	WR	126.25	0.17	0.12	0.06	0.44
U1382A 5R-2W 38-43	WR	134.22	0.25	0.14	0.83	0.79
U1382A 6R-3W 19-25	WR	144.47	0.08	0.12	0.05	0.25
U1382A 6R-3W 64-66	WR	144.88	0.46	0.12	0.17	0.61
U1382A 7R-1W 71-73	WR	152.43	0.21	0.11	0.16	0.47
U1382A 7R-1W 120-123	WR	152.93	0.25	0.12	0.07	0.31
J1382A 10R-1W 85-87	WR	181.37	0.16	0.10	0.11	0.46
U1382A 10R-1W 90-95	WR	181.45	0.11	0.11	0.05	0.36
U1382A 10R-	WR	182.48	0.07	0.11	0.05	0.27

2W 52-57						
U1382A 10R-2W 111-117	WR	183.08	0.11	0.10	0.10	0.44
U1382A 10R-3W 66-71	WR	184.06	0.14	0.11	0.07	0.42
U1382A 10R-3W 76-82	WR	184.17	0.09	0.11	0.05	0.27
U1382A 12R-1W 57-62	WR	200.32	0.24	0.13	0.06	0.34
U1382A 12R-1W 69-72	WR	200.42	0.17	0.13	0.11	0.37
U1382A 12R-1W 104-107	WR	200.77	0.21	0.13	0.19	0.49
U1382A 12R-3W 32-34	WR	202.54	0.21	0.14	0.07	0.40
U1382A 12R-3W 46-51	WR	202.71	0.20	0.14	0.15	0.46
U1383C 2R-1W 125-130	WR	70.80	0.14	0.15	0.39	0.65
U1383C 3R-1W 115-121	WR	77.81	0.31	0.13	0.08	0.46
U1383C 3R-2W 30-33	WR	78.43	0.29	0.13	0.09	0.47
U1383C 3R-3W 57-61	WR	80.10	0.18	0.15	0.41	0.66
U1383C 5R-2W 5-8	WR	97.28	0.33	0.14	0.57	0.71

Sample	Phase	Depth (mbsf)	K_2O (wt%)	Th (ppm)	U (ppm)	$Fe(III)/Fe_{(tot)}$
U1383C 5R-2W 34-37.	WR	97.57	0.19	0.13	0.08	0.35
U1383C 7R-2W 29-32	WR	116.76	0.29	0.13	0.07	0.38
U1383C 7R-2W 86-89	WR	117.33	0.15	0.15	0.65	0.69
U1383C 8R-1W 34-36	WR	124.96	0.25	0.13	0.07	0.31
U1383C 8R-2W 65-69	WR	126.65	0.12	0.15	0.75	0.71
U1383C 9R-4W 81-85	WR	139.50	0.20	0.13	0.07	0.31
U1383C 10R-2W 127-133	WR	146.60	0.18	0.14	0.51	0.69
U1383C 13R-1W 97-101	WR	173.71	0.15	0.11	0.35	0.61
U1383C 13R-1W 109-112	WR	173.82	0.15	0.11	0.06	0.22
U1383C 14R-2W 6-9	WR	183.62	0.20	0.11	0.15	0.57
U1383C 14R-2W 65-69	WR	184.22	0.24	0.10	0.06	0.27
U1383C 16R-1W 16-19	WR	192.99	0.26	0.11	0.19	0.49
U1383C 16R-	WR	193.46	0.12	0.11	0.06	0.33

1W 63-66						
U1383C 19R-1W 70-73	WR	212.33	0.20	0.10	0.28	0.58
U1383C 19R-1W 73-76	WR	212.36	0.15	0.10	0.06	0.27
U1383C 23R-1W 40-44	WR	247.44	0.21	0.09	0.07	0.37
U1383C 23R-1W 89-92	WR	247.92	0.27	0.10	0.20	0.54
U1383C 26R-1W 63-66	WR	276.06	0.52	0.09	0.22	0.56
U1383C 26R-1W 132-136	WR	276.76	0.15	0.09	0.05	0.32
U1383C 27R-1W 9-13	WR	284.93	0.22	0.10	0.46	0.64
U1383C 27R-1W 74-77	WR	285.57	0.13	0.10	0.05	0.22
U1383C 29R-1W 102-105	WR	300.25	0.26	0.10	0.21	0.48
U1383C 30R-1W 16-19	WR	303.89	0.25	0.10	0.05	0.38
U1383C 31R-2W 45-49	WR	313.99	0.43	0.10	0.39	0.58
U1383C 31R-2W 119-123	WR	314.73	0.28	0.10	0.06	0.33
U1383C 32R-1W 27-30	WR	322.00	0.11	0.10	0.06	0.11

U1383C 32R-1W 58-62	WR	322.32	0.31	0.10	0.30	0.58
U1383C 32R-2W 92-95	WR	324.08	0.11	0.10	0.06	0.23
U1383C 32R-3W 1-4	WR	324.31	0.67	0.09	0.31	0.58

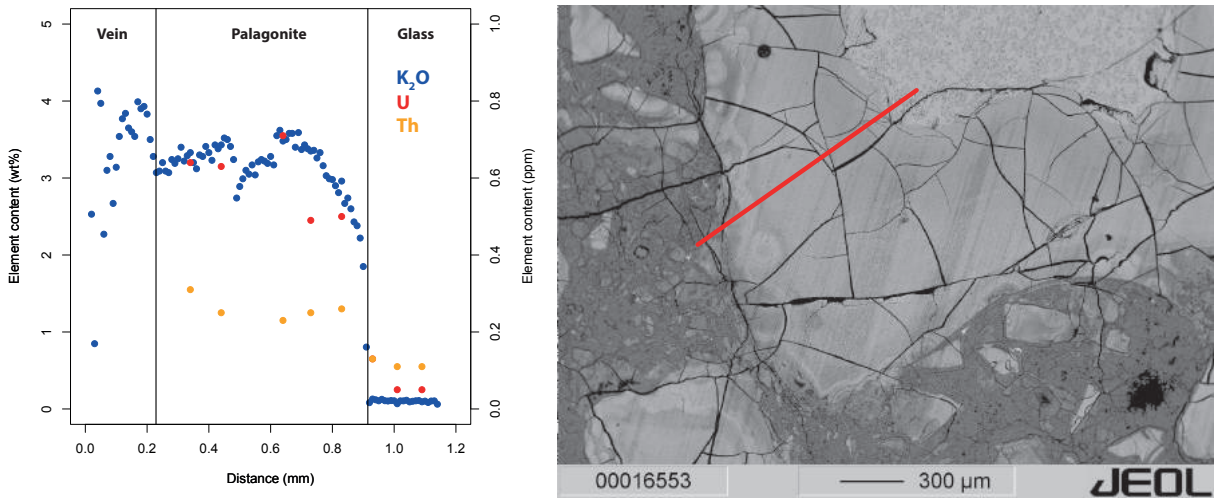

FIG. S1. K_2O, Th, and U content along a traverse, covering vein-filling minerals, palagonite, and fresh glass.

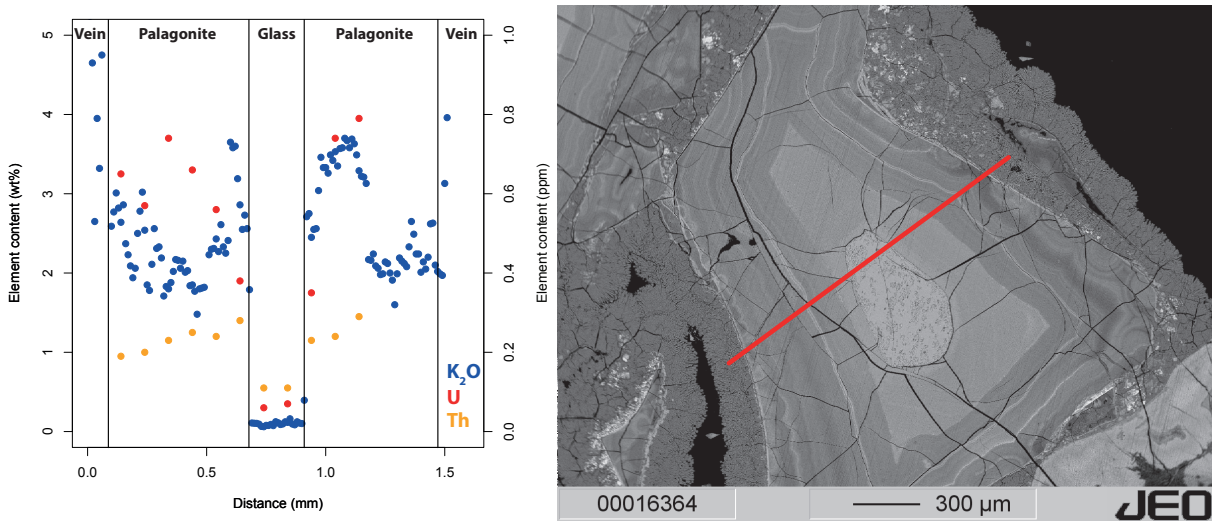

FIG. S2. K_2O, Th, and U content along a traverse, covering vein-filling minerals, palagonite, and fresh glass.

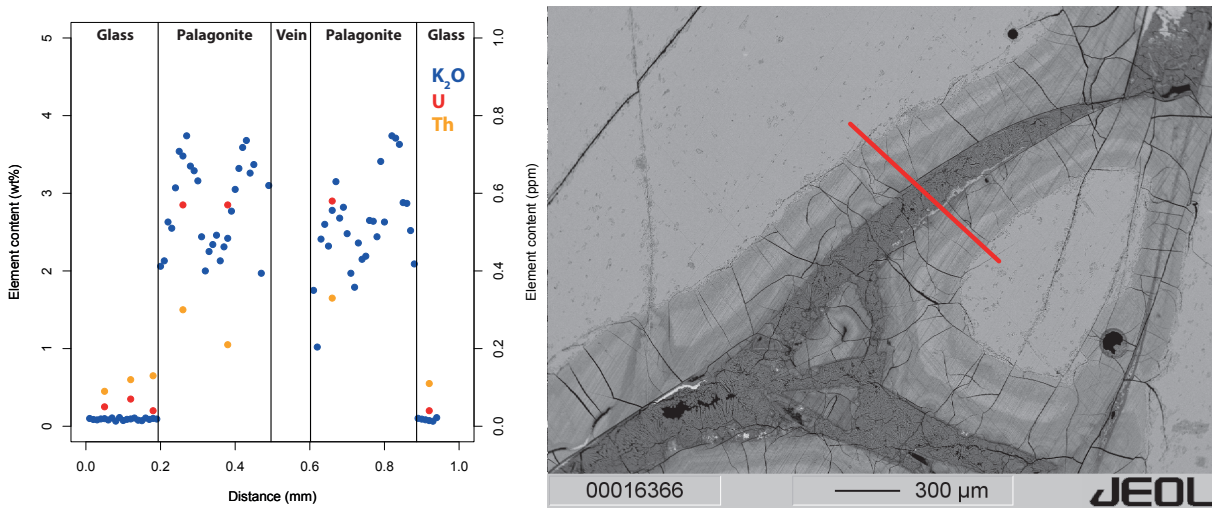

FIG. S2. K_2O, Th, and U content along a traverse, covering vein-filling minerals, palagonite, and fresh glass.

3 Comparing biosignatures from North Pond, Mid-Atlantic Ridge and the Louisville Seamount, off New Zealand

Andreas Türke, Bénédicte Ménez, Wolfgang Bach

3.1 Abstract

Biosignatures in subseafloor basalt glass have been studied as a potential analogue for extraterrestrial habitats for several years. However, little is known about the relationship of the physical and chemical nature of the habitat and the prevalent types of biosignatures. Here, we report and compare strongly varying biosignatures from two distinctly different study sites. We analyzed rock samples for their textural biosignatures and their associated organic molecules. The biosignatures from the 8 Ma North Pond Region, which is built up by young well-oxygenated crust, are characterized by little textural diversity. However, the organic matter associated with those textures, shows evidence for the occurrence of complex molecules like proteins. In contrast, the biosignatures from the Louisville Seamounts (60-80 Ma) are much more texturally diverse, whereas the organic molecules are more degraded and suggest Archaeal origin. We hypothesize that microbial communities change significantly during crustal evolution and suggest that microbes associated with older and severely altered crust, are not responsible for the trace fossils commonly found within subseafloor basalt glass.

3.2 Introduction

Subseafloor basalts are one of the largest and most intriguing habitats on Earth. Oceans cover two-thirds of Earth's surface and the upper 500 m of the underlying igneous crust represents Earth's largest aquifer (e.g., Wheat and Fisher, 2008). The bioenergetical makeup of this habitat is strongly influenced by crustal evolution and its chemical change during seafloor weathering and advancing sedimentation as the igneous crust ages (Bach & Edwards, 2003; Türke et al., 2015).

Putative microbial life in the basaltic ocean crust has been identified in a number of different areas and settings (e.g. in modern ocean crust by Furnes & Staudigel (1999) and Furnes et al. (2001) or in Archean

samples from greenstone belts by Banerjee et al. (2006) and Fliegel et al. (2011)) and by different lines of evidence. Initial work had used textural criteria for microbial activity in subseafloor basalts: putative ichnofossils, preserved as granular and tubular alteration textures in basalt glass (Thorseth et al., 1995; Fisk et al., 1998; Furnes et al., 2001; McLoughlin et al., 2011), which come in different shapes and sizes (Fisk & McLoughlin, 2013). They are usually between 1 – 5 µm in width and tens to hundreds of µm in length and are hypothesized to be due to microbial etching of the volcanic glass. It has been suggested that these microbes thrive on organic matter or oxidize Fe and Mn in the glass for chemoautotrophic energy gain with oxidants like O_2 from seawater. Furthermore, sulfur isotope values in sulfide minerals (Rouxel et al., 2008), phylogenetic studies (Santelli et al., 2008; Lever et al., 2013), and fossilized fungal communities (Ivarsson et al., 2015) provide evidence for an abundant and diverse microbial community within the basaltic ocean crust. Microorganisms have been shown to enhance alteration rates of volcanic glass (Staudigel et al., 1998; Henri et al., 2015) and therefore seem to play an important role in geochemical cycling between oceanic crust and seawater.

Yet, very little has been discovered regarding the relationship between the subseafloor microbial communities and the geological setting (Edwards et al., 2012). There is evidence that fungal communities colonize basalts relatively early, as they are fossilized within secondary minerals like zeolite and calcite, which precipitate as veins in cracks or in vesicles (Ivarsson et al., 2012). But do biosignatures change with ongoing alteration of basaltic ocean crust in seafloor weathering, which affects the bioenergetical and physical conditions of this subseafloor environment? And, furthermore, which organisms form which kind of biosignatures?

Here we report differences in tubular biosignatures and organic matter associated with the samples from the North Pond area, near the Mid-Atlantic Ridge and the Louisville seamounts, off New Zealand, which are two distinctly different areas in terms of their crustal evolution. These differences reveal insights into the changes in the microbial communities in aging ocean crust and their associated biosignatures.

3.3 Material and Methods

3.3.1 Study sites

We analyzed rock samples from drill cores U1372A and U1376A from Integrated Ocean Drilling Program (IODP) Expedition 330 to the Louisville Seamounts and from drill cores U1382A and U1383C from IODP Expedition 336 to North Pond on the western flank of the Mid-Atlantic Ridge.

The Louisville seamount 50 – 80 Ma old trail is a 75 km wide volcanic chain of guyots and seamounts in the South Pacific (Koppers et al., 2013). The entire igneous section of the drill cores has undergone secondary low-temperature weathering (Koppers et al., 2013). Few details are known about the alteration regime, however alteration below 90 meters below seafloor (mbsf) becomes more greenish likely due to reducing conditions.

The North Pond region on the other hand is an 8 Ma old sediment pond structure of 8x15 km located on the western flank of the Mid-Atlantic Ridge, surrounded by steep rift mountains. Here, the hydrology is well contained and characterized by high fluid flux at low temperatures of 2 – 15 °C (Langseth et al., 1992). Given the low age of North Pond, it has only undergone oxidative seafloor weathering, and is not influenced by a more complex alteration history with overprinting due to conductive reheating after sediment sealing (e.g., Teagle et al., 1996).

3.3.2 Sample Preparation

Two types of samples were analyzed for the work presented here:

A) A set of 18 thin sections (11 from Louisville and 7 from North Pond), of which one has > 100 individual tubular alteration textures (the statistics are presented in section 3.1.). These thin sections were not used in the search for organic molecules due to contamination issues in the thin section preparation.

B) Pieces of the same samples were prepared for the identification of organic molecules. The procedure is illustrated in Figure 1. Samples were cut into thin slices, so that all surfaces were fresh cuts (a and b). We used a saw blade sterilized with 5% sodium hypochlorite and sterilized ultrapure water. Afterwards the slices were polished by hand (c) on silicon carbon abrasive discs with ultrapure ethanol to a thickness of approximately 100 µm and analyzed via scanning electron microscopy and Fourier transformed infrared microscopy (FTIR) (d). At all stages the rocks were only handled with sterile nitrile gloves. This procedure should avoid contamination with organic and post sampling colonization.

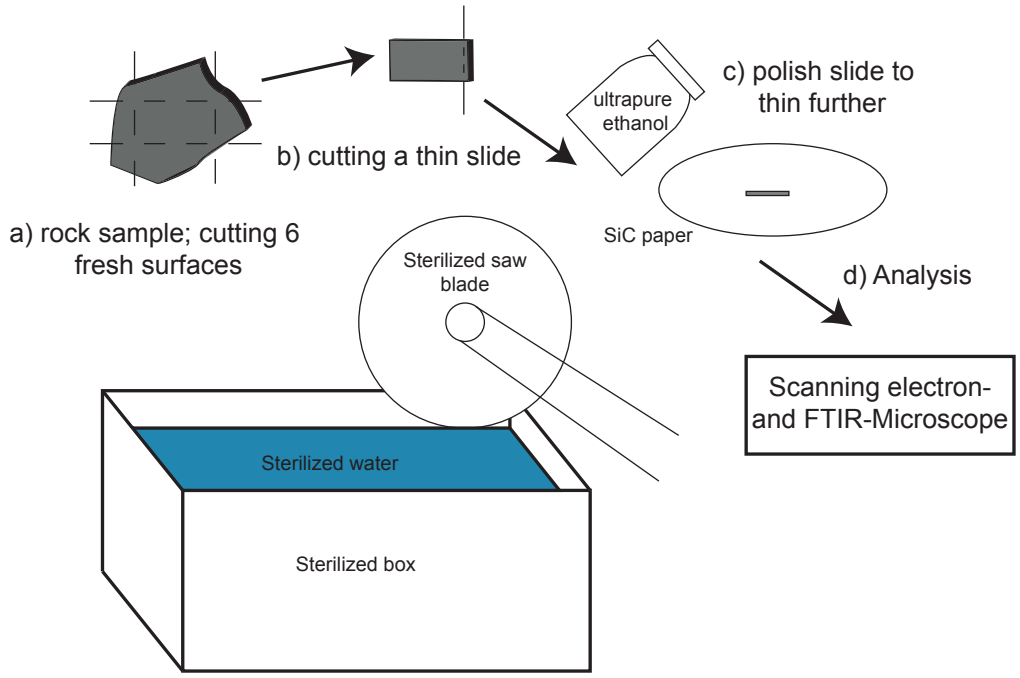

Figure 1: Sketch of the samples preparation procedure using only sterilized equipment. (a) Rock samples were cut into cubes, such that only fresh surfaces remain. (b) Slicing off a thin slide of the rock cube. (c) Polishing the slide using SiC paper as thin as possible, without breaking it. (d) Analyses by FTIR and SEM.

3.3.3 Microtunnel Count

For each of the 18 thin sections, we characterized 100 randomly chosen individual microtunnels under a transmission microscope according to Fisk & McLoughlin's (2013) Atlas of alteration textures in volcanic glass. The textures were classified based on their size (long >= 20µm; short < 20µm; thin < 2µm; thick >= 2µm), content (empty; dark contents; ovoid bodies; filaments; septae), variations in width #1 (constant; tapered), variations in width #2 (none; engorged; bumpy; annulated; mushroom), branching (none; simple, mossy, network, palmate, crown), and content (empty; dark contents; ovoid bodies; filament; septae).

3.3.4 Scanning Electron Microscopy

We used a JEOL JSM-840A scanning electron microscopy (SEM) coupled to energy dispersive X-ray spectrometry (EDS) at the Université Pierre et Marie Curie, Paris, France with and a beam acceleration voltage of T-K kV. Chemical maps have been processed using the Spirit® software. All the samples analyzed by SEM were prepared free of epoxy raisin to avoid contamination (see 2.2).

3.3.5 Fourier Transformation Infrared Microscopy (FTIR)

FTIR measurements were carried out at the Institute de Physique du Globe de Paris, France with a XXX in both transmission and reflectance mode. We acquired the spectra by mapping over areas of several mm^2 with individual spot sizes of 30 x 30 µm. The raw data was converted into –ASCII files with the Omnic Atlus® imaging software by Thermo Scientific TM and afterwards normalized and background-reduced using the ChemoSpec package for the software R (Hanson, 2014).

The following absorption bands were considered indicative of bonds in organic molecules, which potentially originate from microbial cells (Table 1).

Wavenumber (cm^{-1})	Assignment	Potential Origin
2956	CH_3 asymmetrical stretch	Lipids
2920	CH_2 asymmetrical stretch	Lipids
2870	CH_3 symmetrical stretch	Lipids
2850	CH_2 symmetrical stretch	Lipids
1743	C=O stretch	Ester, fatty acids
1653	Amide I, C=O stretch, C-N stretch, N-H bend	Proteins
1567 – 1548	Amide II, N-H bend, C-N stretch	Proteins
1470	CH_3 asymmetrical bend	Lipids
1468	CH_2 scissoring	Lipids
1460	CH_3 asymmetrical bend	Lipids
1430	C-O-H in-plane bending	Carboxylic group
1401	$N^+ (CH_3)_3$ symmetrical bend	Lipids
1320	C-O stretch	Carboxylic group
1299	Amide III, C-N stretch, N-H bend, C=O stretch, O=C-N bend	Proteins

Table 1: Wavenumbers, assignment and potential origin of organic bands as compiled by Preston et al. (2011).

3.3.6 $R_{3/2}$ value

The $R_{3/2}$ value was introduced by Isigu et al. (2009) in order to evaluate spectral characteristics in microfossils. It is the aliphatic CH_3/CH_2 absorbance ratio of the respective stretching band heights. The $R_{3/2}$ value reflects the degree of branching and chain length of aliphatic hydrocarbons. The three domains of life have very different $R_{3/2}$ values for full cells (Eucarya approximately 0.3 – 0.5; Bacteria 0.6 – 0.7; Archaea 0.8 – 1.0). Individual biomolecules for bacteria however, plot significantly higher (proteins) or slightly (membranes) to significantly lower (lipids) (Igisu et al., 2009). We use the $R_{3/2}$ value to compare the fossilized organic matter found within the igneous rocks from the North Pond region and the Louisville Seamounts and unravel their connection to textural biosignatures.

3.4 Results

3.4.1 Tubular alteration textures

The tubular alteration (Figure 2) textures as identified by transmitted light microscopy were classified following Fisk & McLoughlin (2013) (see supplementary figure). Most of the textures described were found within the samples from Louisville (Figure 3), whereas the diversity of textures was lower in the North Pond samples (Figure 4).

The tubules (N = 700) in the North Pond samples are almost exclusively < 2 µm in width (98%) and there are more short tubes (59%), than long tubes (41%). Curvature is wide spread, with 62% of the tubes being curvilinear, 12% being kinked, and 26% convoluted. There were no knotted tubes identified in the North Pond samples. Variation in width is very low, the majority is uniform in width (82%), only 18% of the tubes are tapered, and there is no variation at mid-section and terminus, nor any branching or tunnel contents.

The Louisville tubular alteration textures (N = 1100) on the other hand are much more diverse in every respect. Short and thin tubules are the most abundant ones (47%), similar to North Pond, however long and thin (19%), short and wide (18%), and long and wide tubes (16%) are commonly found as well throughout all the samples. The variation in curvature is less pronounced, but all types are present, with 84% being curvilinear, 13% kinked, 1% knotted, and 2% convoluted. Variations in width are very common. Although most of the tubes are uniform in width (83% curvilinear, and 17% tapered), there is some variation at mid-section and terminus, with 4% engorged, 1% bumpy, 5% annulated, and 3% mushroom

textured. Unlike in the North Pond samples, branching does occur in the Louisville tubes, although 88% of the tubes are not branched. 8% show simple branching, whereas complex branching is less prominent (network 2%, palmate, mossy, and crown < 1%). Furthermore only 72% of the tubules are empty, 14% are filled with dark contents, 6% with ovoid bodies, 6 % show septae, 1% are filled with filaments, and 1% is patterned. Ovoid bodies and septae were exclusively found in long and wide tubules.

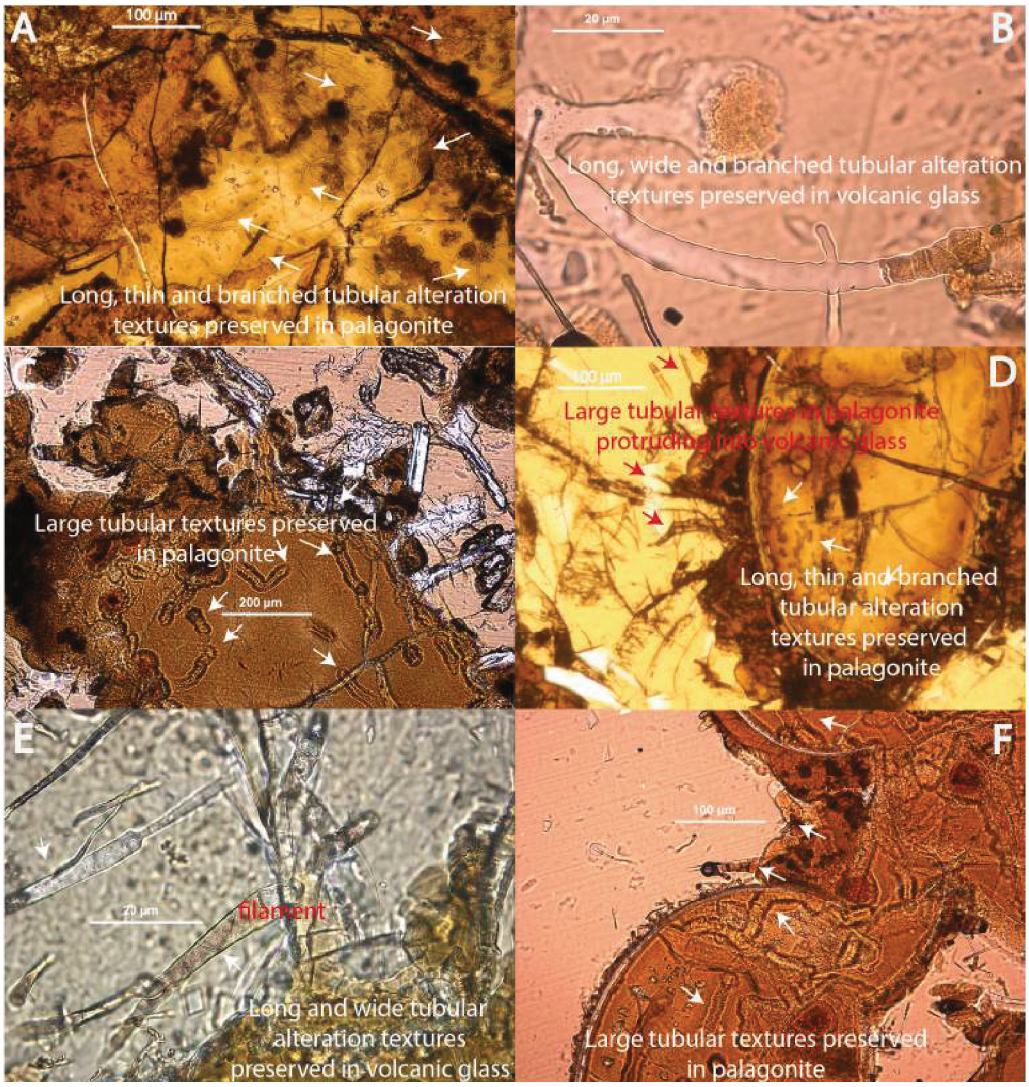

Figure 2: Several tubular alteration textures in volcanic glass under plane polarized light. A and D: Remnants of tubules preserved (or formed?) in palagonite. B and E: Long and wide tubule, which shows significant variation in width at the terminus and simple branching. C and F: Fungal like textures preserved in palagonite. D: Tapered tubule with dark contents, as well as shorter, but wide tubules without any content.

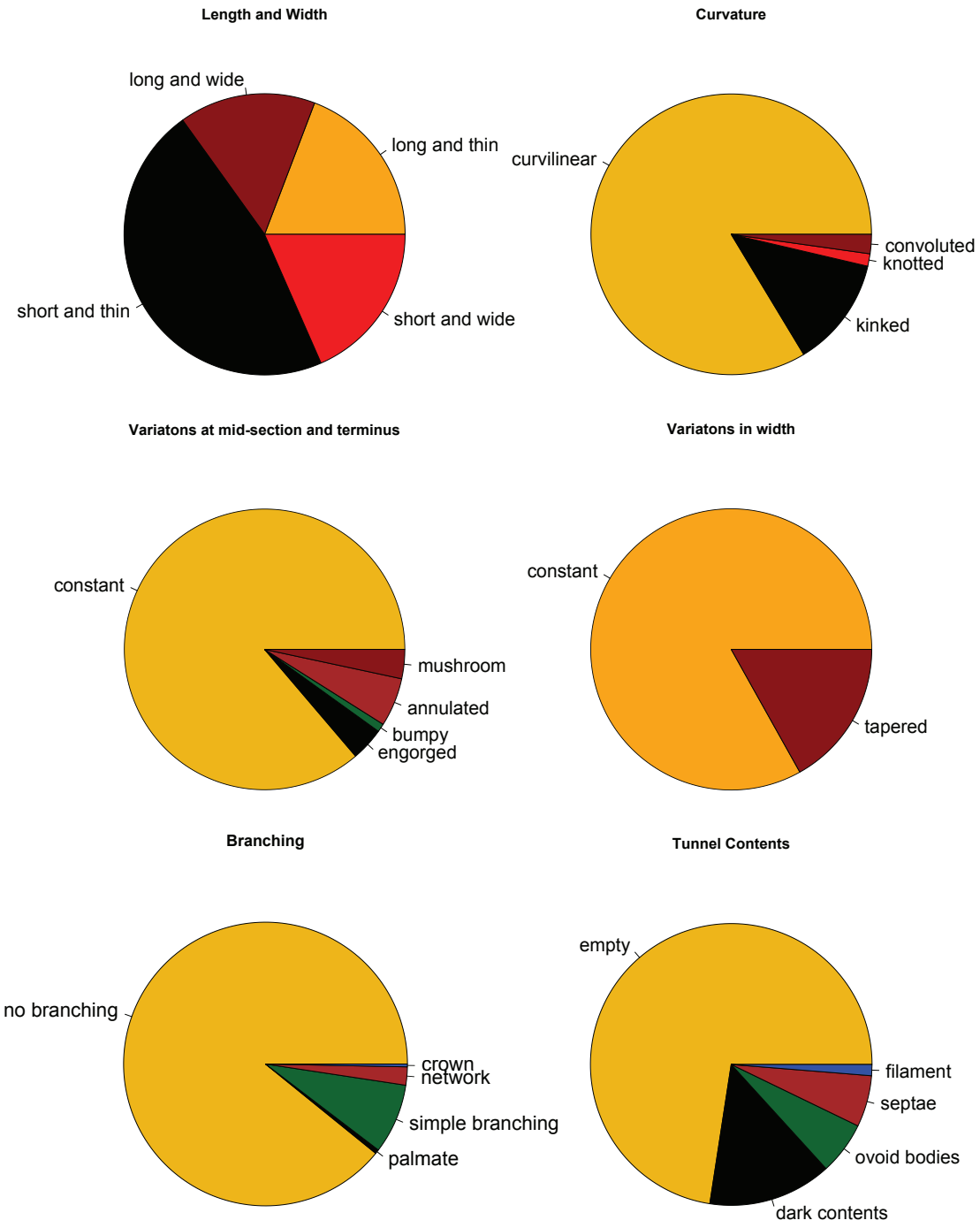

Figure 3: Types of tubular alteration textures in the Louisville samples. Short and thin tubes make up almost 50% of the samples, but longer and thicker tubes are prevalent as well, compared to the North Pond samples. Furthermore, these samples are more diverse in terms of variations in widths, branching, and tunnel contents.

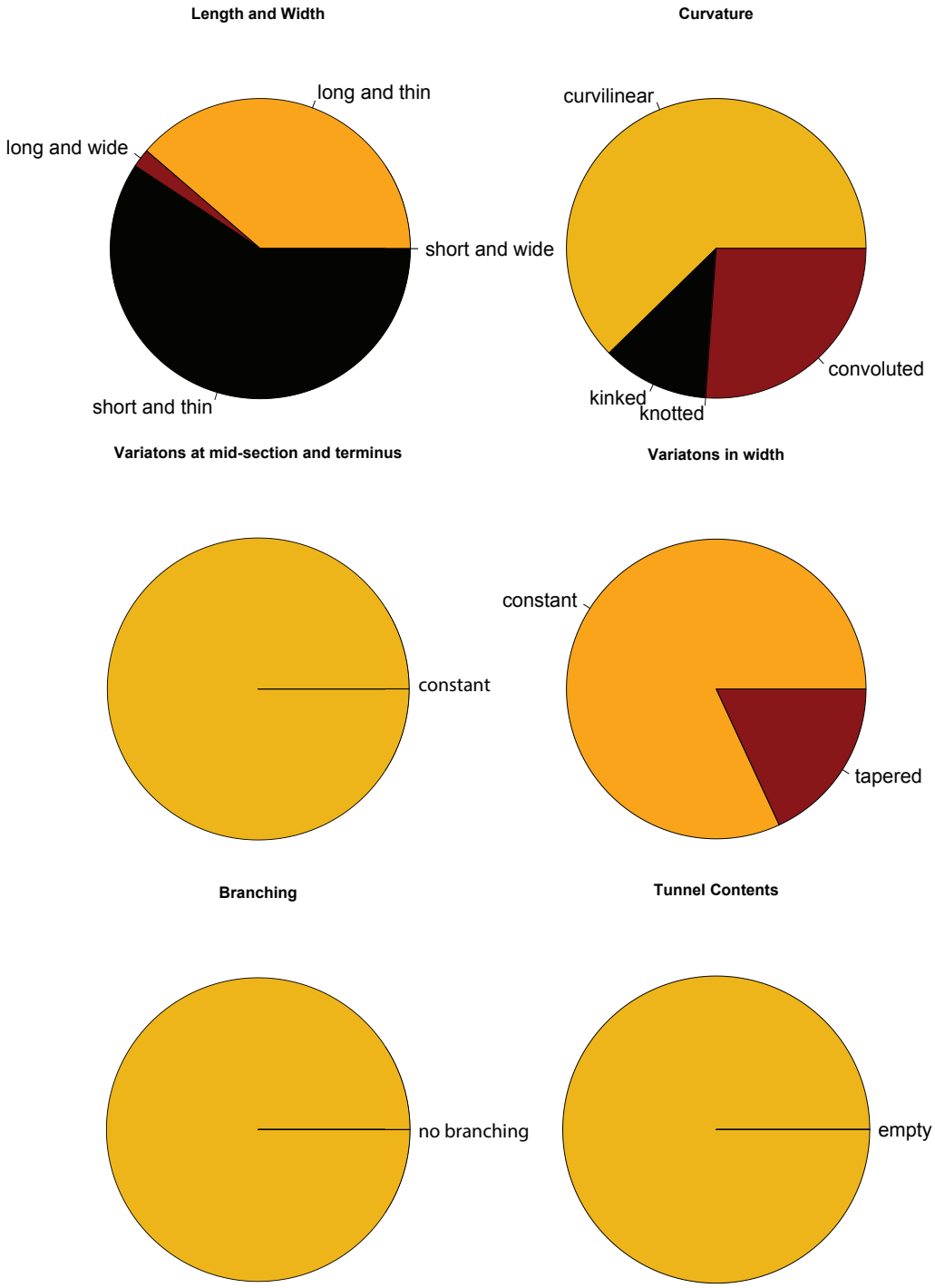

Figure 4: Types of tubular alteration textures in the North Pond samples. Short and thin tubes make the majority of the sample, and thick tubes are almost completely absent. They do not show any branching, are exclusively empty and do not show variations in width.

3.4.2 Organic Molecules

We found organic molecules both in samples from the North Pond Area and the Louisville Seamounts. However, they were distinctly different in their location and composition. The North Pond samples contained only little organic matter, which was exclusively restricted to the palagonite/glass interface (Figure 5). Energy dispersive X-ray spectrometry (EDS) revealed that carbon is not present as a carbonate, nor as SiC contamination from polishing, as it is not associated with Ca, Mg or Si enrichments.

The organic matter showed indications for the presence of lipids (absorption bands at 2956 cm^{-1}, 2920cm^{-1}, 2850 cm^{-1}, and 1460 – 1470 cm^{-1} representing the asymmetrical stretch of CH_2, the asymmetrical stretch of CH_3, the symmetrical stretch of CH_2, and the asymmetrical bend of CH_3 the scissoring of CH_2, respectively). Furthermore, the spectra showed evidence for the presence of esters/fatty acids (absorption band at 1743 cm^{-1} representing the C=O stretch) and proteins (absorption bands at a 1653 cm^{-1}, 1550 cm^{-1}, and 1300 cm^{-1} representing Amide I, II, and III, respectively) (Figure 6).

The samples from Louisville, on the other hand, contained less complex organic matter, which appears to consist exclusively of lipids (absorption bands at 2956 cm^{-1}, 2920cm^{-1}, and 2850 cm^{-1} representing the asymmetrical stretch of CH_3 and CH_2 as well as the symmetrical stretch of CH_2, respectively). These lipids were widely spread in the samples and occurred both in palagonites, and vein filling zeolites and SiO_2 (opal?) (Figure 8 and Figure 9). However, they were never associated with the many etch pits that were observed in the fresh glass (Figure 9), which we identify as the onset of tubular alteration textures.

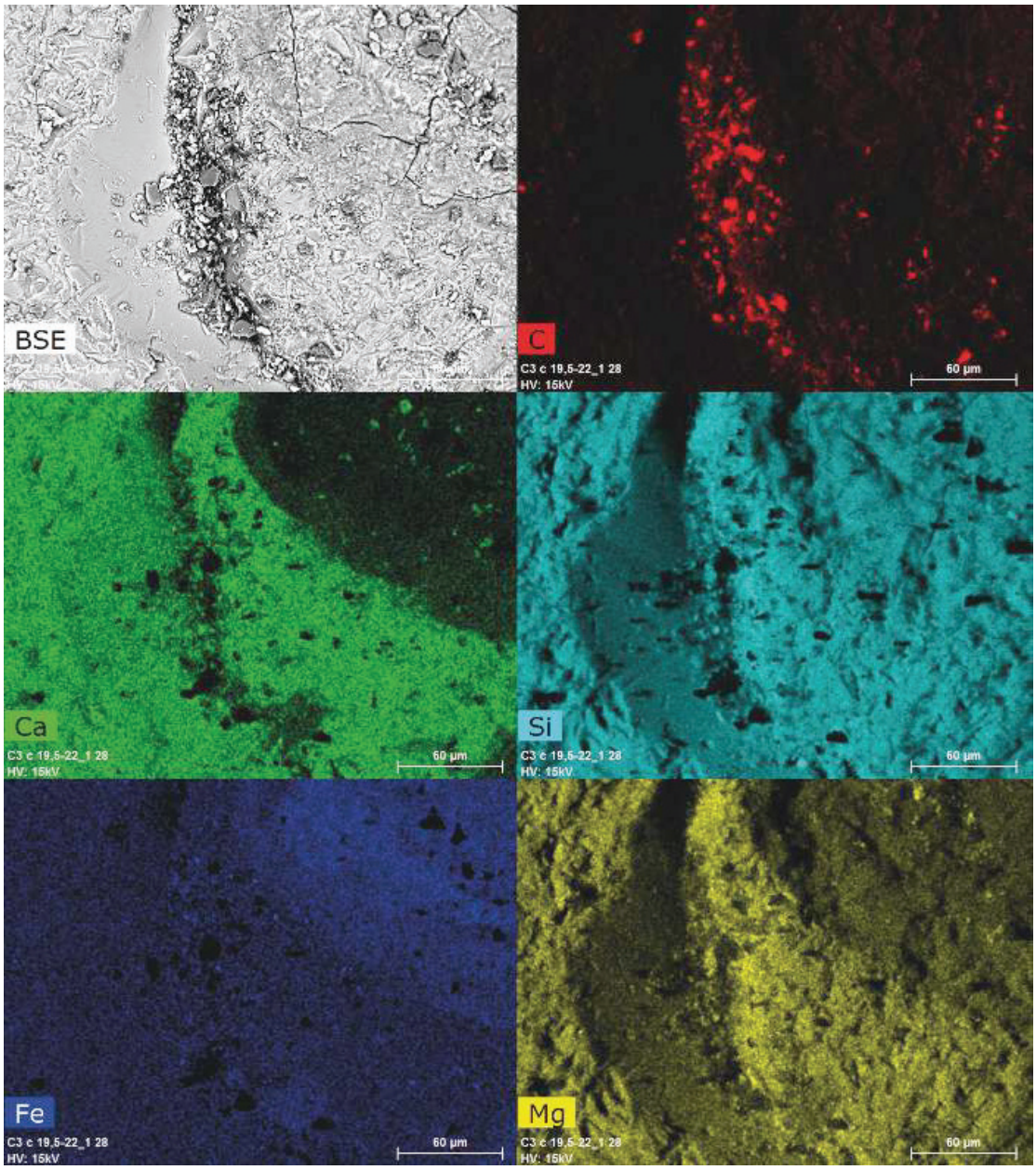

Figure 5: SEM image and associated EDX element maps for C, Ca, Si, Fe, and Mg. The organic matter is located closely to the palagonite/glass interface.

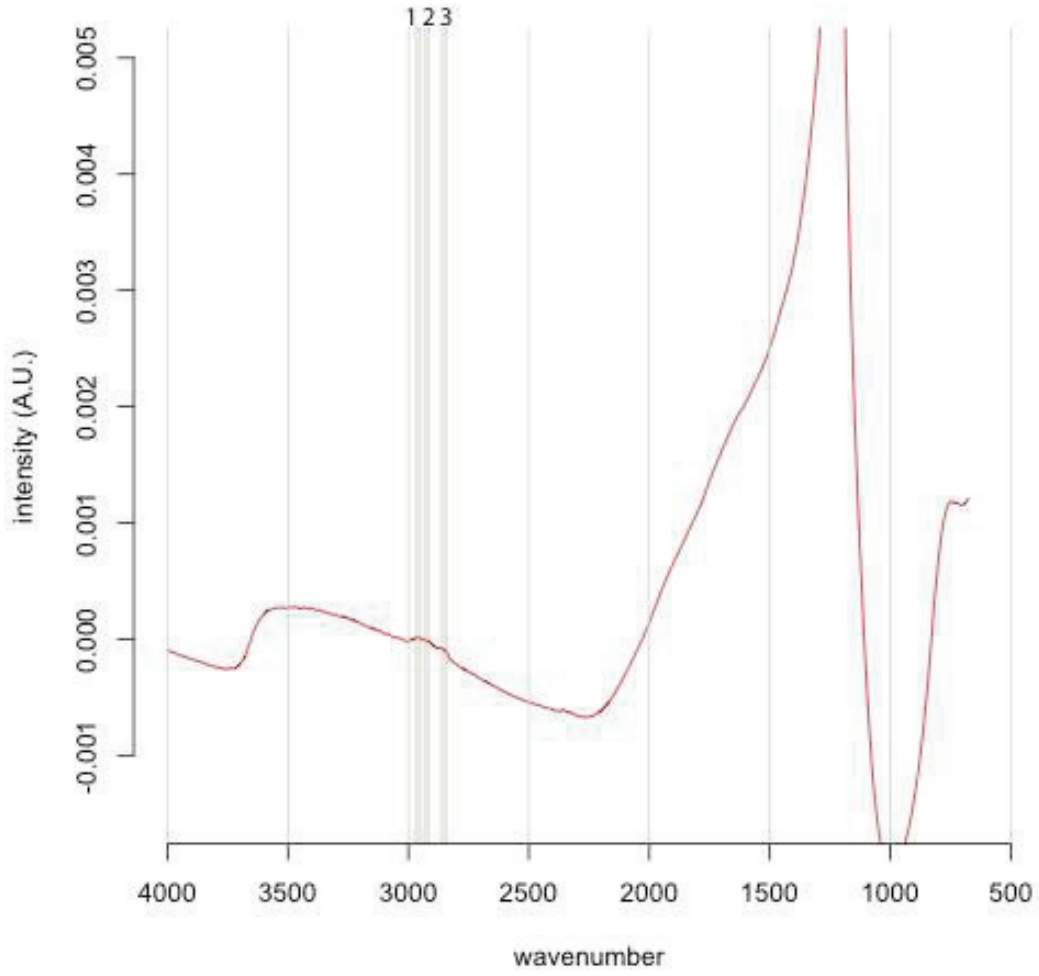

Figure 6: FTIR spectrum of a typical organic molecule in the Louisville samples. The bands that indicate presence of organics are 1: which is the CH_3 asymmetrical stretch, 2: which is the CH_2 asymmetrical stretch, and 3: the CH_2 symmetrical stretch.

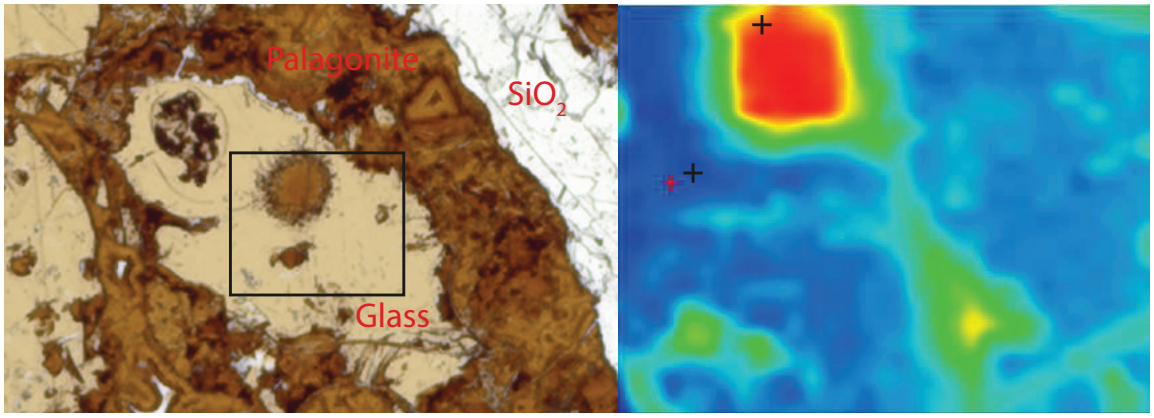

Figure 7: FTIR map of the "negative" split of a thin section, showing the distribution of the CH_3 band. The image indicates the presence of organic matter in a Louisville sample. Its concentration is highest in a palagonite-filled vesicle, from which tubular alteration textures protrude into the surrounding volcanic glass.

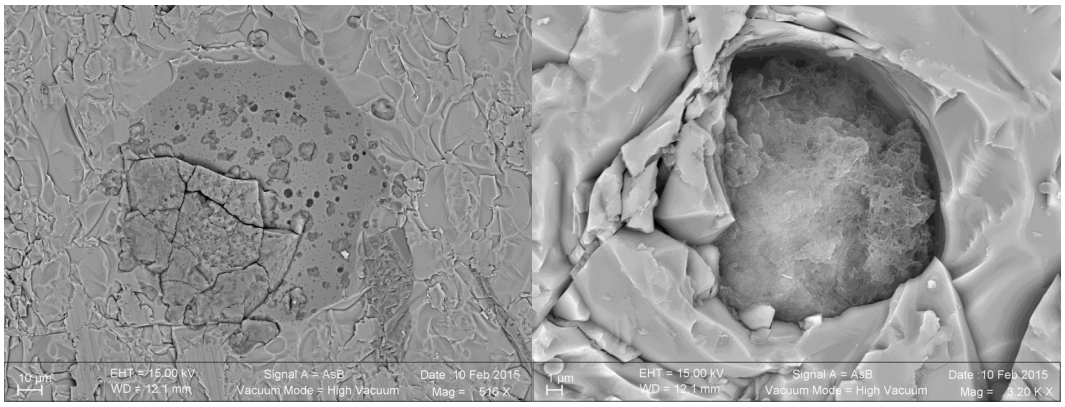

Figure 8: SEM image of a vesicle (same as in Figure 8) in basalt glass filled with palagonite from the Louisville seamount. Several etch pits are visible on the glass surface; the image on the right shows a close up of an etch pit, which protrudes into volcanic glass as a tubular alteration texture.

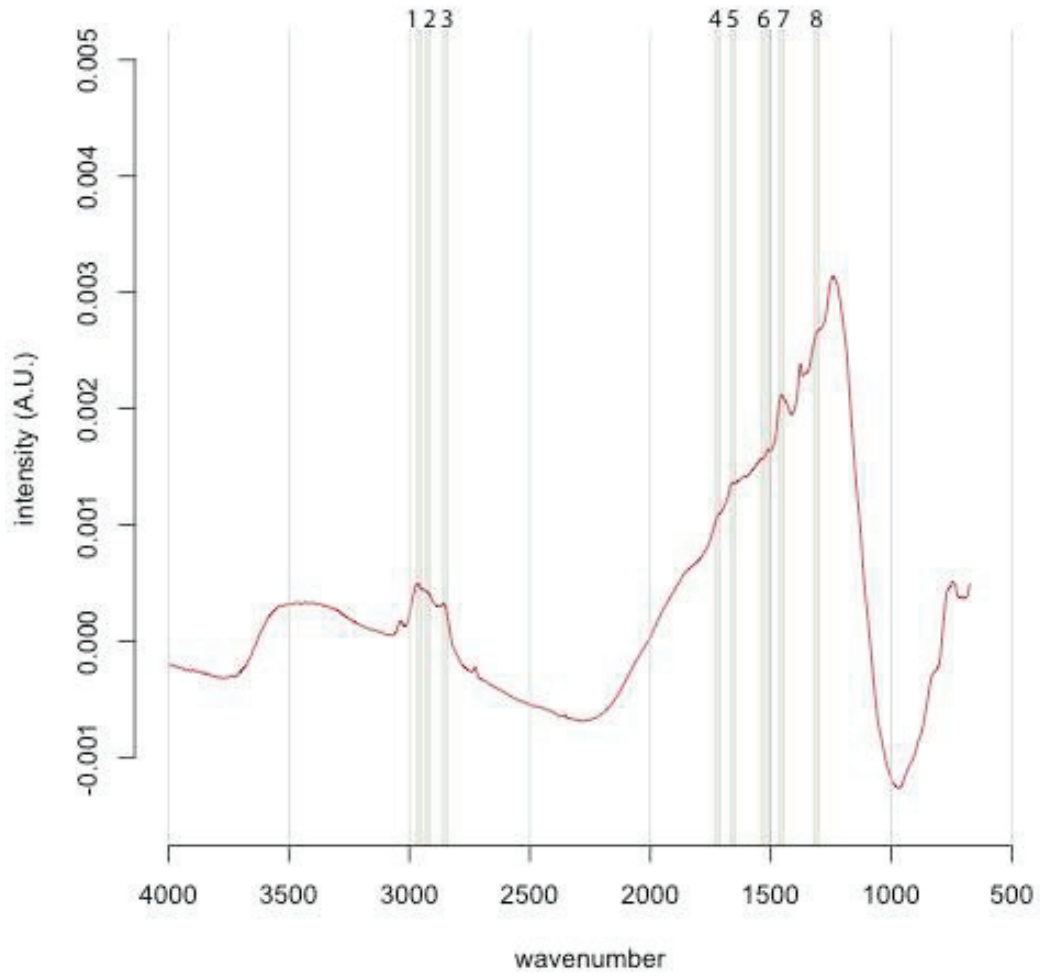

Figure 9: FTIR spectrum of typical organic matter in the North Pond samples. The presence of organics is suggested by the following bands: 1: the CH_3 asymmetrical stretch, 2: the CH_2 asymmetrical stretch, 3: the CH_2 symmetrical stretch, 4: the C=O stretch, 5: which is the Amide I band, 6: which is the Amide II band, 7: the CH_3 and CH_2 scissoring, 8: which is the Amide III band.

3.5 Discussion

3.5.1 Differences in biosignatures

We argue that the differences in the biosignatures of North Pond and Louisville can be explained by their different geological history and its influence on the basaltic aquifer as a habitat. North Pond represents a rather young (8 Ma) area of ridge flank, which has undergone oxidative alteration with temperatures at or

below 20 °C. Here, tubular alteration textures are rare and show little diversity, with only small variations in width, curvature, and branching (Figure 4). The low abundance and diversity might be related to the young age of the crust, which allowed only few and simple alteration textures to form. The organic matter we were able to detect in the North Pond samples via FTIR microscopy was sparse and showed indications of proteins. As proteins are expected to degrade quickly, their presence on the samples may indicate that the organic material is rather fresh and might be indigenous to the rock, rather than brought into the rock by circulating fluids. Both FTIR and SEM analyses revealed that organic matter was exclusively associated with the glass / palagonite interface (Figure 5). No distinct conclusions can be drawn from the $R_{3/2}$ values regarding the microbial community structure, as they span a very wide range (0.45 – 1.2). However, the highest values fall within and even above the range of Archaeal cells (which consist of isoprenoid chains that are highly branched and subsequently have higher $R_{3/2}$ values). This result is consistent with the observation of proteins within the organic matter, since proteins have $R_{3/2}$ values that are increased relative other cellular matter (Igisu, 2011). As spot sizes of 30 µm exceed the size of individual cells, these values likely represent mixed analyses. Therefore, we can only infer that the preserved organic matter at North Pond is likely dominantly Archaeal in origin. However, we cannot exclude the presence of bacterial or eukaryotic organic matter.

The Louisville samples are much older (50 – 80 Ma (Nichols et al., 2014)) and have undergone a longer, but less well constrained history of alteration, and hence the tubular biosignatures are more diverse and complex (Figure 4). The much larger tubular features preserved in palagonites (Figure 2C and 2F) resemble trace fossils of fungal communities found in other basalts (Ivarsson et al., 2012). However, the organic matter preserved was more degraded and only indicated the presence of carbohydrate chains, as commonly found within lipids (Figure 6). No indications for organic matter from fungi (which are Eucaryota) were found, as the $R_{3/2}$ values are all within the archaeal range (Figure 10) (Igisu et al., 2009). The organic matter was detected in secondary void fills such as palagonite in former vesicles (Figure 7) or vein fill with opal (Figure 11). This indicates that the organic matter was either flushed into the aquifer and then fossilized by precipitation within fractures and vesicles, or that the organic matter is indigenous to the rock, and was primarily associated with void spaces.

The relationship between alteration (and thus mineral/fluid interface) and biosignatures is illustrated in Figure 11. Tubular alteration textures in basalt glass form early, when the glass is exposed to fluids in fractures and oxidation of iron and sulfur can supply energy for microbial life. These are later partially replaced by palagonitization, which inhibits supply of energy via oxidation of glass. Eventually tertiary

minerals (like zeolites, carbonates or opal) seal fractures and fluid flow ceases. The organic matter is found within the palagonites and close to the opal, which indicated to us that it is not directly associated with the formation of tubular alteration textures. It rather appears flushed into the rocks by circulating fluids, and then fossilized, or related to a later stage colonization by communities that do not gain energy from alteration and oxidation of glass, but are heterotrophs instead, or possibly use energy sources unrelated to the ongoing alteration of glass. Türke et al. (2015) suggested, that oxidation of radiolytically produced hydrogen or reduction of Fe via hydrogen may be the dominant microbial energy sources in old and thoroughly altered basalts. The Louisville basalts reach U concentrations of up to 3 ppm (Vanderkluysen et al., 2014), so that significant H_2 production is expected. This would be in agreement with the observation that organic matter is found near the palagonite/glass interface in young basalts (North Pond) and within palagonites close to fractures in older basalts (Louisville).

Results from microbiological studies (Tully et al., 2014) suggest that the basalts of the Louisville Seamount Chain still host microbial life. This result is in contrast to our data that suggest no apparent relation between rock alteration and the presence of organic matter. The tow sets of observations may be reconciled if the rocks presently merely provide a substrate for microbes that derive their metabolic energy from seawater, as proposed by Templeton et al. (2009).

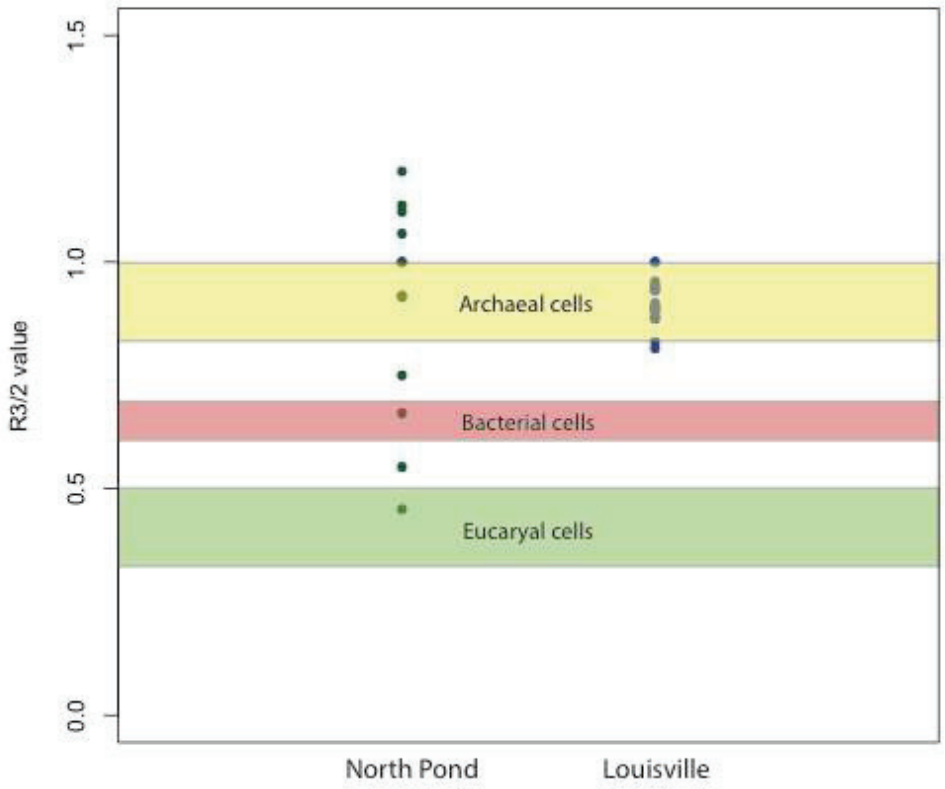

Figure 10: $R_{3/2}$ values of the organic matter found in the North Pond and Louisville samples. The values mostly plot above the values of full bacterial and eucaryal cells in both cases. However, individual biomolecules like membranes and lipids have lower $R_{3/2}$ values than full cells, whereas proteins plot higher.

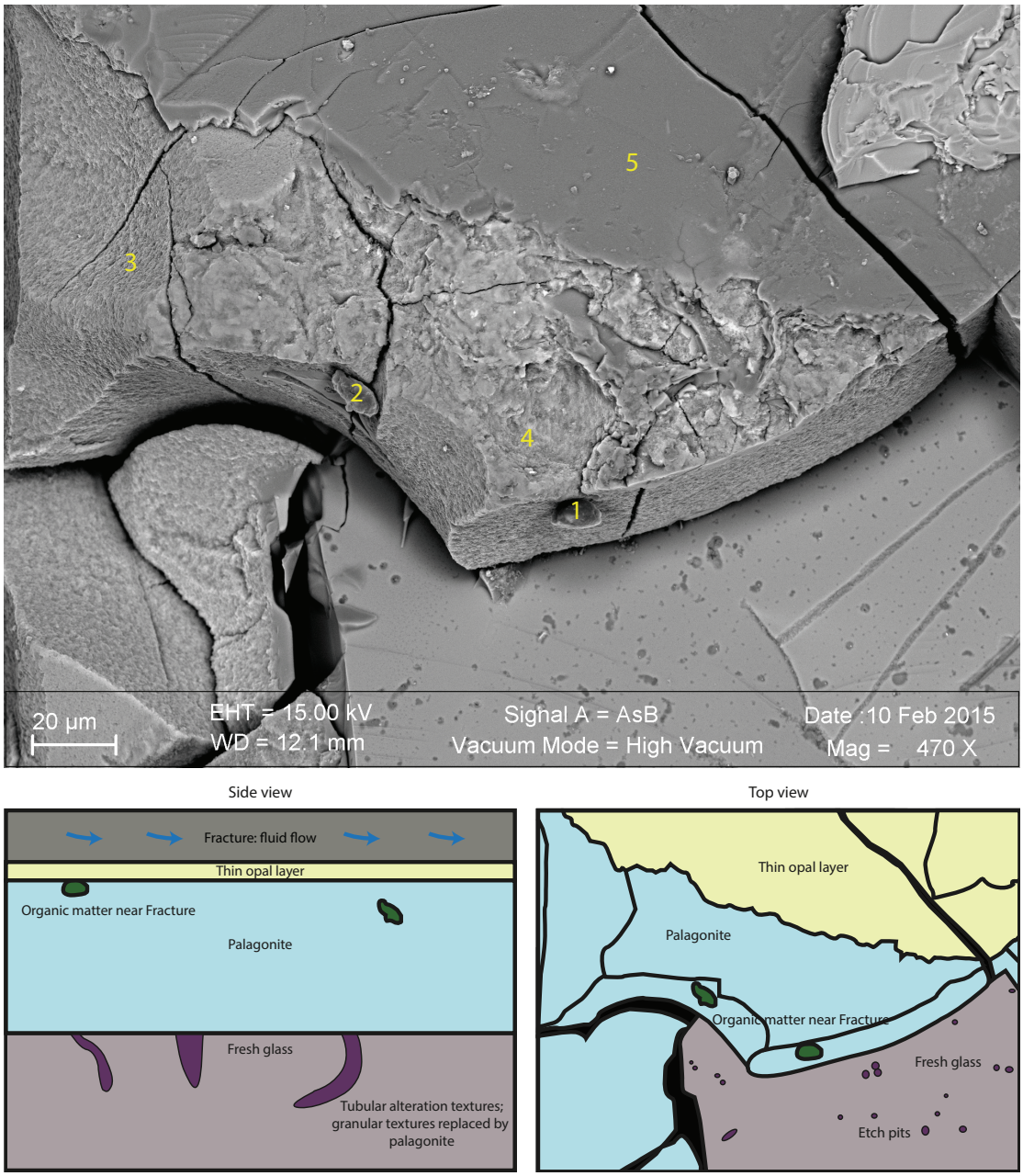

Figure 11: This figure shows and SEM image of organic matter (1 & 2) on a palagonite rim (3 & 4) on top of fresh glass with several etch pits and below an opal filled fracture (5). Below is a sketch as side view and top view, illustrating the spatial distribution of the tubular biosignatures and the organic matter. The tubes originate from the fracture/glass interface into the glass, are then overgrown by palagonite filled by precipitating opal. The organic matter was only found within palagonites, suggesting that it is not associated with formation of tubular alteration textures.

3.6 Conclusion

As the geochemical environment changes significantly during crustal evolution (e.g. oxic in an early stage to suboxic when buried by sediments), basalts might host different communities during different stages of crustal evolution.

Our findings support the idea that microbial life in young basaltic aquifers, which were altered only by oxidation processes, is likely supported by oxidation of iron. The reduced form of iron is found at the glass interface, where the organic matter in the North Pond samples was preserved. Later, fungi can colonize the rock and either feed off the primary producers or from the organic matter that is circulating within the aquifer, In older basaltic crust that has undergone a considerably more complex alteration history, the biosignatures textures are also more complex and diverse. In the latest stages, life seems to be hosted in voids within the rock, such that basalt only acts as a substrate. The organic matter is then preserved when these voids are filled by secondary phases like calcite, zeolite, or opal.

Acknowledgements:

This research used samples and data provided by the Integrated Ocean Drilling Program (IODP). Funding for this research was provided the German Research Foundation DFG (grant BA1605/11) and the MARUM Center for Marine Environmental Sciences.

References:

Bach, W. & Edwards, K.J. (2003). Iron and sulfide oxidation within the basaltic ocean crust: implications for chemolithoautotrophic microbial biomass production. *Geochimica et Cosmochimica Acta*, 67(20), 3871-3887.

Banerjee, N.R., Furnes, H., Muehlenbachs, K., Staudigel, H. & de Wit, M. (2006). Preservation of ~3.4–3.5 Ga microbial biomarkers in pillow lavas and hyaloclastites from the Barberton Greenstone Belt, South Africa. *Earth Planet. Sci. Lett.* 241, 707–722.

Fliegel, D., Wirth, R., Simonetti, A., Schreiber, A., Furnes, H. & Muehlenbachs, K. (2011). Tubular textures in pillow lavas from a Caledonian west Norwegian ophiolite: A combined TEM, LA-ICP-MS, and STXM study. *Geochemistry, Geophysics, Geosystems,* 12.

Furnes, H. & Staudigel, H. (1999). Biological mediation in ocean crust alteration: how deep is the deep biosphere? *Earth Planet. Sci. Lett.* 166, 97–103.

Furnes, H., Staudigel, H., Thorseth, I.H., Torsvik, T., Muehlenbachs, K. & Tumyr, O. (2001). Bioalteration of basaltic glass in the oceanic crust. *Geochemistry Geophysics Geosystems* 2.

Fisk, M.R., Giovannoni, S.J. & Thorseth, I.H. (1998). Alteration of Oceanic Volcanic Glass: Textural Evidence of Microbial Activity. *Science* 281, 978–980.

Fisk, M.R., & McLoughlin, N. (2013). Atlas of alteration textures in volcanic glass from the ocean basins. *Geosphere*, *9*(2), 317-341.

Hanson, B.A. (2014). ChemoSpec: Exploratory Chemometrics for Spectroscopy. R package version 3.0. 1.

Henri, P.A., Rommevaux-Jestin, C., Lensongeur, F., Mumford, A., Emerson, D., Godfroy, A. & Menez, B. (2016). Structural Iron (II) of Basaltic Glass as an Energy Source for Zetaproteobacteria in an Abyssal Plain Environment, Off the Mid Atlantic Ridge. *Front. Microbiol.* 6.

Igisu, M., Ueno, Y., Shimoyima, M., Nakashima, S., Awramik, S.M., Ohta, H. & Maruyama, S. (2009). Micro-FTIR spectroscopic signatures of Bacterial lipids in Proterozoic microfossils. *Precambrian Res.* 173, 19–26.

Igisu, M., Takai, K., Ueno, Y., Nishizawa, M., Nunoura, T., Hirai, M., Kaneko, M., Naraoka, H., Shimojima, M. & Isozaki, Y. (2011). Domain-level identification and quantification of relative prokaryotic cell abundance in microbial communities by Micro-FTIR spectroscopy. *Environ. Microbiol. Rep.* 4, 42–49.

Ivarsson, M., Bengston, S., Belivanova, V., Stampanoni, M., Marone, F. & Tehler, A. (2012). Fossilized fungi in subseafloor Eocene basalts. *Geology* 40, 163–166.

Ivarsson, M., Bengtson, S., Skogby, H., Lazor, P., Broman, C., Belivanova, V., & Marone, F. (2015). A Fungal-Prokaryotic Consortium at the Basalt-Zeolite Interface in Subseafloor Igneous Crust. *PloS one*, *10*(10).

Koppers, A.A.P., Yamazaki, T. & Geldmacher, J. Expedition 330 Scientific Party (2013). IODP Expedition 330: Drilling the Louisville Seamount Trail in the SW Pacific, *Scientific Drilling*, No. 15.

Langseth, M.G., Becker, K., Von Herzen, R.P., and Schultheiss, P. (1992). Heat and fluid flux through sediment on the western flank of the Mid-Atlantic Ridge: a hydrogeological study of North Pond. *Geophys. Res. Lett.* 19:517–520.

Lever, M.A., Rouxel, O., Alt, J.C., Shimizu, N., Ono, S., Coggon, R. M., Shanks III, W.C., Lapham, L., Elvert, M., Prieto-Mollar, X., Hinrichs, K-U., Inagaki, F. & Teske, A. (2013). Evidence for microbial carbon and sulfur cycling in deeply buried ridge flank basalt. *Science*, *339*(6125), 1305-1308.

McLoughlin, N., Wavey, D., Kruber, C., Kilburn, M.R., Thorseth, I.H. & Pedersen, R.B. (2011). A combined TEM and NanoSIMS study of endolithic microfossils in altered seafloor basalt. *Chemical Geology* 289, 154–162.

Nichols, A.R.L., Beier, C., Brandl, P.A. & Krumm, S.H. (2014). Geochemistry of volcanic glasses from the Louisville Seamount Trail (IODP Expedition 330): implications for eruption environments and mantle melting. *Geochemistry, Geophysics, Geosystems*, 15(5) 1718-1738.

Rouxel, O., Shanks, W.C., Bach, W., & Edwards, K.J. (2008). Integrated Fe-and S-isotope study of seafloor hydrothermal vents at East Pacific Rise 9–10 N. *Chemical Geology*, *252*(3), 214-227.

Santelli, C.M., Orcutt, B.N., Banning, E., Bach, W., Moyer, C.L., Sogin, M.L., Staudigel, H. & Edwards, K.J. (2008). Abundance and diversity of microbial life in ocean crust. *Nature*, *453*(7195), 653-656.

Staudigel, H., Yayanos, A., Chastain, R., Davies, G., Verdurmen, E.A.Th., Schiffman, P., Bourcier, R. & De Baar, H. (1998). Biologically mediated dissolution of volcanic glass in seawater. *Earth Planet. Sci. Lett.* 164, 233–244.

Teagle, D.H., Alt, J.C., Bach, W., Halliday, A.N. & Erzinger, J. (1996). Alteration of upper ocean crust in a ridge-flank hydrothermal upflow zone: mineral, chemical, and isotopic constraints. *Proc. Ocean Drill. Program, Sci. Results* 148, 119–150.

Templeton, A.S., Knowles, E.J., Eldridge, D.L., Arey, B.W., Dohnalkova, A.C., Webb, S.M., Bailey, B.E., Tebo, B.M. & Staudigel, H. (2009). A seafloor microbial biome hosted within incipient ferromanganese crusts. *Nat. Geosci.* 2, 872–876.

Thorseth, I.H., Torsvik, T., Furnes, H. & Muehlenbachs, K. (1995). Microbes play an important role in the alteration of oceanic crust. *Chemical Geology* 126, 137–146.

Tully, B.J., Sylvan, J.B., Heidelberg, J.F. & Huber, J.A. (2014). Exploring Genomic Diversity Using Metagenomics of Deep-Sea Subsurface Microbes from the Louisville Seamount and the South Pacific Gyre. *AGU Fall Meeting Abstracts*, Vol. 1, p. 02.

Türke, A., Nakamura, K. & Bach, W. (2015). Palagonitization of basalt glass in the flanks of mid-ocean ridges: implications for the bioenergetics of oceanic intracrustal ecosystems. *Astrobiology* 10/15.

Vanderkluysen, L., Mahoney, J.J., Koppers, A.A., Beier, C., Regelous, M., Gee, J.S. & Lonsdale, P.F. (2014). Louisville Seamount Chain: Petrogenetic processes and

geochemical evolution of the mantle source. *Geochemistry, Geophysics, Geosystems,* 15.

Wheat, C.G. & Fisher, A.T. (2008) Massive, low-temperature hydrothermal flow from a basaltic outcrop on 23 Ma seafloor of the Cocos Plate: Chemical constraints and implications. *Geochemistry, Geophysics, Geosystems,* 9.

Supplementary Data

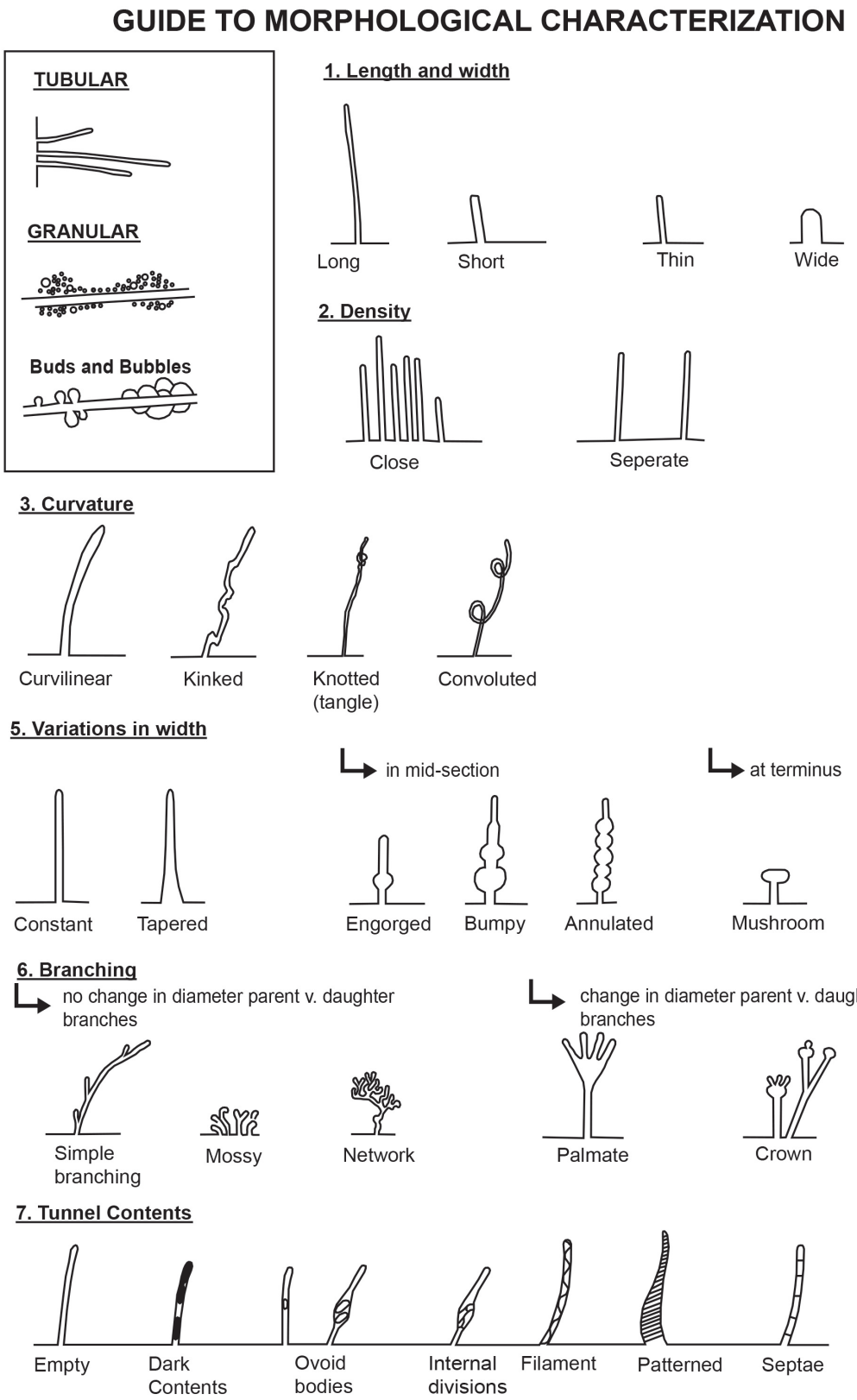

Supplementary Figure: Guide to the morphological characterization of tubular alteration textures slightly modified after Fisk & McLoughlin (2013). We used this guide to characterize the biosignatures described herein.

4 The coupled evolution of void space geometry and alteration reactions in the ageing oceanic crust

Andreas Türke, Wolf-Achim Kahl, Wolfgang Bach

4.1 Abstract

When the upper oceanic crust alters, its geochemistry, hydrology, and physical conditions change considerably, which shapes a very different bioenergetical landscape. In this communication we report geochemical data on altered basalt from the North Pond region, Mid-Atlantic Ridge, as well as micro-tomography measurements of the void space geometry and its evolution during alteration reactions. When fresh basalt reacts with seawater, primary phases (in particularly fresh glass) react to a mixture of clay minerals and palagonite forms as rims around glass shards. When transported off-axis, fluid circulation slows down, as impermeable sediments start to accumulate and fluids can become entrapped to form microenvironments. Within these fluids, SiO_2 concentrations increases due to palagonitization and eventually void space is (partially) filled by zeolites. Alteration of primary phases also changes the mineral interface to the fluid, which is what drives the bioenergetic landscape. For example hydrogen produced by radioactive decay from elements in the basalt has been proposed as an important energy source in old ocean crust. One of the major factors controlling radiolytic H_2 production is the mineralogy in the immediate proximity of void space in the basalts, as the radioactive dosis decreases, while traveling through a mineral matrix. We show that radiolysis is most effective when the void space is small (more radioactive material from minerals in close proximity) and near U, Th, and K bearing minerals.

4.2 Introduction

The majority of Earth' surface is covered by oceans and the majority of the underlying upper oceanic crust are basaltic lavas. These basalts tend to be very fractured, especially where the lava is cooled rapidly in contact with seawater and glassy chilled margins are formed. The high permeability of the upper 500 m

of ocean crust allows seawater to penetrate the crust and water-rock reactions create unique environments, such as the high temperature hydrothermal vents we observe near Mid-Ocean Ridges (MORs). Further off-axis within the ridge flanks, fluid temperatures are lower (usually < 20 °C) and fluid flow is not as channeled. However, ridge flanks cover a huge area of the seafloor and they represent Earth' largest aquifer. The oxidative alteration that occurs in ridge flanks, has significant impact on element cycles like Ca and Mg as a source or U, K, and Fe as a sink. The yearly throughput of fluids through the flanks of MORs rivals the amount of water that is channeled into oceans through river systems globally (Wheat et al., 2003). The alteration of basalts at low temperatures is sluggish and thus microbes are in theory able to catalyze the oxidation of the reduced forms of Fe, Mn, and S that are plentifully available in fresh basalts. There is ample evidence from textural observations, genomics studies, and isotopical studies for the presence and activity of microbes in low temperature alteration environments in ridge flanks (Santelli et al., 2008, Orcutt et al., 2015).

Fresh glass is kinetically the first phase to fall prey to alteration along fractures and around the rims of glass shards. The initial alteration phase of basalt glass is palagonite, which is a mix of clay minerals and/or Fe-(oxy)hydroxides (Stroncik & Schmincke, 2003). The elements released from the glass in the palagonitization process leads to a SiO_2 saturated fluid, from which phases like zeolite can precipitate within fluid filled fractures and void space, eventually sealing fluid pathways in the basaltic ocean crust.

4.3 Material and Methods

4.3.1 The North Pond area

We sampled core from the sites IODP 1382A and 1383C (see supplementary material for a detailed sample list), which are located in the North Pond area, on the western flank of the Mid-Atlantic Ridge. We sampled specifically for pieces of core that contained visibly altered glass, to focus our study on the earliest secondary mineralization (predominantly palagonitization). The North Pond area is a sediment pond structure of 8 x 15 km at 22°45'N, 46°05'W in about 4450 m water depth, which is surrounded by steep and up to 2 km high outcrops, where crustal material is exposed. The crust has been dated at an age of approximately 8 Ma (Shipboard Scientific Party 174B, 1998). The aquifer underneath the sediment pond is hydrologically active and fluid flow at temperatures < 20 °C has been detected (Orcutt et al., 2013). Oxygen has been indicated to flux from the aquifer into the up to 200 m accumulated sediments

(Ziebis et al, 2012), which makes the North Pond area an ideal candidate to study oxidative alteration in the uppermost crustal segment.

4.3.2 Electron Microprobe

Spot measurements for the major element contents were carried out using a Jeol JXA 8900R electron probe microanalyzer (EPMA) at the University of Kiel, Germany. The instrument was operated with an acceleration voltage of 15 kV, a probe current of ~ 20 nA, and a defocussed beam resulting in an elliptical spot of 5 µm in diameter. We analyzed lines as a consecutive series of point measurements with 10 µm spacing.

4.3.3 Laser-Ablation Inductively Coupled Plasma Mass Spectrometry (LA-ICP-MS)

Spot measurements for trace element contents were carried out using a ThermoScientific Element 2 ICP-MS coupled to a NewWave UP193ss laser ablation system at the Geosciences Department at the University of Bremen, Germany. The instrument was operated with an irradiance of ~ 1 GW/cm² for ablation. The beam diameter was set to 75 µm for the spot measurements. Pulse rate was 5 Hz for the palagonites and 10 Hz for basalt glass. Zeolites were not analyzed, as even lower pulse rates ablated the zeolites too quickly. Helium (0.7 L/min) was used as a carrier gas and argon (0.9 L/min) was added as make-up gas. External calibration standard was NIST612 using composition according to Jochum et al. (2011). Silicon was used as internal standard, analyzed prior by EPMA and concentrations were calculated with the Cetac GeoPro™ software. Analytical precision and accuracy were checked regularly by analyzing the SRM BCR-2G (basalt glass; Jochum et al. (2005)) and NIST612 reference materials.

4.3.4 X-ray microtomography method and generation of 3D composite rock model

The spatial information of the 3-D composite rock model used for hydrogen yield calculations has been derived from a X-ray microtomography scan using a CT-ALPHA system (ProCon, Germany) at the Department of Geosciences, University of Bremen, Germany. A rock fragment of hyaloclastite was

scanned with a beam energy of 100 kV, an energy flux of 200 µA, and using a copper filter in a 360°-rotation scan conducted with a step size of 0.225°. Reconstruction of the spatial arrangement of the linear attenuation coefficient in the samples was done with the Fraunhofer software VOLEX, using a GPU-hosted modified Feldkamp algorithm based on filtered backprojection (Feldkamp et al., 1984). As a result of the reconstruction procedure, each image slice consists of isometric voxels (volumetric pixels) with a certain thickness (voxel size: 3.6262 µm). Thus, a stack of images contains true volumetric information. The information about the varied X-ray absorption is encoded as grey values in the black-and-white images. The raw data was filtered with 3-D bilateral filter followed by 2-D non-local-means (Avizo 9.0.1, FEI). Subsequently, for the segmentation (i.e. the recognition of different fabric compounds by the assignment of distinct grey values) the volume data was exported to the software Skyscan™ CTAnalyser (Bruker mikroCT) and treated with an Otsu multilevel 3-D segmentation (mean intensities). Eventually, the volume data was exported as image stack (1791 images at 1549 x 668 voxels), containing four different fabric compounds (pore space; zeolite; palagonite; basaltic glass and primary minerals) to be investigated as model geometry for the hydrogen yield calculations.

4.3.5 3D Radiolysis Model

Radiolysis of water refers to the process of dissociation of water molecules by alpha, beta, and gamma radiation, released by decaying radioactive elements. In natural water-rock systems, U, Th, and K are the dominant sources of radioactivity. Radiation ionizes water molecules and short-lived reactive species, such as aqueous electrons, protons, as well as hydrogen and hydroxyl radicals are formed as primary products of radiolysis (Draganic & Draganic, 1971; LaVerne & Tandon, 2002; Gales et al., 2004). The subsequent reactions then form molecular hydrogen.

We used the average radiation doses per voxel, based on U, Th, and K concentrations and porosities that were reported for the North Pond basalt glasses and palagonites (1 ppm U, 0.2ppm Th, and 2.78 wt% K_2O for palagonite, 0.08 ppm U, 0.05 ppm Th, and 0.22 wt% K_2O for glass, and 0 ppm U, 0 ppm Th, and 4.74 wt% K_2O for zeolites; Türke et al. (2015)). Zeolite dosis was only based on K content, since no trace element data on Zeolite was available. This leads to too conservative total hydrogen yields, as zeolites are known to remove U from seawater (Misaelides et al., 1995; Krestou et al., 2003). The doses emitted from each voxel were then determined for the X-ray microtomography reconstructions of altered basalt and the resulting dosed were calculated based

on the loss of energy from surrounding voxels. We used the model of Dzaugis et al. (2015) for energy loss through the rock matrix. Pore space was assumed to be water saturated, whereas palagonite water content was assumed to be 100% - Total of the EPMA (Pauly et al., 2013), which resulted in 13 % H_2O content.

4.4 Results

4.4.1 Glass Composition

The basalt glass composition of the North Pond samples is given in Table 1. It is very homogeneous and exhibits Mid-Ocean-Ridge basalt (MORB) characteristics. These results are in good agreement with prior analyses of glasses from the North Pond area by Melson et al. (1976).

SiO_2	TiO_2	Al_2O_3	Cr_2O_3	FeO	MnO	MgO	CaO	Na_2O	K_2O
50.60 ± 1.61	1.69 ± 0.15	14.66 ± 0.58	0.04 ± 0.02	10.44 ± 0.30	0.20 ± 0.03	8.47 ± 0.30	10.31 ± 0.23	3.01 ± 0.14	0.22 ± 0.03

Table 1. The average composition of 512 spot measurements of basalt glass measured by EPMA in this study. The error margin is given as 2σ.

For further mass balance calculations of the overall element change in palagonitization at the North Pond area, these values will be used as the initial composition prior to oxidative alteration as palagonites form from volcanic glass.

4.4.2 Secondary minerals

Palagonites

The dominant alteration feature in the selected North Pond samples was palagonitization, which occurred around glass shards. The average composition of the palagonites is given in Table 2.

SiO_2	TiO_2	Al_2O_3	Cr_2O_3	FeO	MnO	MgO	CaO	Na_2O	K_2O
44.19 ± 5.13	2.53 ± 1.04	14.44 ± 3.94	0.05 ± 0.03	16.26 ± 4.31	0.07 ± 0.35	3.36 ± 1.63	1.29 ± 1.84	1.63 ± 0.72	2.78 ± 1.05

Table 2. The average composition of 568 spot measurements of palagonites measured by EPMA in this study. The error margin is given as 2σ.

Palagonites show a very strong depletion in CaO, but also MgO and Na_2O compared to the basalt glass, which was the source material. On the other hand K_2O, FeO, and TiO_2 are enriched. Variations can be large even within a single palagonite rim, and some zonation was observed (exemplary shown in Fig 1). In particular MgO and CaO are less depleted near the palagonite-glass interface, which is the most recent alteration front. SiO_2 exhibits the same zonation, but the depletion is less pronounced. K_2O on the other hand shows the strongest enrichment near fractures (or zeolites in case the fracture is already filled by precipitating minerals), as well as at the palagonite-glass interface. FeO exhibits the same strong enrichment at the palagonite-glass interface, but its content is less variable for the rest of the palagonite rim. The opposite trend can be observed for Al_2O_3, which is more enriched towards the fractures/zeolites.

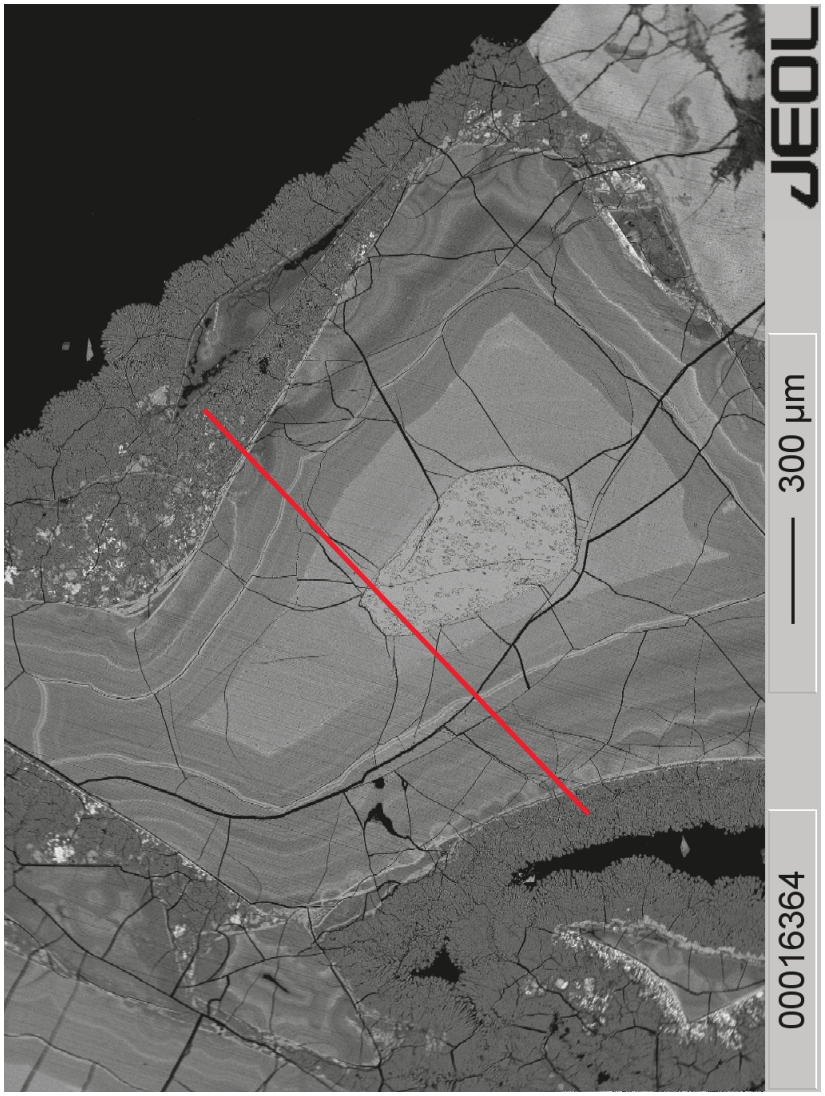
JEOL
300 µm
00016364

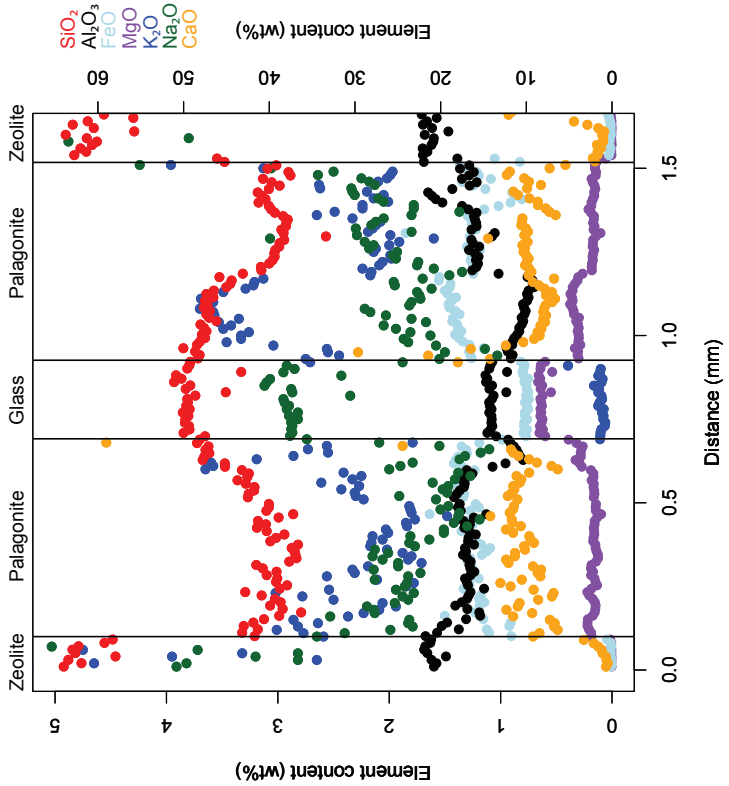
SiO2
Al2O3
FeO
MgO
K2O
Na2O
CaO
Element content (wt%)
0
10
20
30
40
50
60
Zeolite
Palagonite
Glass
Palagonite
Zeolite
0.0
0.5
1.0
1.5
Distance (mm)
Element content (wt%)
0
1
2
3
4
5

Fig 1. Left: EMPA results of the major elements from point analyses spread as a traverse spanning from zeolite through palagonite, fresh glass, palagonite, and zeolite again. K_2O, Na_2O, and CaO are plotted on the left y-axis, whereas SiO_2, Al_2O_3, FeO, and MgO are on the right y-axis. CaO content for the glass is around 10% and is not shown, this scaling was chosen to emphasize the CaO zonation near the palagonite-glass interface. Right: backscattered electron image of the region in that was investigated. The red line indicates the traverse, where spot measurements were carried out. It spans from left to right. The zeolites on the left hand side grew as precipitates, replacing void space in the sample.

The majority of trace elements tend to be slightly enriched in the palagonites, with significant enrichments only in Rb, Ba, Pb, and U, whereas Co is the only trace element that is depleted (Fig 2).

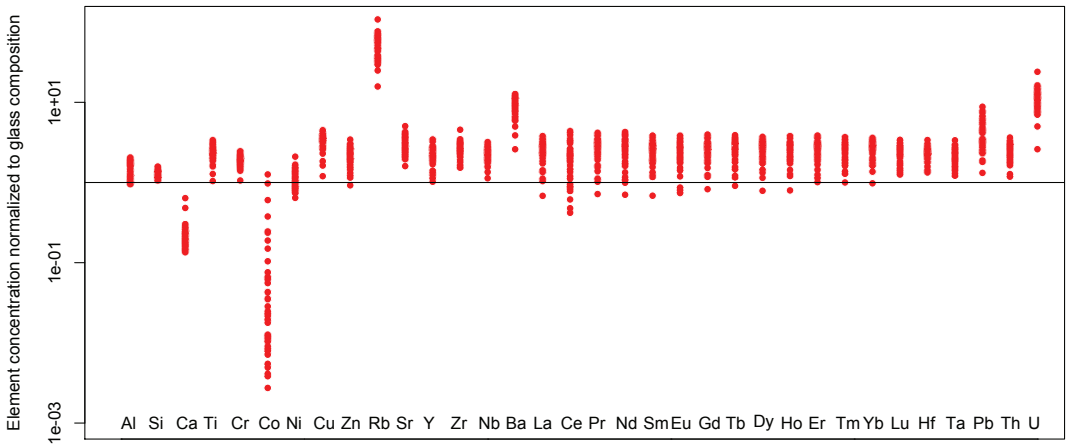

Fig 2. Results of the LA-ICPMS analyses of palagonites. The content of all elements was normalized to the average content of the fresh glass to indicate the enrichment or depletion factor of the respective element.

Zeolites

Based on textural observations zeolites (Fig 1) grow as fracture filling minerals after palagonitization. The average composition of the zeolites measured by EPMA is given in Table 3.

SiO_2	TiO_2	Al_2O_3	Cr_2O_3	FeO	MnO	MgO	CaO	Na_2O	K_2O

55.37 ± 7.75	0.34 ± 0.58	19.85 ± 1.96	0.01 ± 0.02	2.32 ± 3.70	0.27 ± 1.77	1.34 ± 2.41	0.54 ± 0.93	4.13 ± 1.65	4.74 ± 1.71

Table 3. The average composition of 125 spot measurements of zeolites measured by EPMA in this study. The error margin is given as 2σ.

Compared to palagonite as an alteration phase, the precipitated zeolites exhibit even higher K_2O contents. Other than potassium, the other notable cation-forming elements in the zeolites are Na, Ca, Mg, and Fe. The zeolite composition is very diverse (Fig. 3 and 4), but certain groups are distinguishable in particular in the ternary Na_2O, CaO, and K_2O diagram (Fig. 3). Six spot analyses of zeolites very (almost) completely devoid of any potassium and a CaO:Na_2O ratio of roughly 4:1. A large amount of analyses exhibits a K_2O:Na_2O ratio of about 1:1, without any CaO. The remaining spot analyses are characterized by varying CaO/(CaO+Na_2O+K_2O) values of up to 0.4.

Many zeolites within volcanic rocks can be inferred from their chemical composition in a (K+Na)/(K+Na+Ca) and Si/Al diagram (Fig. 4). Here, most of the zeolites plot in the area of phillipsite, chabazite, analcime, and heulandite. Due to fragility of zeolites under a laser, no LA-ICPMS analyses were possible to determine their trace element contents.

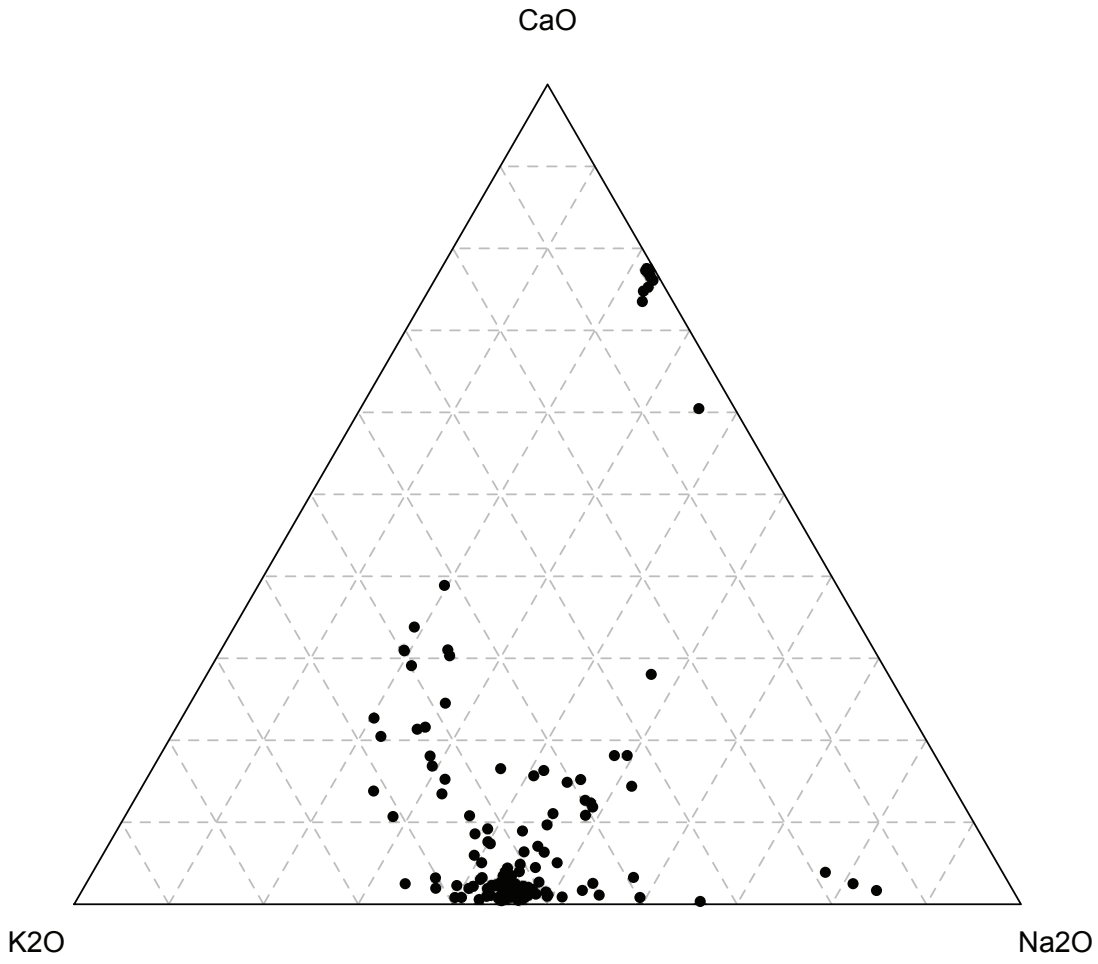

Fig 3. Results from EPMA spot analyses of zeolites in a ternary diagram with CaO, K_2O, and Na_2O as components.

Overall element changes

According Shipboard report of IODP Expedition 336, palagonitization (smectite therein) is the volumetrically more prominent form of secondary minerals compared to zeolites. The major geochemical exchange in oxidative alteration at North Pond occurs as a loss in Ca and to a lesser degree in Mg as shown in Fig. 5. Compared to fresh glass (blue) it is evident, that in palagonites there is depletion in the Na+Ca+K component, which is dominated by the loss of CaO (as Na_2O is only slightly depleted and K_2O even enriched (compare Fig. 1 and Table 2)). Zeolites too, have less Na+Ca+K than fresh glass, but the majority of them show a different behavior in the Mg+Fe component, with many of them devoid of these

elements. Palagonites on the other hand are enriched in Fe (and also strongly oxidized (Türke et al., 2015)).

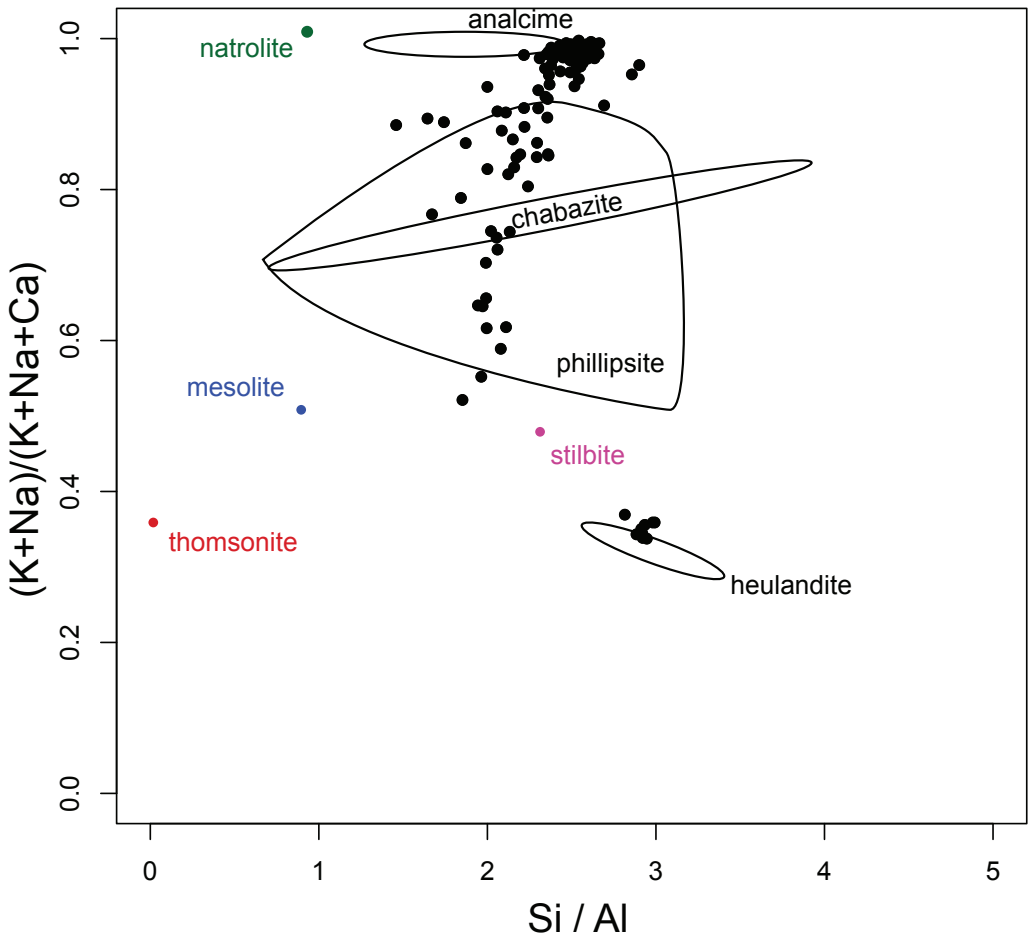

Fig 4. Results from EPMA spot analyses of zeolites with the Si/Al on the x-axis and (K+Na)/(K+Na+Ca) on the y-axis. The idealized mineral formulae of natrolite (green), mesolite (blue), stilbite (pink), and thomsonite (red) are plotted as colored dots. Heulandite, chabasite, phillipsite, and analcime as given as areas (based on results by Chipera & Apps (2001)), due to their higher chemical variability in volcanic rocks.

Figure 6 illustrates the overall strong loss in CaO in the whole rock composition due to its lack in the secondary minerals. The palagonites analyses with > 2 wt% of CaO were mostly very close to the palagonite-glass interface and are a result of the strong zonation.

Overall element changes for the other major elements are rather small as they are either close to the fresh glass contents, or palagonites and zeolites show opposite behaviors. For example, FeO is slightly enriched in palagonites, whereas zeolites' FeO content is only 2.32 wt% on average.

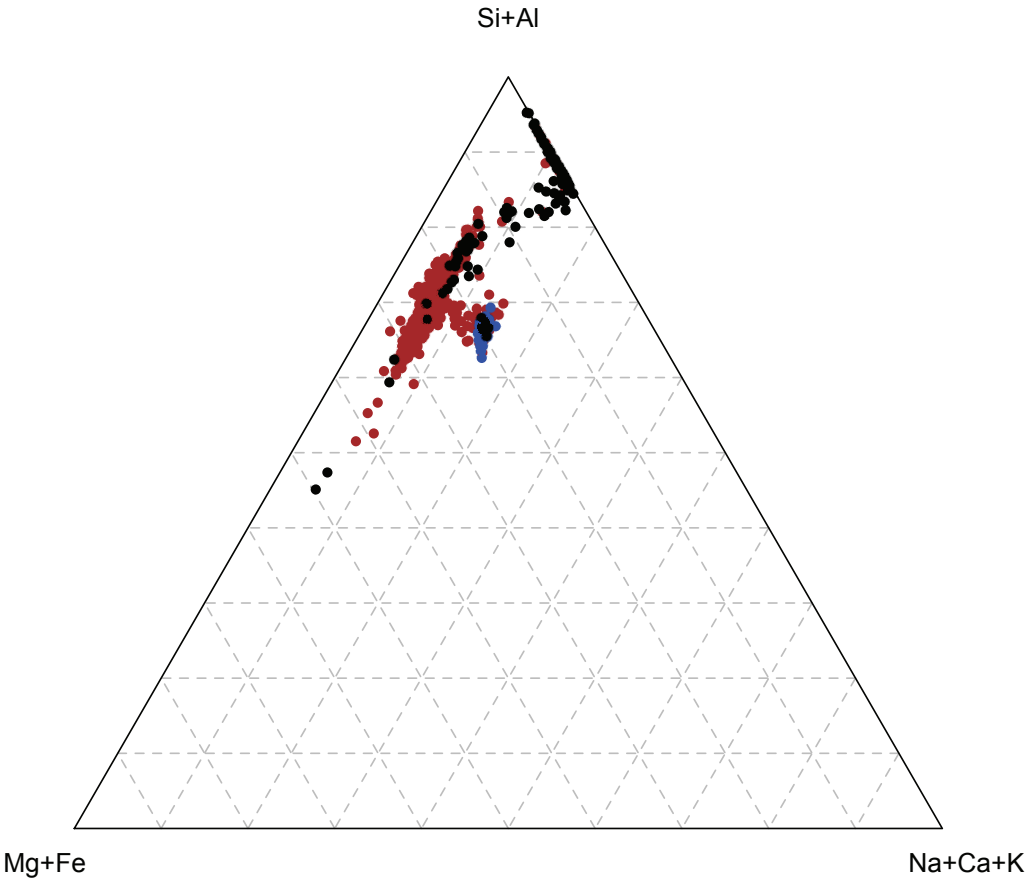

Fig 5. Results of EPMA point analyses plotted in a ternary diagram with Na+Ca+K, Mg+Fe, and Al+Si as components. Fresh glass is plotted in blue, palagonite in brown, and zeolites in black.

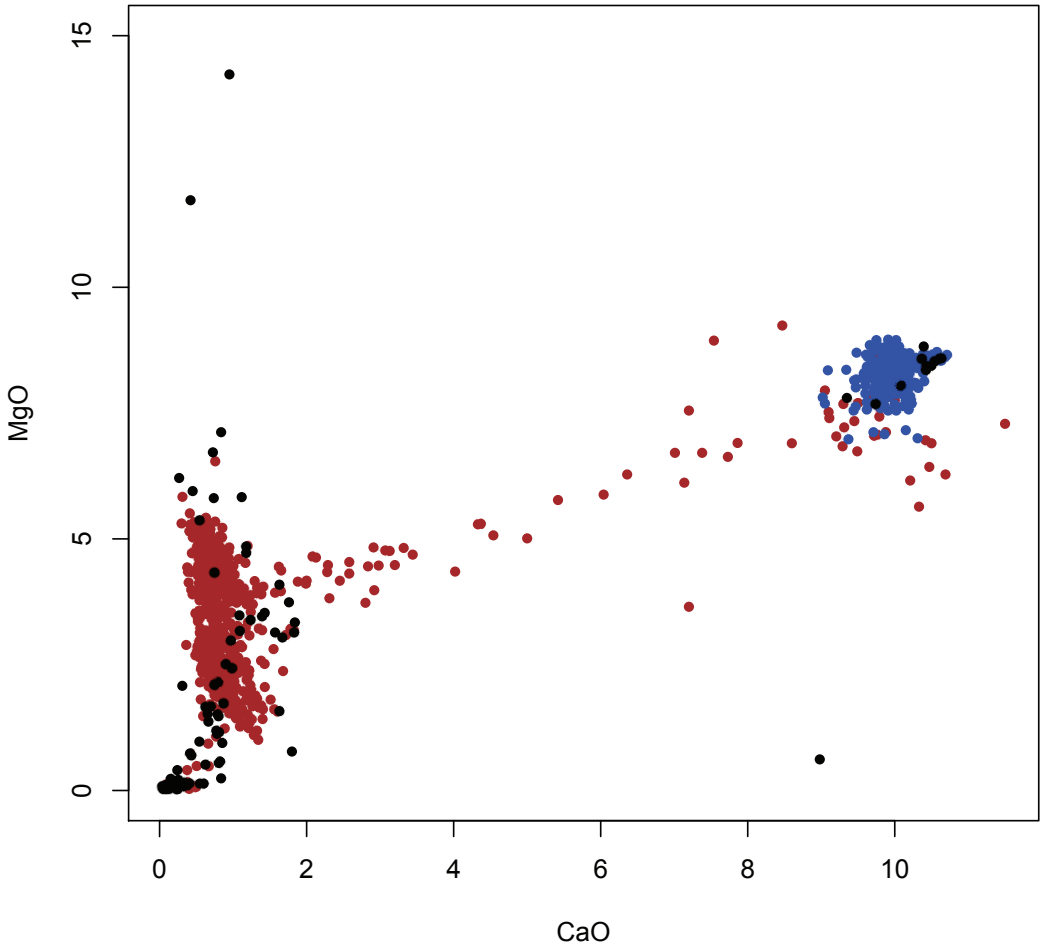

Fig 6. Results of the EPMA CaO and MgO spot analyses. Fresh glass is plotted in blue, palagonites in brown, and zeolites in black. The palagonites show a strong depletion in CaO, with depleted but less homogenous MgO contents. Zeolites exhibit low CaO content and even stronger variation in MgO.

4.4.3 Computer Tomography

The high-resolution microtomography volume reconstructions of a 5.6 mm x 6.4 mm x 2.4 mm fragment of sample U1383C-12-1_68-70 (Fig. 7) illustrates the spacial distribution of alteration phases and their influence on void space geometry. The partially altered piece of hyaloclastitic basalt was initially built up from fresh basalt glass, which occurred as glass shards with ample void space in between the individual shards. The glass was partially replaced by palagonites that grew from the glass-water interface at (former) fractures. Tubular curved palagonite textures of several 10s of µm in length and 1 voxel (3.6 µm) in width are visible at the glass-palagonite interface. Note that the resolution of 3.6 µm does not allow for a reliable specification of the width, it merely means, that the grey value of the voxel was such that the 4-phase composite 3D model described the voxel as palagonite, but does not give any information on the exact shape of the texture within the single voxel.

The void space between the glass shards is mostly filled by zeolites, but some void space still remains. Exceptions are vesicles in fresh glass, which still remain even after palagonitization. Exceptions are vesicles in fresh glass that also prevail after palagonitization, these represent rare cases of preserved void space that is still in direct contact with palagonite.

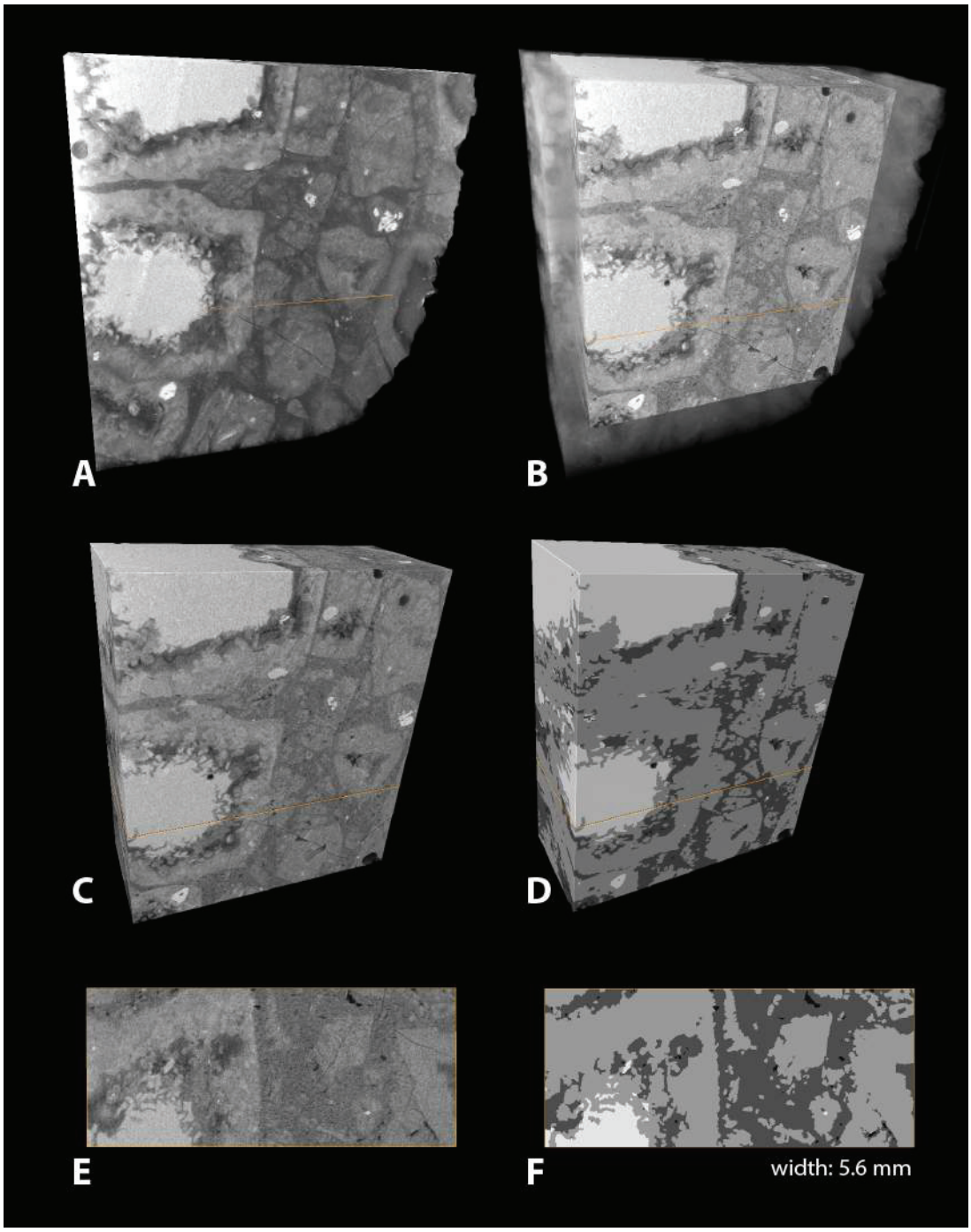

Fig 7. Results of high-resolution X-ray microtomography. (A) Volume reconstruction of a fragment of sample U1383C-12-1_68-70. (B) Localization of the cuboidal sub-volume used for modeling, unconsidered regions are rendered semitransparent. (C) Volume reconstruction, filtered image (3-D bilateral filter). (D) Composite 3-D model of the cuboidal sub-volume, featuring four fabric components: glass, palagonite, zeolite, and void space (from lighter to darker). (E) Reconstructed image (3-D bilateral filter). (F) Image slice (same layer as part E) of the 4-phase composite 3-D model. Note: (i) voxel size in A-F is 3.6 µm; (ii) the location of the image slice (parts E, F) within the cuboid is indicated by the orange plane in parts A-D.

4.5 Discussion

4.5.1 Void space evolution and its effect on radiolytic H_2 production

One of the major factors controlling radiolytic H_2 production is the mineralogy in the immediate proximity of void space in the basalts, as the radioactive dosis decreases, while traveling through a mineral matrix. The impact of the geometry of fractures – i.e. the geometry of water-mineral interfaces – was theoretically studied recently by Dzaugis et al. (2016). They conclude "fracture width [...] greatly influences H_2 production, where microfractures are hotspots for radiolytic H_2 production."

We come to similar conclusions for a rock geometry we observe in in-situ ocean crust basalts that have been altered oxidatively. The radiolytic H_2 yield calculations we present (Fig. 8), assume water saturation in the void space, but ignore mineral bound water in palagonite and zeolite, since the extent of their contribution to radiolytic H_2 production is uncertain. Radiolysis is most effective when the void space is small (more radioactive material from minerals in close proximity) and near U, Th, and K bearing minerals (palagonite as a stronger radioactive source than zeolite). Figure 8 clearly shows this relationship, as the highest H_2 yield occurs in a small vesicle at the right hand side, which is surrounded by palagonite. The larger void space closer to the center has lower H_2 yields, given its size, which means that the trapped fluid is exposed to a lower radioactive dosis. The smaller void space on the left hand side has very low H_2 yields, because it is completely surrounded by tens of µm of zeolite minerals. Even though void space occurs predominantly next to zeolites which precipitate in fractures of vesicles from the trapped fluids, there is ample space available in palagonite as well, which could thus very well act as a micro-scale habitat, in which microbial life fueled by radiolytic H_2 production can be sustained. Our assessment of microfractures is limited by resolution of the microtomography analyses, though, as voxel size was 3.6 µm. The model of Dzaugis et al. (2016) already suggest an order of magnitude less radiolytic H_2 yield after fracture width reaches a few tens of µm. While small fractures like that exist in the rock, a large part of the total void space is made up by structures in the millimeter range. Vesicles tend to be more favorable, as they are occur in glass and when altered, around palagonite.

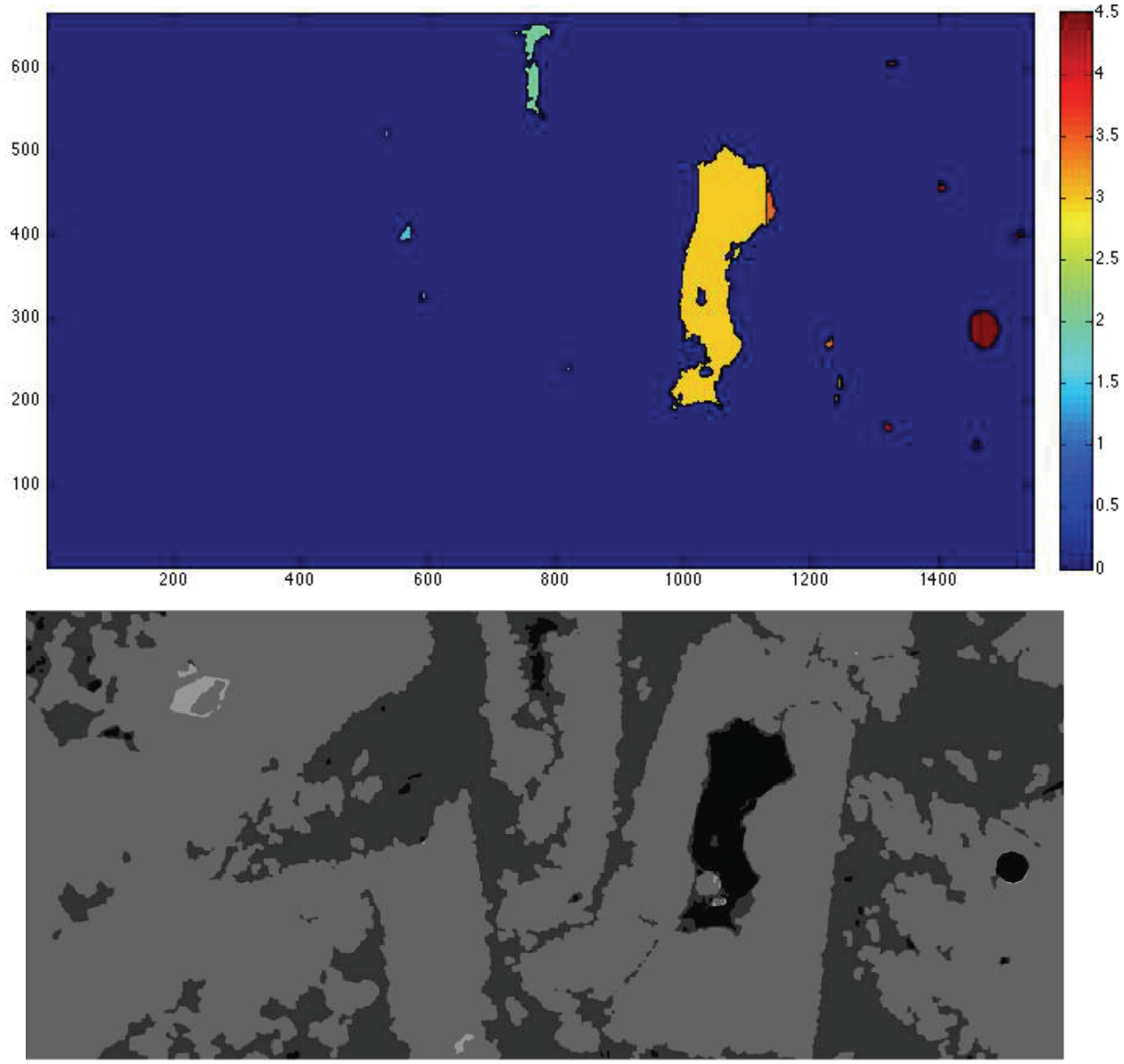

Fig 8. Selected results of high-resolution X-ray microtomography. Top: 3-D calculation of the radiolytic H_2 yield in void space. The H_2 production is highest in small void space that is surrounded by palagonite, as palagonite is the secondary phase with the highest concentration of radioactive elements. Larger void space produces less hydrogen per voxel, as the surrounding fluid filled void space does not contribute additional radioactive decay. Units are 10^{-13} mol/yr/cm^3 H_2. Bottom: four-phase reconstruction of the same selected slice of the composite 3-D model, featuring four fabric components: glass, palagonite, zeolite, and void space (from lighter to darker)

4.5.2 Geochemical changes at the alteration front and its impact on microbial life

Langseth et al. (1992) estimated that about 7.5 billion Liters of seawater flow annually through the basement at North Pond. Fluid measurements from 2014 suggest that approximately 0.6 µg/L of U are lost to the basement per year (Wolfgang Bach, pers. Comm.), which would equate to a very significant sink of 4.5 kg of U per year trapped in secondary minerals in the North Pond region. U is the radioactive element most impactful in H_2 production via radiolysis of water (Blair et al., 2007, Lin et al., 2005, Türke et al., 2015). As these secondary minerals are formed directly at the mineral-fluid interface, the U will contribute to radiolysis with high efficiency.

Additionally the leaching of Si from palagonites creates a fluid with increasing Si(aq) activity. When fluid circulation ceases in the basement, or certain fluid pathways become inactive, Si can accumulate in the fluid and precipitate zeolites. The zeolites then seal fractures and trap fluids within altered basalts. Even though zeolite composition shows some variations, there was no textural correlation to the kind of void space they occurred in. Heulandites, which were identified in spread among several samples, but only as sparsely over the samples, likely present a micro-environment that is less favorable for radiolytic H_2 production, because they do not contain potassium. Within the trapped fluids, radiolytically produced H_2 can accumulate and reach concentrations, which in theory are suitable to sustain hydrogenotrophic microbial life in the remaining void space.

4.6 Conclusion

When basaltic ocean crust alters oxidatively in contact with seawater, its chemical composition and its porosity and permeability changes. Palagonites take up significant amounts of radioactive elements and their decay can produce molecular hydrogen, when in close proximity to water molecules. We conclude that the mineralogy in the immediate proximity of void space in the basalts is the main driving force for H_2 production via radiolysis. It is most effective when the void space is small (more radioactive material from minerals in close proximity) and near U, Th, and K bearing minerals (palagonite as a stronger radioactive source than zeolite). In altered basalt void space occurs predominantly next to zeolites, which precipitate from the trapped fluids in fractures, but also in vesicles. This creates micro-scale habitat, in which microbial life fueled by radiolytic H_2 production can be sustained. Vesicles tend to be more favorable, as they are occur in glass and when altered, around palagonite. A summary of the

possible micro-environments is presented in Figure 9. The possible void space micro environments are; 1) vesicles, 2) fractures in glass, and 3) void space between individual glass shards in a hyaloclastite. In general, the smaller the void space is, the higher are the H_2 production rates. However, as zeolite precipitation begins, H_2 production rates decrease, even though void space decreases, since the fluid interface is no longer at the palagonites. Despite lower production rates, molecular hydrogen can now accumulate to higher fluid concentration, because fluids are trapped and hydrogen is not lost from the rock by fluid circulation anymore.

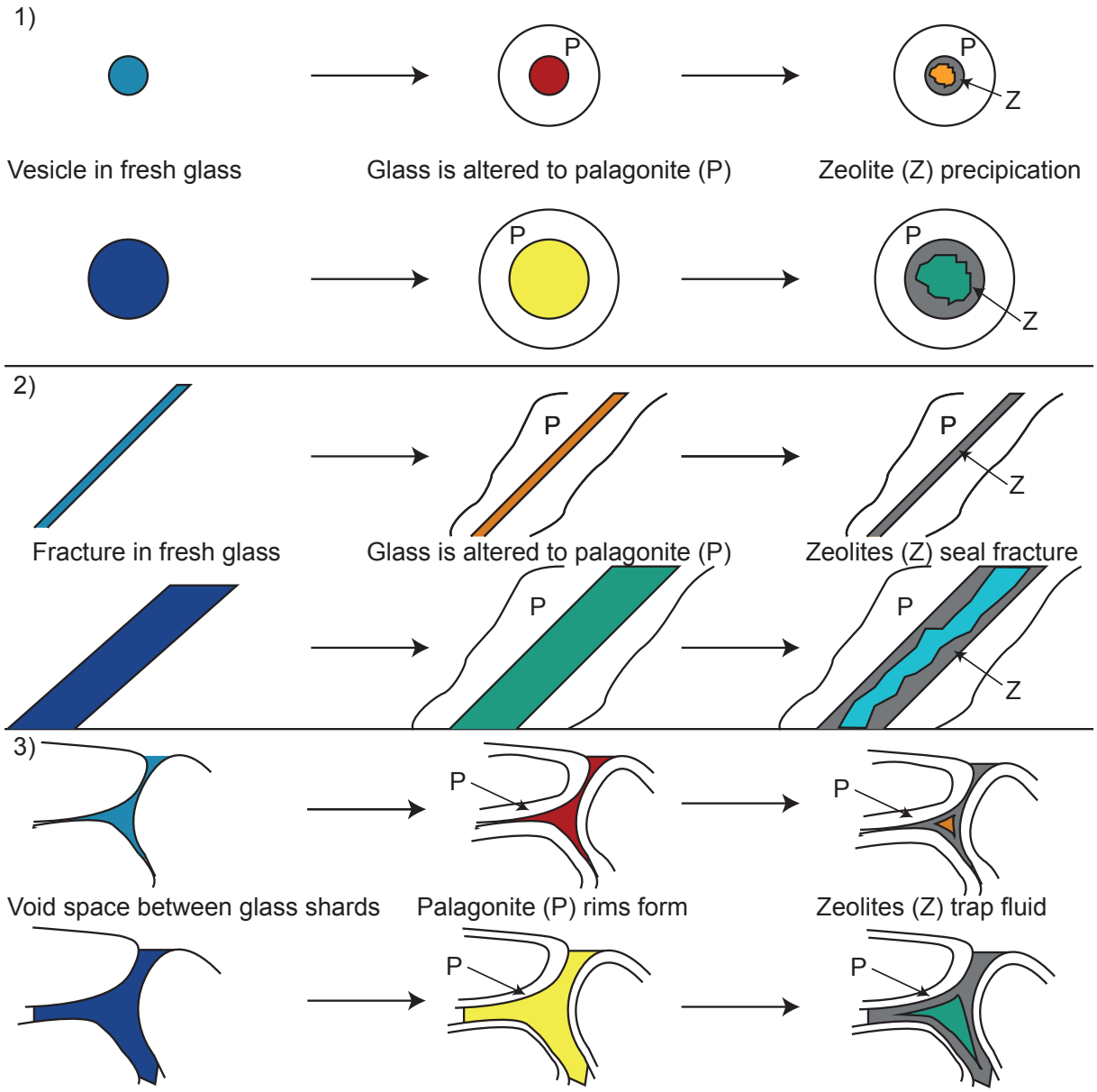

Fig 9. A sketch illustrating the different void space micro-environments in altered basalts. The colors indicate H_2 production rates in the fluid and use the same color scale as Fig. 8 (red highest, blue lowest). The differences in the top and bottom part illustrate the impact of volume of the total void space. The

larger the void space, the lower the production rates. 1) Vesicles in fresh glass, that are altered to palagonite and then precipitate zeolites from the Si enriched entrapped fluid. 2) Fracture in fresh glass with fluid flow through the rock. As palagonite forms, molecular hydrogen is produced. The rates then decrease as zeolites precipitate, however these can seal the fractures and trap fluids, so that H_2 can accumulate. 3) Void space between individual glass shards typically found in hyaloclastitic samples. Void space evolution is very similar to fractures, with a fluid that can eventually be trapped by sealing of zeolites.

However, sampling micro-environments within an already small sample from in-situ volcanic ocean crust is a very challenging task, especially with a focus on microbiology, because a certain amount of material is necessary to detect and genetically identify microbes. We suggest future studies focusing on basement fluid compositions in inclusions trapped within void space in vesicles, as well as zeolite filled fractures, similar to those described in this communication.

Acknowledgements

This research used samples and data provided by the Integrated Ocean Drilling Program (IODP). Funding for this research was provided the German Research Foundation DFG (grant BA1605/11) and the MARUM Center for Marine Environmental Sciences.

References

Blair, C.C., D'Hondt, S., Spivack, A.J. and Kingsley, R.H. (2007) Radiolytic Hydrogen and Microbial Respiration in Subsurface Sediments. Astrobiology Volume 7, Number 6, 951-970.

Chipera, S. J., and Apps, J. A. (2001) Geochemical stability of natural zeolites. Reviews in mineralogy and geochemistry, 45(1), 117-161.

Draganic, I. G., and Draganic Z.D. (1971) The Radiation Chemistry of Water, Academic Press, New York.

Dzaugis, M. E., Spivack, A. J., and D'Hondt, S. (2015) A quantitative model of water radiolysis and chemical production rates near radionuclide-containing solids. Radiation Physics and Chemistry, 115, 127-134.

Dzaugis, M. E., Spivack, A. J., Dunlea, A. G., Murray, R. W., and D'Hondt, S. (2016) Radiolytic hydrogen production in the subseafloor basaltic aquifer. Frontiers in microbiology, 7.

Gales, G., Libert, M-F., Sellier, R., Cournac, L., Chapon, V. & Heulin, T. (2004) Molecular hydrogen from water radiolysis as an energy source for bacterial growth in a basin containing irradiating waste. FEMS Microbiology Letters 240, 155 – 162.

Jochum, K.P., Willbold, M., Raczek, I., Stoll, B., and Herwig, K. (2005) Chemical characterisation of the USGS reference glasses GSA-1G, GSC-1G, GSD-1G, GSE-1G, BCR-2G, BHVO-2G and BIR-1G using EPMA, ID-TIMS, ID-ICP-MS and LA-ICP-MS. Geostandards and Geoanalytical Research 29:285–302.

Jochum, K.P., Weis, U., Stoll, B., Kuzmin, D., Yang, Q., Raczek, I., Jacob, D.E., Stracke, A., Birbaum, K., Frick, D.A., Günther, D., and Enzweiler, J. (2011) Determination of reference values for NIST SRM 610–617 glasses following ISO guidelines. Geostandards and Geoanalytical Research 35:397–429.

Krestou, A., Xenidis, A., and Panias, D. (2003) Mechanism of aqueous uranium (VI) uptake by natural zeolitic tuff. Minerals Engineering, 16(12), 1363-1370.

Langseth, M.G., Becker, K., Von Herzen, R.P. and Schultheiss, P. (1992) Heat and fluid flux through sediment on the western flank of the Mid-Atlantic ridge: a hydrogeological study of North Pond. Geophysical Research Letters 19, 517 – 520.

LaVerne, J. & L. Tandon (2002) H_2 Production in the Radiolysis of Water on CeO_2 and ZrO_2. The Journal of Physical Chemistry B 2002, 106, 380 – 386.

Lin, L., Slater, G.F., Sherwood Lollar, B., Lacrampe-Couloume, G. and Onstott, T.C. (2005) The yield and isotopic composition of radiolytic H_2, a potential energy source for the deep subsurface biosphere. Geochimica et Cosmochimica Acta 69, 893 – 903.

Löffler, F.E., Tiedje, J.M. and Sanford, R.A. (1999) Fraction of Electrons Consumed in Electron Acceptor Reduction and Hydrogen Thresholds as Indicators of Halorespiratory Physiology. Applied and Environmental Microbiology, Sept. 1999, p. 4049 – 4056.

Melson, W.G., Rabinowitz, P.D., Bougault, F., Fujii, T, Graham, A.L., Johnson, P., Lawrence, J., Prosser, E.C., Rhodes, J.M., and Zolotarev, B.P. (1976) Initial Reports of the Deep Sea Drilling Project, Vol. 45.

Misaelides, P., Godelitsas, A., Filippidis, A., Charistos, D., and Anousis, I. (1995) Thorium and uranium uptake by natural zeolitic materials. Science of the Total Environment, 173, 237-246.

Orcutt, B. N., Wheat, G.W., Rouxel, O., Hulme, S., Edwards, K.J., and Bach, W. (2013) Oxygen consumption rates in subseafloor basaltic crust derived from a reaction transport model. Nat. Commun. **4,** 2539.

Orcutt, B. N., Sylvan, J.B., Rogers, D.R., Delaney, J., Lee, R.W., and Girguis, P.R. (2015) Carbon fixation by basalt-hosted microbial communities. Front. Microbiol. 6, 1–14.

Pauly, B. D., Schiffman, P., Zierenberg, R., and Clague, D. (2011) Environmental and chemical controls on palagonitization. Geochemistry Geophys. Geosystems 12, Q12017.

Santelli, C.M., Orcutt, B.N., Banning, E., Bach, W., Moyer, C.L., Sogin, M.L., Staudigel, H., and Edwards, K.L. (2008) Abundance and diversity of microbial life in ocean crust. Nature 453, 653 – 656.

Shipboard Scientific Party. in Proc. ODP, Initial Reports, 174B (eds Becker, K. and Malone, M. J.) 25–35 (Ocean Drilling Program, 1998).

Türke, A., Nakamura, K., and Bach, W. (2015) Palagonitization of Basalt Glass in the Flanks of Mid-Ocean Ridges : Implications for the Bioenergetics of Oceanic Intracrustal Ecosystems. Astrobiology 15, 10. doi:10.1089/ast.2014.1255

Wheat, C. G.,McManus, J.,Mottl, M. J., and Giambalvo, E. (2003) Oceanic phosphorous imbalance: the magnitude of the ridge-flank hydrothermal sink. Geophys.Res. Lett. 30,OCE5.1– OCE5.4.

Ziebis, W., McManus, J., Ferdelman, T., Schmidt-Schierhorn, F., Bach, W., Muratli, J., Edwards, K. J., and Villinger, H. (2012) Interstitial fluid chemistry of sediments underlying the North Atlantic gyre and the influence of subsurface fluid flow. Earth and Planetary Science Letters, 323 – 324, 79 – 91.

4.7 Supplementary material

Sample	Lithology	Depths (mbsf)
336 U1382A 4R-3W 18/21	Pillow lava	125.99 – 126.02
336 U1382A 5R-1W 116/119	Pillow lava	133.66 – 133.69
336 U1382A 10R-2W 132/137	Massive flow	183.23 – 183.28
336 U1383C 7R-1W 21/25	Pillow lava	115.21 – 115.25
336 U1383C 12R-1W 68/70	Pillow lava	163.78 – 163.80
336 U1383C 13R-1W 39/43	Pillow lava	173.09 – 173.13
336 U1383C 19R-1W 67/69	Pillow lava	212.27 – 212.29
336 U1383C 20R-1W 22/25	Pillow lava	219.42 – 219.45
336 U1383C 20R-1W 139/141	Pillow lava	220.59 – 220.61
336 U1383C 22R-1W 24/27	Pillow lava	237.94 – 237.97
336 U1383C 24R-1W 6/9	Pillow lava	256.26 – 256.29

Table S1. List of all samples analyzed as thin sections within this study and their respective lithology and depth as meters below seafloor (mbsf).

5 Conclusion and Outlook

The oxidative alteration of ocean crust plays a vital role in shaping the conditions under microorganisms have to cope with in the subseafloor. This thesis aimed at unraveling the geochemical and physical changes that result from palagonitization and precipitation of zeolites that occur later on in crustal evolution. When ocean crust ages and moves off-axis, impermeable sediments will cover the igneous parts eventually and the hydrology of the ocean crust is impacted significantly. Circulation ceases and fluids can get trapped, which can lead to fluid compositions that do not resemble seawater as much, as they do in ridge flanks near the MORs. These changes also shape the bioenergetical landscape, i.e. the thermodynamics of chemical reactions, which microorganisms can exploit for their energy gain. Basalt that is exposed to oxygenated aqueous solutions, forms rims of palagonite along fractures at the expense of glass. Radioactive elements are enriched in palagonite relative to fresh glass, as shown in the (LA)-ICPMS and EMPA analyses of fresh glass, adjacent palagonite crusts, and zeolites. They reach concentrations where radiolytic production of molecular hydrogen may play a significant role for microbial energy gain. In older flanks, crustal sealing and sediment accumulation have slowed down seawater circulation and radiolytically produced hydrogen might reach concentrations of > 1 nM, which allows for hydrogenotrophic metabolism to occur.

Based on these results, the hypothesis that microbial ecosystems in ridge flank habitats undergo a transition in the principal energy carrier, fueling carbon fixation from Fe oxidation in very young crust to H_2 consumption in older crust, was formed. Unless the H_2 is swept away by rapid fluid flow (i.e., in young flanks), it may easily accumulate to levels high enough to support chemolithoautotrophic life.

Void space in basalts plays a crucial role in determining how trapped crustal fluids evolve chemically and thus how the bioenergetical regime changes in these cavities. The accompanied changes in bioenergetical conditions raise the question of whether the upper oceanic crust is habitable only for a short duration of its existence or throughout the entire phase from formation at the MOR to the subduction at the continental margin.

Alteration of primary phases also changes the mineral interface to the fluid. One of the major factors controlling radiolytic H_2 production is the mineralogy in the immediate proximity of void space in the basalts, as the radioactive doses decrease, while traveling through a mineral matrix.

Microtomography was used to observe the relationship of secondary phases that are precipitated or formed from primary phases and the void space, which is retreating in favor of precipitating minerals. The 3-D CT scans of altered basalts revealed that void space occurs predominantly next to zeolites, which precipitate from the trapped fluids in fractures, but also in vesicles. This creates micro-scale habitats, which have to be considered individually and can be different from the overall crustal fluid compositions. Different types of micro-environments also behave differently in terms of radiolytic H_2 production. Vesicles tend to show the highest production rates, as they occur in glass, and when altered around palagonite.

The possible void space micro-environments are; 1) vesicles, 2) fractures in glass, and 3) void space between individual glass shards in a hyaloclastite. In general, the smaller the void space is, the higher are the H_2 production rates. However, as zeolite precipitation begins, H_2 production rates decrease, even though void space decreases, since the fluid interface is no longer at the palagonites. Despite lower production rates, this is the state where molecular hydrogen can accumulate to higher fluid concentration, because fluids are trapped and hydrogen is not lost from the rock by fluid circulation.

Furthermore, biosignatures in young well-oxygenated crust, are characterized by little textural diversity. However, the organic matter associated with those textures, shows evidence for the occurrence of complex molecules like proteins. In contrast, the biosignatures from severely altered basalts are much more texturally diverse, whereas their associated organic molecules are more degraded and suggest Archaeal origin. This implies that microbial communities change significantly during crustal evolution and suggests that microbes associated with older crust, are not responsible for the trace fossils commonly found within subseafloor basalt glass.

Similar habitats on other planetary surfaces are theoretically possible; as accumulation of radiolytically produced hydrogen merely requires the presence of H_2O molecules and a porous medium, from which the hydrogen is not lost. The multimethodical approach to address habitability and syngenecity questions of potential biosignatures that was attempted in this thesis hopefully contributes new insights into astrobiological research.

Acknowledgements

I thank my supervisor Wolfgang Bach for giving me the opportunity to conduct a PhD thesis in the working group Petrology of the Ocean Crust. His guidance and support when necessary were vital in concluding this project, but I am especially grateful for the creative freedom he allowed me.

I also thank Magnus Ivarsson for his role as second supervisor and for reviewing this thesis. Meeting him at conferences to discuss science and other aspects of life was always a delightful experience.

Furthermore, I would like to thank Simone Kasemann and Heiko Pälike for being part of my thesis committee and providing valuable feedback.

I thank my co-authors Benedicte Menez, Kentaro Nakamura, and Wolf-Achim Kahl for their scientific expertise and work they contributed to this thesis.

Patrick Monien was vital for the success of my thesis with his dedication and support in the lab for which I am very grateful.

I thank the entire working group for their pleasant daily company and conversations at the coffee table.

I am grateful to my parents for setting me on a path that allowed me pursuing my passion for scientific work.

A special place is reserved for my friends. These are the comrades I have; there are no better. We all shared good times. Here is the list, to whom I dedicate my love:

To Christian

To Bastian

To Andrea

To Julia

To Alex

To Elmar

To Alex

To Dario

To Lena

To Lisa

To Carlos

To Katharina

To Yves

To Rike

To Florian

To Janis

Be happy now because tomorrow you are dying.

6 Erklärung

Versicherung an Eides Statt

gem. § 5 Abs. 5 der Promotionsordnung vom 15.07.2015

Ich, _____
(Vorname, Name, Anschrift, ggf. Matr.-Nr.)

versichere an Eides Statt durch meine Unterschrift, dass ich die vorstehende Arbeit selbständig und ohne fremde Hilfe angefertigt und alle Stellen, die ich wörtlich dem Sinne nach aus Veröffentlichungen entnommen habe, als solche kenntlich gemacht habe, mich auch keiner anderen als der angegebenen Literatur oder sonstiger Hilfsmittel bedient habe, und die zu Prüfungszwecken beigelegte elektronische Version der Dissertation mit der abgegebenen gedruckten Version identisch ist.

Ich versichere an Eides Statt, dass ich die vorgenannten Angaben nach bestem Wissen und Gewissen gemacht habe und dass die Angaben der Wahrheit entsprechen und ich nichts verschwiegen habe.

Die Strafbarkeit einer falschen eidesstattlichen Versicherung ist mir bekannt, namentlich die Strafandrohung gemäß § 156 StGB bis zu drei Jahren Freiheitsstrafe oder Geldstrafe bei vorsätzlicher Begehung der Tat bzw. gemäß § 161 Abs. 1 StGB bis zu einem Jahr Freiheitsstrafe oder Geldstrafe bei fahrlässiger Begehung.

_____ _____

Ort, Datum Unterschrift